Perturbative analysis of two-qubit gates on transmon qubits

von

Susanne Richer

Masterarbeit in Physik
vorgelegt der Fakultät für Mathematik, Informatik und Naturwissenschaften der RWTH Aachen im September 2013
angefertigt im Institut für Quanteninformation

bei

Prof. Dr. Barbara M. Terhal,
Prof. Dr. David P. DiVincenzo

Abstract

This thesis treats different schemes for two-qubit gates on transmon qubits and their perturbative analysis. The transmon qubit is a superconducting qubit that stands out due to its very low sensitivity to charge noise, leading to high coherence times. However, it is also characterized by its low anharmonicity, making it impossible to neglect the higher transmon levels.
Coupled systems of superconducting qubits and resonators can be treated in cavity QED. In the dispersive regime, where qubit and resonator are far detuned from each other, perturbative methods can be used for the derivation of effective Hamiltonians. Several such methods are presented here, among which the Schrieffer-Wolff transformation results to be the most adequate.
As the anharmonicity of the transmon qubit is low, higher transmon levels play a significant role in two-qubit gate schemes. These gates can be driven using microwave pulses, where certain resonance conditions between the transmon levels are used to tune up the desired two-transmon interaction effects. The Schrieffer-Wolff transformation will be used to see how these effects arise.

Contents

Acknowledgements

I would like to thank my supervisors Barbara Terhal and David DiVincenzo for mentoring me during the past year. You are both not only great physicists but also gifted teachers. Thank you very much for your patience and your inspiring enthusiasm. It has been a pleasure to work with you.
Thanks to Jay Gambetta, on whose work a part of this thesis is based and who was so kind to share some of his calculations with me.
Special thanks goes to Eva Kreysing and Stefan Hassler for being the best office mates in the world. It was amazing to always be able to talk to you about any physics or non-physics problems. We had a great time together and I will miss working with you.
Thanks to Helene Barton for making me feel at home in the institute from the first day I came here and to all my other co-workers for making the IQI such a friendly place.
Last but not least, I would like to thank my parents for all their support and encouragement during my studies and for always believing in me more than I did myself and all my crazy friends without whom I would have never gotten anywhere near a degree. Thank you so much!

1. Introduction

Since first proposed by Richard Feynman in 1982 [1], the idea of building a quantum computer has evoked a great amount of research interest. The immense potential of quantum computers became evident in 1994, when Peter Shor developed a quantum algorithm for the factorization of integers that was substantially faster than any known classical algorithm [2]. Ever since, research groups all over the planet have been working incessantly on the realization of quantum computers, making the field one the most intriguing in the world.

However, in spite of more than two decades of intense research, quantum computation is still in its infancy. The first step on the long way to a quantum computer is to replace the classical bit with its instances 0 and 1 by a *quantum bit* or *qubit* with two possible quantum states $|0\rangle$ and $|1\rangle$. In principle, any quantum-mechanical two-level system could be used as a qubit. In contrast to classical bits, these qubits obey the laws of quantum mechanics, allowing them, for example, to be in a superposition of states rather than in one state only. Possible realizations of qubits could be for instance the ground state and excited state of a two-level atom or the two directions of an electron spin, up and down. One of the most promising among the many conceivable realizations of qubits are superconducting qubits, that is electrical circuits with quantized energy levels. Even though these elements consist of many atoms, we will see that they effectively act like single artificial atoms. Among superconducting qubits we distinguish between charge qubits [3], flux qubits [4], and phase qubits [5], depending on the relevant quantum number.

Having found a physical realization of qubits, the next question is how to manipulate them coherently. We have to be able to initialize the qubits in a desired state, do one- and two-qubit gates and read-out their state with high fidelity. As these gates will never be perfect, we will also need methods to correct the errors that occur during computation [6].

While a lot of research is done on the subject of quantum computation, the ultimate goal of finally building a quantum computer continues to be decades away from its realization. Nevertheless, the field exhibits a great amount of physical phenomena that are worth studying just for the sake of gaining knowledge.

This thesis will treat superconducting qubits, most notably the *transmon* qubit [7]. Chapter 2 includes a detailed description of transmon qubits in cavity quantum electrodynamics. We will see that the analysis of these qubits requires systematic methods for the derivation of effective Hamiltonians. In chapter 3, such methods are presented and compared with special regard to the Schrieffer-Wolff transformation [8, 9], which is a unitary transformation in quasi-degenerate perturbation theory. This transformation will be used in chapter 4 for the analysis of gates involving one or two qubits. Finally, chapter 5 contains conclusions and an outlook on possible future work.

2. Transmon qubits in cavity QED

Superconducting qubits are promising physical realizations of quantum bits and therefore a field with high research interest. These qubits are made of superconducting circuits including dissipationless elements such as capacitors, inductors and Josephson junctions. It turns out that the physical description of these circuits is strikingly similar to the field of cavity quantum electrodynamics

2.1. Cavity QED and Jaynes-Cummings model

Cavity quantum electrodynamics (cavity QED) describes the interaction between atoms and light inside a reflective cavity. Such a cavity is a resonator in which certain resonant frequencies oscillate with much higher amplitude than any non-resonant frequency. Therefore atoms in a cavity interact almost exclusively with these resonant modes, i.e. with photons of well-defined frequencies. While in free space a photon emitted by the atom is lost, it stays confined in the cavity and might be reabsorbed, leading for example to Rabi oscillations. The Hamiltonian of a light mode with frequency ω_c can be described as a harmonic oscillator, that is

$$H_{\text{field}} = \omega_c \left(a^\dagger a + \frac{1}{2} \right), \tag{2.1}$$

where $a = \sum_n \sqrt{n+1}|n\rangle\langle n+1|$ is the photon annihilation operator. We will omit the vacuum term $\omega_c/2$ in further calculations.
Consider an atom interacting with a mode of light inside a cavity. Even though the cavity might have more than one resonant mode, we suppose that all other modes are far away from the atom's transition frequency and can therefore be neglected. Assuming that the atom can be modeled as a two-level system with ground state $|0\rangle$ and excited state $|1\rangle$, its Hamiltonian can be written as

$$H_{\text{atom}} = -\frac{\omega_a}{2}\sigma^z, \tag{2.2}$$

where ω_a is the transition frequency of the atom and $\sigma^z = |0\rangle\langle 0| - |1\rangle\langle 1|$ is the Pauli-Z matrix. The Hamiltonian of the interacting atom-cavity system is given by

$$H = H_{\text{field}} + H_{\text{atom}} + H_{\text{int}} = \omega_c a^\dagger a - \frac{\omega_a}{2}\sigma^z + g(a^\dagger + a)(\sigma^+ + \sigma^-), \tag{2.3}$$

where g is the coupling strength between the atom and the field and where $\sigma^+ = |1\rangle\langle 0|$ and $\sigma^- = |0\rangle\langle 1|$ are the atomic raising and lowering operators, respectively.
It is instructive to look at this Hamiltonian in a rotating frame, where the atom stands still. Such a rotating frame is defined by the unitary transformation $U = e^{iH^0 t}$ with $H^0 = H_{\text{field}} + H_{\text{atom}}$. This transformation leads to an interaction picture Hamiltonian

$$H_I(t) = UHU^\dagger + i\dot{U}U^\dagger = g\left(a^\dagger\sigma^+ e^{i\omega_\Sigma t} + a^\dagger\sigma^- e^{i\Delta t} + a\sigma^+ e^{-i\Delta t} + a\sigma^- e^{-i\omega_\Sigma t}\right),$$

where $\Delta = \omega_c - \omega_a$ is the detuning between the atom and the cavity and $\omega_\Sigma = \omega_c + \omega_a$ is the sum of the two frequencies. We see that we are left with the interaction term only, which now includes terms rotating at either Δ or ω_Σ. In the case of near resonance, where $|\Delta| \ll \omega_\Sigma$, we assume that the effect of the fast-rotating terms at frequency ω_Σ (also called counter-rotating terms) averages out and can therefore be neglected. This is called the *rotating wave approximation* (RWA). The resulting Hamiltonian, transformed back into the Schrödinger frame, is the so-called *Jaynes-Cummings Hamiltonian*

$$H = \omega_c a^\dagger a - \frac{\omega_a}{2}\sigma^z + g(a^\dagger \sigma^- + a\sigma^+). \tag{2.4}$$

The effect of the counter-rotating terms, which the Jaynes-Cummings model neglects, is further examined in section 3.1.3.
In the remaining interaction part, the $a^\dagger\sigma^-$-term represents the emission of a photon in combination with a deexcitation of the atom, while the $a\sigma^+$-term describes the reverse process. Thus, the Hamiltonian couples the levels $|n+1, 0\rangle$ and $|n, 1\rangle$, where n is the photon number and $|0\rangle$ and $|1\rangle$ the ground state and excited state of the atom, respectively. The eigenstates of the Jaynes-Cummings Hamiltonian are the so-called *dressed states*, which are superposition states of these two, namely

$$|n, +\rangle = \sin\left(\frac{\vartheta_n}{2}\right)|n+1, 0\rangle + \cos\left(\frac{\vartheta_n}{2}\right)|n, 1\rangle \tag{2.5}$$

$$|n, -\rangle = \cos\left(\frac{\vartheta_n}{2}\right)|n+1, 0\rangle - \sin\left(\frac{\vartheta_n}{2}\right)|n, 1\rangle \tag{2.6}$$

with $\tan(\vartheta_n) = -\frac{2g\sqrt{n+1}}{\Delta}$. The corresponding eigenenergies yield

$$E_{|n,\pm\rangle} = \omega_c\left(n + \frac{1}{2}\right) \pm \frac{\Delta}{2}\sqrt{1 + \frac{4g^2(n+1)}{\Delta^2}}, \tag{2.7}$$

which are depicted in figure 2.1.

2.1.1. Dispersive regime

Figure 2.1 shows the energies of the dressed states as a function of the atom-cavity detuning Δ. While the uncoupled states are degenerate for zero detuning, we see an avoided crossing for the dressed states.
If Δ is large compared to the coupling strength g, the dressed states tend to the uncoupled ones

$$E_{|n,\pm\rangle} \to \omega_c\left(n + \frac{1}{2}\right) \pm \frac{\Delta}{2} = \begin{cases} \omega_c(n+1) - \frac{\omega_a}{2} = E_{|n+1,0\rangle} \\ \omega_c n + \frac{\omega_a}{2} = E_{|n,1\rangle}. \end{cases} \tag{2.8}$$

This is the so-called dispersive regime, where the coupling can be treated as a perturbation. In this regime, we assume that we can use the uncoupled eigenstates and derive an effective Hamiltonian, which shows that the coupling only leads to an energy shift on the unperturbed eigenenergies. As a first approximation, we can expand the eigenenergies for $g \ll \Delta$ to give

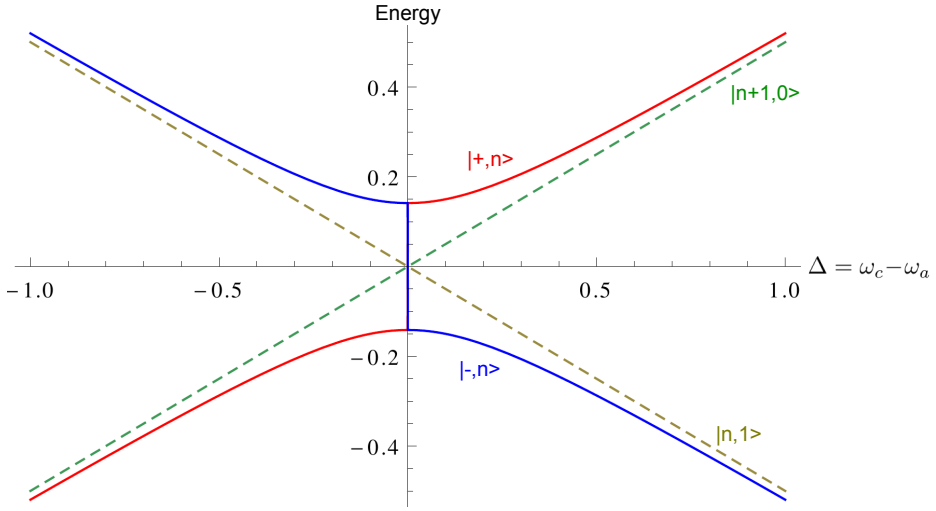

Figure 2.1.: Energy of the dressed states (equation 2.7) as a function of the detuning $\Delta = \omega_c - \omega_a$ for $\omega_c = 0$ in arbitrary units. For large detuning $\Delta \gg g$, the dressed states tend to the uncoupled ones.

$$E_{|n,\pm\rangle} \to \begin{cases} \left(\omega_c + \frac{g^2}{\Delta}\right)(n+1) - \frac{\omega_a}{2} \\ \left(\omega_c - \frac{g^2}{\Delta}\right) n + \frac{\omega_a}{2}. \end{cases}$$

Comparing these to the uncoupled levels (equation 2.8), we see that the cavity frequency undergoes a shift, whose sign depends on the state of the atom. This shift, called AC-Stark shift, is very convenient for read-out purposes, as we can detect the state of the atom by measuring the cavity's resonant frequency.
In section 3, different methods for the derivation of effective Hamiltonians are presented with special regard to the Jaynes-Cummings Hamiltonian (equation 2.4) including a more systematic derivation of the Stark-shift and the additional Lamb shift.

2.2. Circuit QED

Circuit quantum electrodynamics studies the behavior of certain electrical circuits that have great similarities to single atoms and cavities. Thus, it is possible to transfer much of the physics derived in cavity QED to these circuits.
As described in [10], transmission line resonators are used as a circuit analogue to cavities in order to read out and control superconducting qubits. A transmission line resonator can be modeled as a quantum LC oscillator consisting of an inductor with inductance L and a capacitor with capacitance C. Its Hamiltonian is

$$H = \frac{q^2}{2C} + \frac{\Phi^2}{2L},$$

where q is the charge stored in the capacitor and Φ is the flux through the inductor. Using $q = i\sqrt[4]{\frac{C}{4L}}(a^\dagger - a)$ and $\Phi = \sqrt[4]{\frac{L}{4C}}(a^\dagger + a)$, we can write this as a quantum harmonic

oscillator with frequency $\omega_r = \sqrt{1/(LC)}$

$$H = \omega_r \left(a^\dagger a + \frac{1}{2} \right) \tag{2.9}$$

in analogy to the cavity Hamiltonian equation 2.1 with the creation and annihilation operators as defined above. The constant term will be omitted in further calculations.
Though this is a very simplified description of a transmission line resonator, it is adequate for this purpose. As described in [10], a transmission line resonator should really be treated as the continuum limit of a chain of transmission oscillators, leading to a Hamiltonian like 2.9, but with many modes. However, these other modes are assumed to be far off-resonant and therefore negligible. Just as with real cavities, we will consider only one relevant mode here.

2.2.1. The Transmon qubit

We have thus found an electrical circuit that can model a cavity. However, it is not possible to use an LC oscillator as a qubit, because its levels are all equally spaced. It is therefore impossible to take two of the levels as a qubit as they can not be separately addressed. Thus, we need an element in the circuit that brings in the necessary anharmonicity: the Josephson junction.
A Josephson junction is a superconducting circuit element that consists of two superconductors separated by a thin insulating barrier. A superconducting current can pass this junction when Cooper pairs tunnel through the barrier. The Josephson junction can be seen as a non-linear inductor that induces a phase-shift across the junction.
The *transmon* qubit (see [7]), which this thesis primarily treats, is based on the Cooper pair box qubit (see [11], [3]), which consists of a Josephson junction and an additional capacitance, as depicted in figure 2.2.

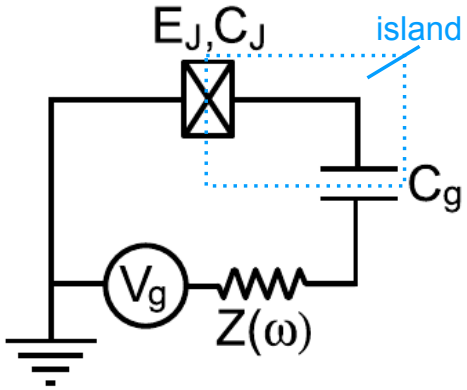

Figure 2.2.: Circuit diagram of a Cooper pair box qubit, which consists of a Josephson junction with Josephson energy E_J and capacitance C_J and an additional capacitance C_g. The charge offset $n_g = C_g V_g / 2e$ on the island can be controlled via the gate voltage V_g. The circuit diagram also includes an environmental impedance $Z(\omega)$. (Figure taken from [3], page 4.)

The state of the Cooper pair box qubit is determined by the number of Cooper pairs on the superconducting island between the capacitor and the Josephson junction. Thus, the Cooper pair box qubit is a charge qubit, as the charge is the relevant quantum number in this setup.
As described in [10], the Hamiltonian of the Cooper pair box can be written as

$$H = \frac{q^2}{2C} - E_J \cos\left(2\pi \frac{\Phi}{\Phi_0}\right),$$

where $C = C_g + C_J$ is the capacitance and $q = -n2e$ is the discrete charge, with n being the number of Cooper pairs that have crossed the junction. Φ is the flux through the Josephson junction and $\Phi_0 = h/(2e)$ is the superconducting flux quantum. E_J is the so-called Josephson energy, a constant that characterizes the junction. Using the number operator $\hat{n}$ and the dimensionless phase operator $\hat{\varphi} = 2\pi\Phi/\Phi_0$ for the superconducting phase across the Josephson junction, we can write this as

$$H = 4E_C(\hat{n} - n_g)^2 - E_J \cos(\hat{\varphi}), \tag{2.10}$$

where $E_C \equiv e^2/(2C)$ is the charging energy, $n_g = C_g V_g/2e$ is a possible offset charge and $\hat{n}$ and $\hat{\varphi}$ are canonically conjugate variables with $\hat{n} = \frac{\partial}{\partial\hat{\varphi}}$ and $[\hat{n}, e^{\pm i\hat{\varphi}}] = \pm e^{\pm i\hat{\varphi}}$ (see [12]).
The biggest problem of the Cooper pair box qubit is that it is highly sensitive to charge noise leading to short coherence times. Therefore, Koch et al. proposed in [7] a further development of the Cooper pair box qubit, the *transmon*.
Figure 2.3 shows how the charge noise sensitivity changes with the ratio between E_J and E_C. While the Cooper pair box qubit operates in a regime where $E_J/E_C \sim 1$ (figure 2.3a), the transmon is operated in a regime where this ratio is significantly higher (several tens up to several hundreds according to [7]), that is in a regime where the charge sensitivity is almost zero (see figure 2.3d). This leads to an enhancement of the dephasing time T_2 due to charge noise by two orders of magnitude ($T_2 = 0.4\,\mathrm{ms}$ due to charge noise for the transmon opposed to $T_2 = 1\,\mu\mathrm{s}$ due to charge noise for the Cooper pair box qubit, see Table I in [7]). While charge noise is the dominant noise channel for the Cooper pair box qubit, the coherence time of a transmon is only limited by relaxation processes according to [7].
This decrease in charge noise comes at the cost of a decreased anharmonicity, which makes it more difficult to separately address certain levels of the transmon. However, while the sensitivity to charge noise decreases exponentially with E_J/E_C, the anharmonicity decreases only algebraically as shown in [7]. Nevertheless, its low anharmonicity might be the crucial weakness of the transmon.
Looking at figure 2.3d, we see that in the transmon regime, the energy levels are independent of the charge offset n_g. Therefore, we can remove this term from the Hamiltonian using the unitary gauge transformation

$$U = e^{-in_g\hat{\varphi}}$$

as described in [13], because of

$$U(\hat{n} - n_g)U^\dagger = \hat{n}.$$

This gauge transformation changes the boundary conditions in φ and therefore the eigenenergies. However, as stated in [13], the wave function is exponentially small at the boundary

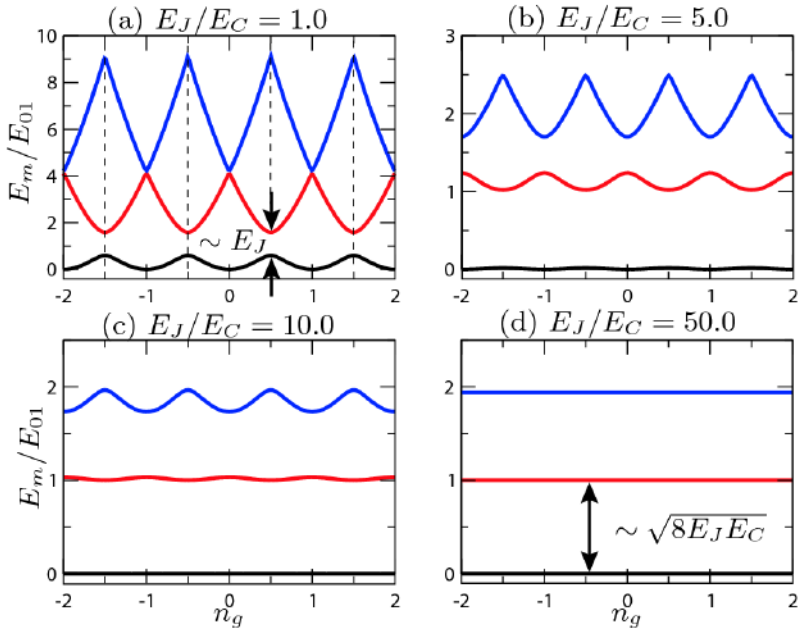

Figure 2.3.: Eigenenergies of the lowest levels of 2.10 as a function of the offset charge n_g. We see that for $E_J/E_C = 1$ (Cooper pair box regime), the levels are highly anharmonic and highly sensitive to slight changes in n_g. While E_J/E_C increases, both the anharmonicity and the charge sensitivity decrease. (Figure taken from [7], page 3.)

$\pm\varphi$ for large E_J/E_C, so this effect will be negligible in the transmon regime. Thus, we leave out the charge offset in 2.10 and expand for small φ

$$H = 4E_C\hat{n}^2 - E_J\left(1 - \frac{\hat{\varphi}^2}{2} + \frac{\hat{\varphi}^4}{24}\right).$$

This is possible for weak anharmonicity, as the transmon should be a harmonic oscillator with a small perturbation. Using $\hat{n} = \frac{i}{2}\sqrt[4]{\frac{E_J}{2E_C}}(c^\dagger - c)$ and $\hat{\varphi} = \sqrt[4]{\frac{2E_C}{E_J}}(c^\dagger + c)$, this is

$$H = \sqrt{8E_CE_J}\left(c^\dagger c + \frac{1}{2}\right) - E_J - \frac{E_C}{12}(c^\dagger + c)^4,$$

where $c = \sum_j \sqrt{j+1}|j\rangle\langle j+1|$ is the lowering operator for the transmon. Now, omitting the constant terms, we find

$$H = \omega_0 c^\dagger c + \frac{\delta}{12}(c^\dagger + c)^4$$

with $\omega_0 \equiv \sqrt{8E_CE_J}$ and $\delta \equiv -E_C$. Leaving out the fast-oscillating terms such as $c^{\dagger 4}$ in a rotating wave approximation (and the constant term), we find

$$H = \omega_0 c^\dagger c + \frac{\delta}{2}((c^\dagger c)^2 + c^\dagger c) = \left(\omega_0 + \frac{\delta}{2}\right)c^\dagger c + \frac{\delta}{2}(c^\dagger c)^2.$$

If we define $\omega \equiv \omega_0 + \delta$, we find for the transition frequencies that

$$\omega_{j+1} - \omega_j = \omega + \delta j,$$

where ω_j is the eigenvalue of H and δ the anharmonicity. Using this and $c^\dagger c = \sum_j j|j\rangle\langle j|$, we can write the transmon Hamiltonian as

$$H_{\text{transmon}} = \omega c^\dagger c + \frac{\delta}{2} c^\dagger c(c^\dagger c - 1) = \left(\omega - \frac{\delta}{2}\right) c^\dagger c + \frac{\delta}{2}(c^\dagger c)^2, \tag{2.11}$$

which is the ansatz Poletto et al. make in [14] or equally

$$H_{\text{transmon}} = \sum\nolimits_j \underbrace{\left(\left(\omega - \frac{\delta}{2}\right) j + \frac{\delta}{2} j^2\right)}_{\omega_j} |j\rangle\langle j|$$

as in [7]. The transmon Hamiltonian in equation 2.11 is a so-called Duffing oscillator, that is a harmonic oscillator plus a quartic term. If the anharmonicity was sufficiently large, the two lowest levels could be treated as a two-level qubit. We make the two-level approximation, i.e. we pretend the levels with $j \geq 2$ do not exist, and find

$$\sum_{j=0}^{1} \omega_j |j\rangle\langle j| = \omega|1\rangle\langle 1| = -\frac{\omega}{2}(|0\rangle\langle 0| - |1\rangle\langle 1|) + \frac{\omega}{2}(|0\rangle\langle 0| + |1\rangle\langle 1|) = -\frac{\omega}{2}\sigma^z + const.$$

Thus, for large anharmonicity, the transmon could be approximated as a qubit with Hamiltonian

$$H_{\text{qubit}} = -\frac{\omega_q}{2}\sigma^z. \tag{2.12}$$

However, as we will see in section 4.2, the higher levels of the transmon play a significant role in many two-qubit gates, making the two-level approximation invalid for transmons. The qubit Hamiltonian (equation 2.12) is equal to the Hamiltonian of a two-level atom (equation 2.2), while the transmon Hamiltonian $H_{\text{transmon}} = \sum_j \omega_j |j\rangle\langle j|$ is equivalent to the Hamiltonian of a multi-level atom. This is why circuit QED is very similar to cavity QED. A system of a transmon or a two-level qubit coupled to a resonator will behave very similar to a system of an atom in a cavity.

In [7], Koch et al. present the transmon as depicted in figure 2.4, consisting of two Josephson junctions in a dc-SQUID setup, which are shunted by two large capacitances C_g and C_B. These large capacitances lead to the small charging energy $E_C = e^2/2C$ with $C = C_J + C_B + C_g$ that distinguishes the transmon from the Cooper pair box qubit. The transmon is coupled to a LC oscillator acting as a read-out cavity, see figure 2.4.

In [12], Reed describes how the coupling between a transmon and a transmission line resonator works. The standing wave in the resonator (see figure 2.4b) induces a voltage difference across the two islands, leading to a dipole coupling term

$$H_{\text{coupling}} = 2e\beta V_{rms}^0 \hat{n}(a^\dagger + a) = g_{ij} \sum_{i,j} |i\rangle\langle j|(a^\dagger + a),$$

where $\beta = C_g/C$, $|i\rangle$ are the uncoupled transmon states and

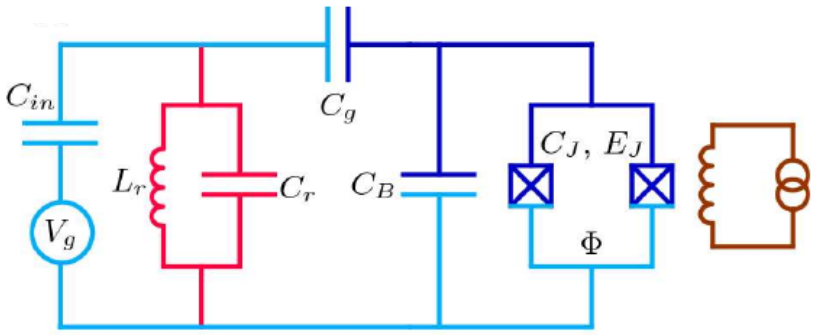

(a) Effective circuit diagram of a transmon qubit coupled to a transmission line resonator (colored in red). The superconducting island between the two Josephson junctions and the capacitances C_g and C_B is depicted in dark blue. The effective Josephson energy can be tuned via flux tuning (see section 2.2.2) using the flux bias line (colored in brown).

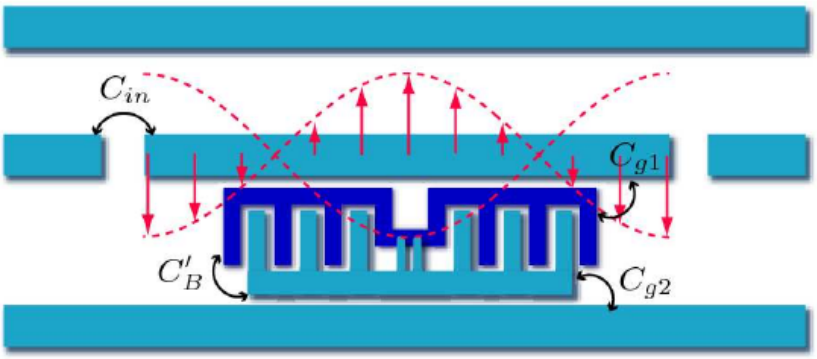

(b) Simplified schematic of the transmon-cavity system.

Figure 2.4.: Taken from [7], page 2.

$$g_{ij} = 2e\beta V^0_{rms}\langle i|\hat{n}|j\rangle = g^*_{ji}$$

are the matrix elements of the coupling energy. Using $\hat{n} = \frac{i}{2}\sqrt[4]{\frac{E_J}{2E_C}}(c^\dagger - c)$ we see that only nearest-neighbor transmon states are coupled and find

$$H_{\text{coupling}} = ig(c^\dagger - c)(a^\dagger + a)$$

with

$$g \equiv \sqrt[4]{\frac{E_J}{2E_C}}e\beta V^0_{rms}. \tag{2.13}$$

Applying the unitary transformation $U = e^{-ic^\dagger c\frac{\pi}{2}}$ leads to

$$H_{\text{coupling}} = g(c^\dagger + c)(a^\dagger + a),$$

which is the multi-level equivalent of the coupling term in equation 2.3. The rotating wave approximation leads to a generalized Jaynes-Cummings Hamiltonian

$$H = \omega_r a^\dagger a + \sum\nolimits_j \omega_j |j\rangle\langle j| + g(a^\dagger c + a c^\dagger)$$

for the coupled system of transmon and resonator. However, as opposed to equation 2.4, this Hamiltonian does not have an analytical solution like the dressed states in equations 2.5 and 2.6. Only in the dispersive limit are there analytical solutions for the effective Hamiltonian (see section 3.1.4).
Looking at equation 2.13, we see that the coupling strength increases with E_J/E_C, leading to high coupling energies for the transmon compared to the Cooper pair box. In [7] they state that the coupling strength is limited to 10% of the resonator frequency ω_r. They report typical values for the coupling strength as $g/(2\pi) \sim 20 - 100\,\mathrm{MHz}$, while the transmon transition frequencies are of around $\omega_{01}/(2\pi) \sim 10\,\mathrm{GHz}$.
Recently, according to [15], the coherence time of the transmon was improved to yield $T_1 \sim T_2 \sim 55 - 60\,\mu\mathrm{s}$, which is a significant enhancement compared to $\sim 1\,\mu\mathrm{s}$ for the Cooper pair box qubit.

2.2.2. Flux tuning

For some of the gates described in chapter 4, it is necessary to have tunable qubits. Looking at figure 2.3a, which shows the eigenenergies of the lowest levels as a function of the charge offset n_g in the Cooper pair box regime, it is clear that the transition frequency of a Cooper pair box qubit can be tuned via n_g. The qubit is usually parked at a so-called *sweet-spot* of coherence at $n_g = \frac{1}{2}$, where it is least sensitive to charge fluctuations. By changing n_g, the transition frequency of the qubit can be easily tuned. Thus, the interaction between two qubits can be turned on and off.
In the transmon regime though, tuning n_g does not lead to any changes in the transition frequencies, as we can see in figure 2.3d. However, it is possible to tune the transmon via E_J. As described in [7], a tunable transmon consists of two parallel Josephson junctions that are typically not identical. Therefore, as shown in Appendix A, the Josephson energy in equation 2.10 has to be adjusted to give

$$E_J \to E_{J\Sigma} \cos\left(\pi \frac{\Phi}{\Phi_0}\right) \sqrt{1 + d^2 \tan^2\left(\pi \frac{\Phi}{\Phi_0}\right)},$$

where $E_{J\Sigma} = E_{J1} + E_{J2}$ and $d \equiv \frac{E_{J2} - E_{J1}}{E_{J1} + E_{J2}} \approx 0.1$ is the junction asymmetry that is typically of around 10%, as it is difficult to fabricate identical junctions with current fabrication techniques. This makes it possible to tune E_J and therefore $\omega_0 = \sqrt{8 E_C E_J}$ via the flux through the SQUID and thereby tune the transmon.

2.2.3. Measurement and readout

Reading out the state of a qubit is possible via microwave radiation on the cavity. As shown in section 2.1.1, the resonance frequency of the cavity undergoes a shift where the sign depends on the state of the qubit, see figure 2.5. This can be used in order to read out the state of the qubit. In a transmission line resonator, only photons at the resonance frequency are transmitted, while the others are reflected. Thus, if we irradiate the cavity at one of the shifted frequencies $\omega_r \pm g^2/\Delta$ and measure the transmitted photons, we

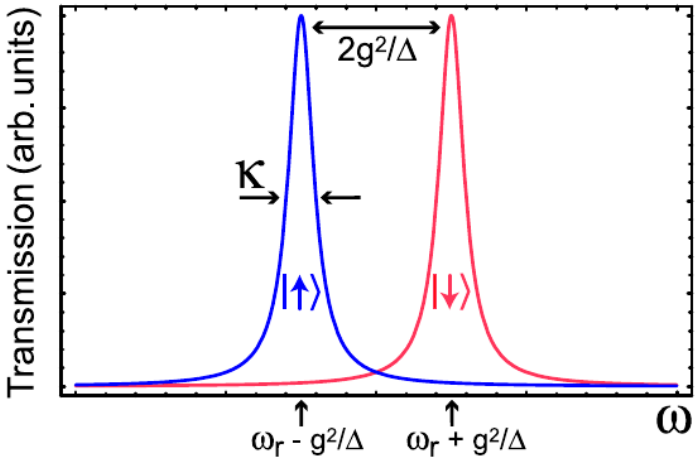

Figure 2.5.: The resonance frequency of the cavity undergoes a dispersive shift dependent on the state of the qubit. If the shift $\frac{g^2}{\Delta}$ is larger than the linewidth κ of the cavity, the two peaks are clearly separated and the state of the qubit can be measured by a microwave pulse with frequency $\omega_r \pm \frac{g^2}{\Delta}$. (Figure taken from [3], page 7.)

effectively measure the state of the qubit. However, as we can see in figure 2.5, the different states of the qubit can only be dissolved, if the cavity line width κ is smaller than the dispersive shift $\kappa < g^2/\Delta$ (compare [3]).

For the case that the cavity line width κ is too large to dissolve the two peaks, there is another possibility to read out the qubit state as described by Blais in [3]. Consider a qubit coupled to a cavity that is assumed to be empty in the beginning. The cavity is populated via a drive pulse at the bare cavity frequency ω_r

$$H^d(t) = \xi(t)(a^\dagger e^{-i\omega_r t} + a e^{i\omega_r t}),$$

where $\xi(t)$ is the pulse envelope. After turning off the drive again, the system is in a state

$$|\Psi\rangle = |\alpha\rangle(c_0|0\rangle + c_1|1\rangle) = e^{-\frac{|\alpha|^2}{2}} \sum_{n=0}^{\infty} \frac{\alpha^n}{\sqrt{n!}} |n\rangle(c_0|0\rangle + c_1|1\rangle),$$

where $|\alpha\rangle$ is a coherent state. The system is now left to evolve freely for a time t under the effect of the dispersive Hamiltonian

$$H_{\text{eff}} = (\omega_r + \chi\sigma^z)\, a^\dagger a - \frac{1}{2}(\omega_q - \chi)\, \sigma^z,$$

which will be derived in section 3.1.2 with $\chi = g^2/\Delta$. While all pure qubit terms and pure cavity terms lead to phase factors only, the $\chi\sigma^z a^\dagger a$-term entangles the qubit state with the cavity state. It is

$$
\begin{aligned}
e^{-i\chi\sigma^z a^\dagger a t}|\alpha\rangle(c_0|0\rangle + c_1|1\rangle) &= e^{-\frac{|\alpha|^2}{2}} \sum_{n=0}^{\infty} \frac{\alpha^n}{\sqrt{n!}} e^{-i\chi\sigma^z n t}|n\rangle(c_0|0\rangle + c_1|1\rangle) \\
&= c_0 e^{-\frac{|\alpha|^2}{2}} \sum_{n=0}^{\infty} \frac{\left(\alpha e^{-i\chi t}\right)^n}{\sqrt{n!}}|n\rangle|0\rangle + c_1 e^{-\frac{|\alpha|^2}{2}} \sum_{n=0}^{\infty} \frac{\left(\alpha e^{i\chi t}\right)^n}{\sqrt{n!}}|n\rangle|1\rangle \\
&= c_0|\alpha e^{-i\chi t}\rangle|0\rangle + c_1|\alpha e^{i\chi t}\rangle|1\rangle.
\end{aligned}
$$

Thus, the state of the qubit can be determined by measuring the phase of the transmitted photons by homodyne detection.

3. Deriving effective Hamiltonians

In this chapter, different methods for the derivation of effective Hamiltonians are presented and compared. As an illustration of these methods, we apply them to the Jaynes-Cummings Hamiltonian derived in section 2.1.

3.1. Schrieffer-Wolff transformation

Quasi-degenerate perturbation theory (see [8], [9]) is a method for the derivation of effective Hamiltonians in which the low-energy and high-energy subspaces are decoupled using a unitary transformation called the Schrieffer-Wolff transformation.
Let us assume that the exact Hamiltonian

$$H = H^0 + H' = H^0 + \epsilon V$$

is composed of an unperturbed part H^0 with known eigenvalues and eigenfunctions and a small perturbation $H' = \epsilon V$. We assume that the eigenfunctions of H^0 can be divided into two subsets A and B which are separated by a spectral gap Δ. These subspaces interact weakly due to H', but we assume that the perturbation is so weak that the spectral gap is never closed, i.e.

$$|\epsilon| \leq \epsilon_c = \frac{\Delta}{2||V||}$$

(see equation 3.1 in [9]). Now the Schrieffer-Wolff transformation is defined as

$$H_{\text{eff}} = e^{-S} H e^{S}, \tag{3.1}$$

where S is chosen such that the block off-diagonal elements in H_{eff} disappear up to the desired order. As Roland Winkler describes in [8], the perturbation can be decomposed into a sum $H' = H^1 + H^2$, where H^1 is purely block diagonal and H^2 purely block off-diagonal (see figure 3.1).
Now, the question is how to determine S. Using the Campbell-Baker-Hausdorff formula (see appendix B, equation B.1) we can write

$$H_{\text{eff}} = e^{-S} H e^{S} = \sum_{j=0}^{\infty} \frac{1}{j!} [H, S]^{(j)},$$

where $[H, S]^{(j)} = [[H, S]^{(j-1)}, S]$ and $[H, S]^{(0)} = H$. As S must be anti-hermitian and block off-diagonal, the block off-diagonal elements in H_{eff} are

$$H^o_{\text{eff}} = \sum_{j=0}^{\infty} \frac{1}{(2j+1)!} [H^0 + H^1, S]^{(2j+1)} + \sum_{j=0}^{\infty} \frac{1}{(2j)!} [H^2, S]^{(2j)} \stackrel{!}{=} 0. \tag{3.2}$$

We can write S as a Taylor series of successive approximations to S

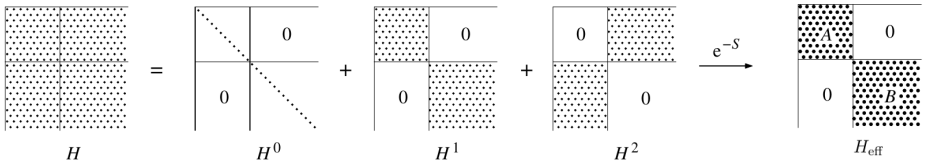

Figure 3.1.: The original Hamiltonian consists of an unperturbed diagonal part H^0 and a perturbation that can be decomposed into a block diagonal term H^1 and a block off-diagonal term H^2. The coupling between the blocks A and B is eliminated via the unitary transformation e^{-S} (Schrieffer-Wolff transformation) yielding a block diagonal effective Hamiltonian. (Figure taken from [8], appendix B, page 202.)

$$S = \sum_{j=1}^{\infty} S^{(j)},$$

where $S^{(j)}$ is of j-th order in ϵ and $S^0 = 0$. Assuming that H^1 and H^2 are of first order in ϵ, we can derive the following equations defining $S^{(j)}$

$$[H^0, S^{(1)}] = -H^2 \tag{3.3}$$
$$[H^0, S^{(2)}] = -[H^1, S^{(1)}] \tag{3.4}$$
$$[H^0, S^{(3)}] = -[H^1, S^{(2)}] - \frac{1}{3}[[H^2, S^{(1)}], S^{(1)}] \tag{3.5}$$

(see [8]), using the condition that the effective Hamiltonian should be block diagonal to each order in j (equation 3.2). According to [9] the transformation S is unique, so we just need to find an ansatz that satisfies equations 3.3-3.5. Up to second order in ϵ the effective Hamiltonian yields

$$H_{\text{eff}} = H^0 + H^1 + [H^2, S^{(1)}] + \frac{1}{2}[\underbrace{[H^0, S^{(1)}]}_{=-H^2}, S^{(1)}] = H^0 + H^1 + \frac{1}{2}[H^2, S^{(1)}]. \tag{3.6}$$

3.1.1. Schrieffer-Wolff full diagonalizing transformation

The Schrieffer-Wolff transformation as presented in section 3.1 according to Winkler ([8]) leads to an effective Hamiltonian that is block diagonal. The operator S is chosen such that all terms that couple the two blocks disappear to the desired order (equations 3.3-3.5). Thus, by choosing S, we choose the frame to which we want to transform our Hamiltonian.
In the appendix of [14], Gambetta et al. present a Schrieffer-Wolff-like full diagonalization technique, where S is chosen such that all but the diagonal elements disappear.
Starting with

$$H = H^0 + \lambda V,$$

where λ is a small parameter in the perturbation term, they define their Schrieffer-Wolff transformation as

$$H_{\text{eff}} = e^{iS} H e^{-iS} = \sum_{m=0}^{\infty} \lambda^m H^{(m)},$$

where $H^{(m)}$ are the successive approximations to H_{eff} with $H^{(0)} = H^0$. This definition is a little different from Winkler's definition (equation 3.1), but it is essentially the same transformation. For $m > 0$ they define

$$H^{(m)} = i[S^{(m)}, H^0] + H_x^{(m)}, \tag{3.7}$$

where $H_x^{(m)}$ includes all the other commutators (see equation 1.4 in the appendix of [14]). This is the definition of the Schrieffer-Wolff transformation we will use in the *mathematica* sheets for the interpretation of the bSWAP and the MAP gate (see appendices C and D). Now Gambetta et al. distinguish between two ways of choosing S, whether we want the effective Hamiltonian to be block diagonal or completely diagonal. For the full diagonalization, we want $H^{(m)}$ to be diagonal in the eigenbasis $|p\rangle$ of H^0, that is

$$\langle p|H^{(m)}|q\rangle = \delta_{pq}.$$

Taking the matrix element $\langle p|...|q\rangle$ of equation 3.7 for $p \neq q$ yields

$$\begin{aligned}\langle p|H^{(m)}|q\rangle = 0 = i\langle p|S^{(m)}\left(\sum\nolimits_r |r\rangle\langle r|\right)H^0|q\rangle - i\langle p|H^0\left(\sum\nolimits_r |r\rangle\langle r|\right)S^{(m)}|q\rangle \\ + \langle p|H_x^{(m)}|q\rangle = iE_q^{(0)}\langle p|S^{(m)}|q\rangle - iE_p^{(0)}\langle p|S^{(m)}|q\rangle + \langle p|H_x^{(m)}|q\rangle,\end{aligned}$$

where $E_p^{(m)} = \langle p|H^{(m)}|p\rangle$ are the eigenvalues of $H^{(m)}$. This defines S to be

$$\langle p|S^{(m)}|q\rangle = \frac{-i\langle p|H_x^{(m)}|q\rangle}{E_p^{(0)} - E_q^{(0)}}.$$

Using this choice of S, the Schrieffer-Wolff transformation can be used as a perturbative diagonalization technique.

3.1.2. Jaynes-Cummings Hamiltonian

As an illustration of the Schrieffer-Wolff method, we will derive an effective Hamiltonian for a system of a qubit coupled to a cavity as derived in chapter 2. We start with the Jaynes-Cummings Hamiltonian

$$H = \underbrace{\omega_r a^\dagger a - \frac{\omega_q}{2}\sigma^z}_{H^0} + \underbrace{g(a^\dagger\sigma^- + a\sigma^+)}_{H'}. \tag{3.8}$$

The eigenfunctions $\{|\Psi_n\rangle\}$ of H can be divided into two weakly interacting subsets A and B, where A $\widehat{=}$ qubit in state 0 and B $\widehat{=}$ qubit in state 1. (We could also choose our blocks to be A $\widehat{=}$ even number of photons in the cavity and B $\widehat{=}$ odd number of photons. For the calculation in this section, this does not make a difference.)

Two interacting states $|\Psi_m\rangle = |0, n+1\rangle$ and $|\Psi_l\rangle = |1, n\rangle$ from blocks A and B will always be separated by an energy gap Δ, because of

$$E_m - E_l = \omega_r(n+1) - \frac{\omega_q}{2} - \left(\omega_r n + \frac{\omega_q}{2}\right) = \omega_r - \omega_q \equiv \Delta. \tag{3.9}$$

In the so-called dispersive regime (compare section 2.1.1), where g is much smaller than the detuning $\Delta = \omega_r - \omega_q$ between qubit and cavity, H' can be treated as a perturbation. In our case, there is no interaction within the sets A and B and H' takes the form

$$H' = H^1 + H^2 = \begin{pmatrix} \blacksquare & \\ & \blacksquare \end{pmatrix} = H^2,$$

as the block-diagonal part H^1 is zero. To find $S^{(1)}$ we make the ansatz

$$S^{(1)} = \alpha a^\dagger \sigma^- - \alpha^* a \sigma^+,$$

as we assume that S will include similar terms as H^2 and we know that S has to be anti-hermitian. Solving equation 3.3 with this ansatz yields

$$S^{(1)} = -\frac{g}{\Delta}(a^\dagger \sigma^- - a\sigma^+). \tag{3.10}$$

The first correction to H^0 is

$$\begin{aligned}
\frac{1}{2}[H^2, S^{(1)}] &= -\frac{g^2}{2\Delta}[a^\dagger\sigma^- + a\sigma^+, a^\dagger\sigma^- - a\sigma^+] \\
&= \frac{g^2}{2\Delta}(a^\dagger a\sigma^-\sigma^+ - aa^\dagger\sigma^+\sigma^- - aa^\dagger\sigma^+\sigma^- + a^\dagger a\sigma^-\sigma^+) = \frac{g^2}{2\Delta}(2a^\dagger a[\sigma^-, \sigma^+] - 2\sigma^+\sigma^-) \\
&= \frac{g^2}{2\Delta}(2a^\dagger a \underbrace{(|0\rangle\langle 0| - |1\rangle\langle 1|)}_{=\sigma^z} - 2\underbrace{|1\rangle\langle 1|}_{=\frac{I-\sigma^z}{2}}) = \frac{g^2}{2\Delta}(2a^\dagger a + 1)\sigma^z - \underbrace{\frac{g^2}{\Delta}I}_{=const.},
\end{aligned}$$

where the constant will be neglected. Thus, the effective Hamiltonian to second order in g is

$$H_{\text{eff}} = H^0 + \frac{1}{2}[H^2, S^{(1)}] = \left(\omega_r + \frac{g^2}{\Delta}\sigma^z\right) a^\dagger a - \frac{1}{2}\left(\omega_q - \frac{g^2}{\Delta}\right)\sigma^z. \tag{3.11}$$

Comparing this to equation 3.8, we note that H_{eff} is of the same form as the original H^0, but with frequencies shifted by $\chi \equiv \frac{g^2}{\Delta}$. The shift in the cavity frequency is called AC-Stark-shift, while the shift in the qubit frequency is a Lamb shift.
In order to see what happens in higher order, we have to determine $S^{(3)}$ (as the perturbation is purely block off-diagonal, $S^{(2)} = 0$ due to equation 3.4). $S^{(3)}$ has to satisfy

$$[H^0, S^{(3)}] = -\frac{1}{3}\left[[H^2, S^{(1)}], S^{(1)}\right] = \frac{4g^3}{3\Delta^2} a^\dagger a(a^\dagger\sigma^- + a\sigma^+).$$

Guessing the ansatz

$$S^{(3)} = \alpha a^\dagger a(a^\dagger\sigma^- - a\sigma^+),$$

where the constant has to be real for $S^{(3)}$ to be anti-hermitian, we find

$$S^{(3)} = \frac{4g^3}{3\Delta^3} a^\dagger a (a^\dagger \sigma^- - a\sigma^+).$$

The next corrections will be of fourth order in g (the third order corrections disappear if $H^1 = 0$). We find

$$\begin{aligned} H_{\text{eff}} = H^0 + \frac{1}{2}[[H^0, S^{(1)} + S^{(3)}], S^{(1)} + S^{(3)}] + \frac{1}{24}[[[[H^0, S^{(1)}], S^{(1)}], S^{(1)}], S^{(1)}] \\ + [H^2, S^{(1)} + S^{(3)}] + \frac{1}{6}[[[H^2, S^{(1)}], S^{(1)}], S^{(1)}] \\ = H^0 + \frac{1}{2}[H^2, S^{(1)}] + \frac{1}{2}[H^2, S^{(3)}] + \frac{1}{8}\left[[H^0, S^{(3)}], S^{(1)}\right], \end{aligned}$$

where equations 3.3 and 3.5 were used. The two new commutators turn out to be the same, i.e.

$$\left[[H^0, S^{(3)}], S^{(1)}\right] = \frac{4g^4}{3\Delta^3}\left(a^\dagger a(2a^\dagger a + 1)\sigma^z - 2a^\dagger a + \frac{1}{2}\sigma^z\right) = [H^2, S^{(3)}].$$

The effective Hamiltonian up to fourth order in g is

$$\begin{aligned} H_{\text{eff}} = H^0 + \frac{1}{2}[H^2, S^{(1)}] + \frac{5}{8}[H^2, S^{(3)}] = \left(\omega_r - \frac{5g^4}{3\Delta^3} + \left(\frac{g^2}{\Delta} + \frac{5g^4}{6\Delta^3}\right)\sigma^z\right) a^\dagger a \\ + \frac{5g^4}{3\Delta^3}\sigma^z (a^\dagger a)^2 - \frac{1}{2}\left(\omega_q - \left(\frac{g^2}{\Delta} + \frac{5g^4}{6\Delta^3}\right)\right)\sigma^z. \end{aligned}$$

We see that apart from further corrections to the second order terms, there appears a shift on the cavity frequency, which is independent of the qubit's state and an anharmonic quartic cavity term. This cavity anharmonicity is known as the nonlinear Kerr effect, which describes a change in the refractive index of a material proportional to the square of the applied electric field.

3.1.3. Bloch-Siegert shift

The Bloch-Siegert shift is an energy shift that appears due to the counter-rotating terms, which the Jaynes-Cummings model neglects (see section 2.1). In order to see where this shift comes from, we start with

$$H = \underbrace{\omega_r a^\dagger a - \frac{\omega_q}{2}\sigma^z}_{H^0} + \underbrace{g(a^\dagger \sigma^+ + a^\dagger \sigma^- + a\sigma^+ + a\sigma^-)}_{H' = H^2}$$

and make the following ansatz for $S^{(1)}$

$$S^{(1)} = \alpha_1 a^\dagger \sigma^+ + \alpha_2 a^\dagger \sigma^- - \alpha_2^* a\sigma^+ - \alpha_1^* a\sigma^-,$$

as $S^{(1)}$ has to be anti-hermitian. By solving

$$[H^0, S^{(1)}] = -H^2,$$

we find $S^{(1)}$ to be

$$S^{(1)} = -\frac{g}{\omega_\Sigma}(a^\dagger\sigma^+ - a\sigma^-) - \frac{g}{\Delta}(a^\dagger\sigma^- - a\sigma^+)$$

with $\omega_\Sigma = \omega_r + \omega_q$, so we just add some extra terms to $S^{(1)}$ for the counter-rotating terms. The effective Hamiltonian yields to be

$$H_{\text{eff}} = H^0 + \frac{1}{2}[H^2, S^{(1)}] = H^0 + \left(\frac{g^2}{2\Delta} - \frac{g^2}{2\omega_\Sigma}\right)(2a^\dagger a + 1 + a^{\dagger 2} + a^2)\sigma^z. \tag{3.12}$$

Comparing this to 3.6, we see an additional shift proportional to $g^2/(2\omega_\Sigma)$, which is called Bloch-Siegert shift. In addition to this shift, we see two-photon terms that are not there in equation 3.11.

3.1.4. Full transmon

In analogy to section 3.1.2, we derive an effective Hamiltonian for the full transmon Hamiltonian (see section 2.2.1)

$$H = \underbrace{\omega_r a^\dagger a + \sum\nolimits_j \omega_j |j\rangle\langle j|}_{=H^0} + \underbrace{g(a^\dagger c + a c^\dagger)}_{=H'=H^2} \tag{3.13}$$

using the Schrieffer-Wolff transformation. We divide the eigenstates again into two weakly interacting subsets A and B, where A will include the even transmon level (or photon number) states and B the odd ones. In both cases, we can treat $H' = H^2$ as a block off-diagonal perturbation for small g.
Supposing that $S^{(1)}$ will be similar to equation 3.10, we make the ansatz

$$S^{(1)} = \alpha a^\dagger c - \alpha^* a c^\dagger \tag{3.14}$$

with $c = \sum_j \sqrt{j+1}|j\rangle\langle j+1|$ as defined above. Substituting this into

$$[H^0, S^{(1)}] = -H^2$$

yields

$$S^{(1)} = -g\sum\nolimits_j \frac{\sqrt{j+1}}{\omega_r - \omega - \delta j}(a^\dagger|j\rangle\langle j+1| - a|j+1\rangle\langle j|) = -g(a^\dagger\tilde{c} - a\tilde{c}^\dagger),$$

where $\tilde{c} = \sum_j \frac{\sqrt{j+1}}{\omega_r - \omega - \delta j}|j\rangle\langle j+1|$ is a changed annihilation operator that includes the energy difference between the coupled levels $|n+1, j\rangle$ and $|n, j+1\rangle$. We see that it is due to the anharmonicity that this energy difference depends on the transmon level number and we have to use $\tilde{c}$. Having found a representation for $S^{(1)}$, we can calculate the transformed Hamiltonian up to second order in g. The first correction yields

$$\frac{1}{2}[H^2, S^{(1)}] = \frac{g^2 a^2}{2} \sum_j \left(\frac{\sqrt{j+2}\sqrt{j+1}}{\omega_r - \omega - \delta j} - \frac{\sqrt{j+2}\sqrt{j+1}}{\omega_r - \omega - \delta(j+1)} \right) |j+2\rangle\langle j|$$
$$+ \frac{g^2 a^{\dagger 2}}{2} \sum_j \left(\frac{\sqrt{j+2}\sqrt{j+1}}{\omega_r - \omega - \delta j} - \frac{\sqrt{j+2}\sqrt{j+1}}{\omega_r - \omega - \delta(j+1)} \right) |j\rangle\langle j+2|$$
$$+ g^2 a^\dagger a \sum_j \frac{j+1}{\omega_r - \omega - \delta j} |j\rangle\langle j| - g^2 \underbrace{aa^\dagger}_{=a^\dagger a+1} \sum_j \frac{j+1}{\omega_r - \omega - \delta j} |j+1\rangle\langle j+1|.$$

Dropping the two-photon terms (for low anharmonicity, the prefactor in the brackets should tend to zero), leaves us with

$$\frac{1}{2}[H^2, S^{(1)}] = g^2 a^\dagger a \sum_j \left(\frac{j+1}{\omega_r - \omega - \delta j} - \frac{j}{\omega_r - \omega - \delta(j-1)} \right) |j\rangle\langle j|$$
$$- g^2 \sum_j \frac{j}{\omega_r - \omega - \delta(j-1)} |j\rangle\langle j| = g^2 \sum_j \left(a^\dagger a(\mu_{j+1} - \mu_j) - \mu_j \right) |j\rangle\langle j|,$$

where $\mu_j = \frac{j}{\omega_r - \omega - \delta(j-1)}$. Thus, the transformed Hamiltonian for the full transmon is

$$H_{\text{eff}} = H^0 + \frac{1}{2}[H^2, S^{(1)}] = \left(\omega_r + \sum_j g^2(\mu_{j+1} - \mu_j)|j\rangle\langle j| \right) a^\dagger a + \sum_j \left(\omega_j - g^2 \mu_j \right) |j\rangle\langle j|$$
$$= \left(\omega_r + \sum_j \chi_j |j\rangle\langle j| \right) a^\dagger a + \sum_j \tilde{\omega}_j |j\rangle\langle j| \quad (3.15)$$

with

$$\chi_j \equiv g^2(\mu_{j+1} - \mu_j) = \frac{g^2(\omega_r - \omega + \delta)}{(\omega_r - \omega - \delta j)(\omega_r - \omega - \delta(j-1))} \quad (3.16)$$

and

$$\tilde{\omega}_j \equiv \omega_j - g^2 \mu_j = j\omega + \frac{\delta}{2}(j-1)j + \frac{j g^2}{\omega - \omega_r + (j-1)\delta}, \quad (3.17)$$

which is equal to Gambetta's result in [16] (equation 42). Just as in the two-level case (equation 3.11), we see both the Stark-shift on the cavity frequency that depends on the state of the transmon and the Lamb shift on the transmon's frequency.

3.2. Adiabatic Elimination

Alongside Schrieffer-Wolff, there are various methods for the derivation of effective Hamiltonians, as for example adiabatic elimination as presented in [17].
In many physical problems the possible states of a system can be divided into relevant and irrelevant states. This is the case whenever these two blocks are only weakly coupled to each other. Thus, we are interested in an effective Hamiltonian for the relevant states only, which may however couple to each other via virtual intermediate states from the

irrelevant block. In [17], they start with an interaction picture Hamiltonian that can be written as

$$H_I = \begin{pmatrix} \boldsymbol{\omega} & \frac{1}{2}\boldsymbol{\Omega} \\ \frac{1}{2}\boldsymbol{\Omega}^\dagger & \boldsymbol{\Delta} \end{pmatrix},$$

where the submatrices stand for the relevant states $\boldsymbol{\omega}$, the irrelevant states $\boldsymbol{\Delta}$ and the coupling $\boldsymbol{\Omega}$ between these two blocks. They assume that in this interaction picture, the Hamiltonian is time-independent and that the frequencies involved in $\boldsymbol{\Delta}$ are much larger than any frequencies involved in $\boldsymbol{\omega}$ and $\boldsymbol{\Omega}$. We can split the Schrödinger equation in two, writing

$$i\dot{\Psi}(t) = \boldsymbol{\omega}\Psi(t) + \frac{1}{2}\boldsymbol{\Omega}\epsilon(t) \tag{3.18}$$

$$i\dot{\epsilon}(t) = \frac{1}{2}\boldsymbol{\Omega}^\dagger\Psi(t) + \boldsymbol{\Delta}\epsilon(t), \tag{3.19}$$

where $\Psi(t)$ denotes the relevant states and $\epsilon(t)$ the irrelevant states which will be eliminated. Equation 3.19 can be rewritten as

$$\epsilon(t) = -\frac{i}{2}\int_0^t dt' e^{-i\boldsymbol{\Delta}(t'-t)}\boldsymbol{\Omega}^\dagger\Psi(t'),$$

where we assumed $\epsilon(0) = 0$. According to zeroth-order Markov approximation, we can set $\Psi(t') \approx \Psi(t)$ in the integral which then gives

$$\epsilon(t) = -\frac{i}{2}\left(\frac{1 - e^{-i\boldsymbol{\Delta}t}}{i\boldsymbol{\Delta}}\right)\boldsymbol{\Omega}^\dagger\Psi(t) \approx -\frac{1}{2\boldsymbol{\Delta}}\boldsymbol{\Omega}^\dagger\Psi(t),$$

where the fast-oscillating term $e^{-i\boldsymbol{\Delta}t}$ was left out. A short-cut for this Markov-approximation procedure would be to set $\dot{\epsilon}(t) = 0$ in equation 3.19.
Inserting this into equation 3.18 gives

$$H_{\text{eff}} = \boldsymbol{\omega} - \boldsymbol{\Omega}\frac{1}{4\boldsymbol{\Delta}}\boldsymbol{\Omega}^\dagger, \tag{3.20}$$

which is an effective Hamiltonian for the relevant states only.

3.2.1. Jaynes-Cummings via adiabatic elimination

In comparison to section 3.1.2, we try to derive an effective Hamiltonian for a system of a qubit coupled to a resonator. We start with

$$H = \omega_r a^\dagger a - \frac{\omega_q}{2}\sigma^z + g(a^\dagger\sigma^- + a\sigma^+)$$

and for simplicity go to a rotating frame at frequency ω_r for both the resonator and the qubit, i.e. we use the transformation

$$U = e^{i\omega_r(a^\dagger a - \frac{1}{2}\sigma^z)}. \tag{3.21}$$

In this frame, the resonator terms disappear and we are left with

$$H = \frac{\Delta}{2}\sigma^z + g(a^\dagger\sigma^- + a\sigma^+),$$

where $\Delta = \omega_r - \omega_q$. We aim to decouple the excited state from the ground state, as we can assume that the weak coupling between them will only lead to an energy shift. This division of the states corresponds to the blocks A and B that we want to decouple in Schrieffer-Wolff.
A requirement for adiabatic elimination is that both $\boldsymbol{\omega}$ and $\boldsymbol{\Omega}$ contain only frequencies that are small compared to the frequency of the excited state which we wish to eliminate. We can achieve this by a simple energy shift and write

$$H - \frac{\Delta}{2}I = \begin{pmatrix} 0 & ga^\dagger \\ ga & -\Delta \end{pmatrix} \equiv \begin{pmatrix} \boldsymbol{\omega} & \frac{1}{2}\boldsymbol{\Omega} \\ \frac{1}{2}\boldsymbol{\Omega}^\dagger & \boldsymbol{\Delta} \end{pmatrix}.$$

Using the formula derived above (equation 3.20), the effective Hamiltonian for the ground state only yields

$$H_{\text{eff}} = \boldsymbol{\omega} - \boldsymbol{\Omega}\frac{1}{4\boldsymbol{\Delta}}\boldsymbol{\Omega}^\dagger = \frac{g^2}{\Delta}a^\dagger a,$$

which is (except for a constant) the correction term we also get via Schrieffer-Wolff. However, this might not be the perfect example for the illustration of adiabatic elimination. We will get more insight from cases with more than one relevant state, as for example a Raman process.

3.2.2. Raman process in comparison to Schrieffer-Wolff

As a further illustration of adiabatic elimination, we consider a three level Raman process with Hamiltonian

$$H = \sum_{i=0}^{2}\omega_i|i\rangle\langle i| + \frac{1}{2}\sum_{i=0}^{1}\Omega_i\left(|i\rangle\langle i+1|e^{i\omega_{L_i}t} + h.c.\right),$$

where the ground state $|g\rangle \equiv |0\rangle$ is weakly coupled to the target state $|t\rangle \equiv |2\rangle$ via a far-detuned excited state $|e\rangle \equiv |1\rangle$, see figure 3.2. The system is driven by two detuned lasers.
We suppose here that $\omega_g, \omega_t < \omega_e$ and $\omega_g = \omega_0 = 0$. The laser drives are detuned by $\Delta_0 = \omega_e - \omega_{L_0}$ and $\Delta_1 = (\omega_e - \omega_t) - \omega_{L_1}$. Using

$$H_0 = \omega_0|0\rangle\langle 0| + \sum_{i=1}^{2}\left(\omega_0 + \sum_{k=0}^{i-1}\omega_{L_k}\right)|i\rangle\langle i|$$

we can move this to a time-independent interaction picture via

$$H_I = e^{iH_0t}(H - H_0)e^{-iH_0t}$$

and shift everything by $-\frac{1}{2}\delta = \frac{\Delta_0 - \Delta_1}{2}$ giving

$$H_I = \begin{pmatrix} -\frac{1}{2}\delta & 0 & \frac{1}{2}\Omega_0 \\ 0 & \frac{1}{2}\delta & \frac{1}{2}\Omega_1 \\ \frac{1}{2}\Omega_0 & \frac{1}{2}\Omega_1 & \Delta \end{pmatrix} \equiv \begin{pmatrix} \boldsymbol{\omega} & \frac{1}{2}\boldsymbol{\Omega} \\ \frac{1}{2}\boldsymbol{\Omega}^\dagger & \boldsymbol{\Delta} \end{pmatrix} \tag{3.22}$$

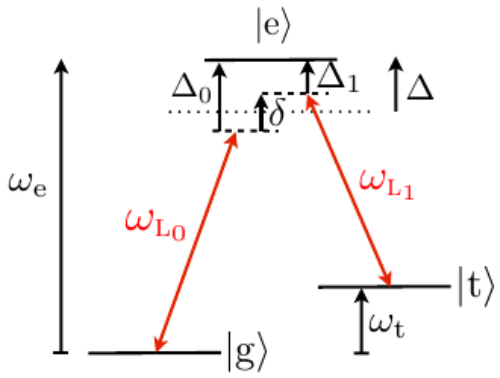

Figure 3.2.: In this Raman process, the ground state $|g\rangle$ and the target state $|t\rangle$ are far off-resonantly coupled via the excited state $|e\rangle$. The transitions are driven by two detuned lasers with frequencies ω_{L_0} and ω_{L_1}. (Figure taken from [17], page 3.)

in the $\{|g\rangle, |t\rangle, |e\rangle\}$-basis, where $\Delta = \frac{1}{2}(\Delta_0 + \Delta_1)$ is the average detuning from the intermediate state. We assume here, that both ω and $\mathbf{\Omega}$ are much smaller than $\mathbf{\Delta}$. Then we can apply adiabatic elimination and use the formula by Paulisch et al. (equation 11 in [17]), which gives

$$H_{\text{eff}} = \boldsymbol{\omega} - \mathbf{\Omega}\frac{1}{4\mathbf{\Delta}}\mathbf{\Omega}^\dagger = \begin{pmatrix} -\frac{1}{2}\left(\delta + \frac{|\Omega_0|^2}{2\Delta}\right) & -\frac{\Omega_0\Omega_1}{4\Delta} \\ -\frac{\Omega_1\Omega_0}{4\Delta} & \frac{1}{2}\left(\delta - \frac{|\Omega_1|^2}{2\Delta}\right) \end{pmatrix}. \tag{3.23}$$

In order to compare the two presented methods, we derive an effective Hamiltonian for this Raman process with a Schrieffer-Wolff transformation. Starting again with the Hamiltonian in the interaction picture (equation 3.22), we define

$$H^0 = \frac{1}{2}\delta(|2\rangle\langle 2| - |0\rangle\langle 0|) + \Delta|1\rangle\langle 1|$$

as the unperturbed Hamiltonian and

$$H^2 = \frac{\Omega_0}{2}(|0\rangle\langle 1| + |1\rangle\langle 0|) + \frac{\Omega_1}{2}(|1\rangle\langle 2| + |2\rangle\langle 1|)$$

as the block off-diagonal perturbation, where we assume that Ω_0 and Ω_1 are much smaller than the gap between the blocks A $\widehat{=}\ \{|g\rangle, |t\rangle\}$ and B $\widehat{=}\ \{|e\rangle\}$. We make the ansatz

$$S^{(1)} = c_1|0\rangle\langle 1| - c_1^*|1\rangle\langle 0| + c_2|1\rangle\langle 2| - c_2^*|2\rangle\langle 1|.$$

By solving

$$[H^0, S^{(1)}] = -H^2,$$

we find

$$S^{(1)} = \frac{\Omega_0}{\delta + 2\Delta}(|0\rangle\langle 1| - |1\rangle\langle 0|) + \frac{\Omega_1}{\delta - 2\Delta}(|1\rangle\langle 2| - |2\rangle\langle 1|).$$

The effective Hamiltonian in the $\{|g\rangle, |t\rangle, |e\rangle\}$-basis yields

$$H_{\text{eff}} = H^0 + \frac{1}{2}[H^2, S^{(1)}]$$
$$= \begin{pmatrix} -\frac{1}{2}\left(\delta + \frac{|\Omega_0|^2}{\delta+2\Delta}\right) & \frac{\Omega_0\Omega_1}{4(\delta-2\Delta)} - \frac{\Omega_0\Omega_1}{4(\delta+2\Delta)} & 0 \\ \frac{\Omega_1\Omega_0}{4(\delta-2\Delta)} - \frac{\Omega_1\Omega_0}{4(\delta+2\Delta)} & \frac{1}{2}\left(\delta + \frac{|\Omega_1|^2}{\delta-2\Delta}\right) & 0 \\ 0 & 0 & \Delta + \frac{|\Omega_0|^2}{\delta+2\Delta} - \frac{|\Omega_1|^2}{\delta-2\Delta} \end{pmatrix}.$$

For $\delta \ll 2\Delta$ we can do a Taylor expansion in $\frac{\delta}{2\Delta}$ giving

$$\frac{\Omega^2}{\delta \pm 2\Delta} = \pm\frac{\Omega^2}{2\Delta}\sum_{k=0}^{\infty}\left(\mp\frac{\delta}{2\Delta}\right)^k,$$

which to zeroth order gives the same result as in 3.23. This is exactly the condition in which adiabatic elimination can be applied. For Schrieffer-Wolff, it is only important, that the gap between the blocks is large compared to $\mathbf{\Omega}$, so $\delta \gg \Delta$ would be allowed, too. In addition, Schrieffer-Wolff gives an effective Hamiltonian for the excited state, which is completely eliminated in adiabatic elimination. In total, the Schrieffer-Wolff result is more general and complete than the one obtained via adiabatic elimination. However, the most usual case for a Raman process would be $\delta = 0$, which would mean that the detuning from the excited state is the same for both drives. In this case, adiabatic elimination and Schrieffer-Wolff give the same result (to this order).

3.3. Time-averaging

In [18], James and Jerke propose another possible method for the derivation of effective Hamiltonians. Using a time-averaging method, where fast-oscillating terms are left out in an interaction picture Hamiltonian, they derive an easy formula for second order effective Hamiltonians. This method can be used both for explicitly time-dependent Hamiltonians and for Hamiltonians that acquire a time-dependence in an interaction picture.
In the interaction picture, the time evolution operator obeys the relation

$$i\frac{d}{dt}U(t) = H_I(t)U(t). \tag{3.24}$$

We want to find an effective Hamiltonian for the time-averaged evolution operator, i.e.

$$i\frac{d}{dt}\overline{U(t)} = H_{\text{eff}}(t)\overline{U(t)}, \tag{3.25}$$

where the overline stands for the time-averaging. If we apply this time-averaging to equation 3.24 and compare it to equation 3.25, we find for the effective Hamiltonian

$$H_{\text{eff}}(t) = \left(\overline{H_I(t)U(t)}\right)\left(\overline{U(t)}\right)^{-1}, \tag{3.26}$$

where $U(t)$ can be expanded via Magnus expansion to give

$$U(t) = \mathcal{T}e^{-i\int_0^t H_I(t't)dt'} = e^{-it(H^{(0)}+H^{(1)}+H^{(2)}+\ldots)}.$$

The lowest terms of the expansions are

$$H^{(0)} = \frac{1}{t}\int_0^t H_I(t')dt'$$
$$H^{(1)} = -\frac{i}{2t}\int_0^t dt' \int_0^{t'} dt''[H_I(t'), H_I(t'')].$$

Now, if we write the exponential function in $U(t)$ as an expansion in a small parameter ϵ, this gives

$$U(t) = \mathbf{1} - it\epsilon H^{(0)} + (-it\epsilon)^2 H^{(1)} + ...,$$

we can do a Taylor expansion for equation 3.26 giving

$$H_{\text{eff}}(t) = \overline{H_I(t)} + (\overline{H_I(t)U_1(t)} - \overline{H_I(t)}\ \overline{U_1(t)}) + 2(\overline{H_I(t)U_2(t)} - \overline{H_I(t)}\ \overline{U_2(t)} - \overline{H_I(t)U_1(t)}\ \overline{U_1(t)} + \overline{H_I(t)}\ \overline{U_1(t)}\ \overline{U_1(t)}) + ...$$

with $U_j = (-it)^j H^{(j-1)}$. As this effective Hamiltonian is in general not hermitian, we have to make it hermitian by adding the complex conjugate and dividing by two. This gives

$$H_{\text{eff}}(t) = \overline{H_I(t)} + \frac{1}{2}(\overline{[H_I(t), U_1(t)]} - [\overline{H_I(t)}, \overline{U_1(t)}]) + (\overline{[H_I(t), U_2(t)]} - [\overline{H_I(t)}, \overline{U_2(t)}] - \overline{H_I(t)U_1(t)}\ \overline{U_1(t)} - \overline{U_1(t)}\ \overline{H_I(t)U_1(t)} + \overline{H_I(t)}\ \overline{U_1(t)}\ \overline{U_1(t)}) + \overline{U_1(t)}\ \overline{U_1(t)})\ \overline{H_I(t)} + ... \tag{3.27}$$

The formula, which James and Jerke provide, only includes the first two of these commutators. For an interaction Hamiltonian with a harmonic time dependence such as

$$H_I(t) = \sum_{n=1}^{N} h_n e^{-i\omega_n t} + h_n^\dagger e^{i\omega_n t},$$

where the frequency range is much smaller than the frequencies themselves, we find

$$H_{\text{eff}} = \sum_{m,n=1}^{N} \frac{1}{\bar{\omega}_{mn}}[h_m^\dagger, h_n]e^{i(\omega_m - \omega_n)t} \tag{3.28}$$

with $\frac{2}{\bar{\omega}_{mn}} \equiv \frac{1}{\omega_m} + \frac{1}{\omega_n}$ and assuming that

$$\overline{e^{\pm i\omega_n t}} = 0$$
$$\overline{e^{\pm i(\omega_n + \omega_m)t}} = 0$$
$$\overline{e^{\pm i(\omega_n - \omega_m)t}} = e^{\pm i(\omega_n - \omega_m)t}$$

While 3.28 seems to be an easy formula, going one order further is already much more

complicated (just looking at equation 3.27). In fact, it is not so easy to calculate $U_2(t)$ for a simple interaction Hamiltonian, let alone all the commutators including $U_2(t)$.
So while the James and Jerke formula is quite easy for one very special case (see section 3.3.1), it is not as easy to generalize as the Schrieffer-Wolff method.

3.3.1. Jaynes-Cummings via time-averaging

As an illustration of the time-averaging method presented above, we use their formula to derive an effective Hamiltonian for the Jaynes-Cummings Hamiltonian

$$H = \underbrace{\omega_r a^\dagger a - \frac{\omega_q}{2}\sigma^z}_{H^0} + \underbrace{g(a^\dagger\sigma^- + a\sigma^+)}_{H'},$$

which we split into an unperturbed part H^0 and a perturbation H'. We can move this Hamiltonian to an interaction picture where H^0 disappears using the unitary transformation

$$U(t) = e^{iH^0 t}$$

and find

$$H_I = UHU^\dagger + i\dot{U}U^\dagger = g(a^\dagger\sigma^- e^{it\Delta} + a\sigma^+ e^{-it\Delta}) \equiv h_1^\dagger e^{it\omega_1} + h_1 e^{-it\omega_1},$$

where $\omega_1 \equiv \Delta = \omega_r - \omega_q$ and $h_1 \equiv ga\sigma^+$. Now, using the time-averaging formula by James and Jerke (see [18]), the effective Hamiltonian yields

$$H_{\text{eff}} = \frac{1}{\omega_1}[h_1^\dagger, h_1]e^0 = \frac{g^2}{\Delta}[a^\dagger\sigma^-, a\sigma^+] = \frac{g^2}{2\Delta}(2a^\dagger a + 1)\sigma^z,$$

which is the same correction we get with the Schrieffer-Wolff method.
Now, we take a step back and do the same time-averaging procedure before doing the rotating wave approximation, i.e. we include the counter-rotating terms and start with

$$H = \underbrace{\omega_r a^\dagger a - \frac{\omega_q}{2}\sigma^z}_{H^0} + \underbrace{g(a^\dagger\sigma^+ + a^\dagger\sigma^- + a\sigma^+ + a\sigma^-)}_{H'_S},$$

H' transforms according to

$$\begin{aligned} H_I = g(a^\dagger\sigma^- e^{it\Delta} + a\sigma^+ e^{-it\Delta} + a^\dagger\sigma^+ e^{it\omega_\Sigma} + a\sigma^- e^{-it\omega_\Sigma}) \\ \equiv h_1^\dagger e^{it\omega_1} + h_1 e^{-it\omega_1} + h_2^\dagger e^{it\omega_2} + h_2 e^{-it\omega_2}, \end{aligned}$$

where $\omega_1 \equiv \Delta = \omega_r - \omega_q$, $\omega_2 \equiv \omega_\Sigma = \omega_r + \omega_q$, $h_1 \equiv ga\sigma^+$ and $h_2 \equiv ga\sigma^-$.

The effective Hamiltonian according to James and Jerke is

$$H_{\text{eff}} = \sum_{m,n=1}^{N} \frac{1}{\bar{\omega}_{mn}} [h_m^\dagger, h_n] e^{i(\omega_m - \omega_n)t} = \frac{1}{\omega_1}[h_1^\dagger, h_1]e^0 + \frac{1}{\omega_2}[h_2^\dagger, h_2]e^0$$
$$= \frac{g^2}{\Delta}[a^\dagger\sigma^-, a\sigma^+] + \frac{g^2}{\omega_\Sigma}[a^\dagger\sigma^+, a\sigma^-] = \frac{g^2}{2\Delta}\left(1 - \frac{\Delta}{\omega_\Sigma}\right)(2a^\dagger a + 1)\sigma^z.$$

Just as with Schrieffer-Wolff, the Bloch-Siegert shift appears when we include the counter-rotating terms. However, in contrast to 3.12, we do not see any two-photon terms here as terms with $e^{\pm i(\omega_n + \omega_m)t}$ disappear in the time-averaging.
This time-averaging procedure is only justified if the frequency range is much smaller than the frequencies themselves, i.e. $\omega_\Sigma - \Delta \ll \Delta \Leftrightarrow 3\omega_q \ll \omega_r$.

3.4. Ordinary perturbation theory

Another standard method for the derivation of effective Hamiltonians is ordinary time-independent perturbation theory. Let us consider a Hamiltonian

$$H = H^0 + \lambda V,$$

where H^0 is an unperturbed Hamiltonian with known eigenfunctions and V is a small perturbation. We assume that the eigenenergies of H can be written as successive approximations to the eigenenergies of H^0 in terms of the ordering parameter λ

$$E_j = E_j^{(0)} + \lambda\langle j^{(0)}|V|j^{(0)}\rangle + \lambda^2 \sum_{k\neq j} \frac{|\langle k^{(0)}|V|j^{(0)}\rangle|^2}{E_j^{(0)} - E_k^{(0)}} + ...$$

For the Jaynes-Cummings problem this gives

$$E_{|n,0/1\rangle} = \left(\omega_r \pm \frac{g^2}{\omega_r - \omega_q}\right) n \mp \frac{\omega_q}{2}$$

to second order in g. Comparing this to the result obtained via Schrieffer-Wolff (equation 3.11), we see that while we can derive the Stark-shift with this method, we can not see the Lamb shift on the qubit frequency here. Furthermore, this method only serves to find the eigenenergies, but not an effective Hamiltonian.
In conclusion, among the methods for the derivation of effective Hamiltonians compared here, the Schrieffer-Wolff transformation seems to be the method that gives the best results with least effort for time-independent quasi-degenerate Hamiltonians.

4. Gates

In order to use the superconducting qubits presented in chapter 2 for a quantum computer, we have to be able to perform gates on them.
Single-qubit gates can be performed with high precision using microwave pulses (see for example chapter 5 in [12]). High fidelity two-qubit gates though, are still a big challenge today.

4.1. Coherent control

As described in section 2.2.3, the state of a qubit can be measured via microwave radiation on the cavity. However, it is also possible to coherently control a qubit via microwave driving without measuring it.

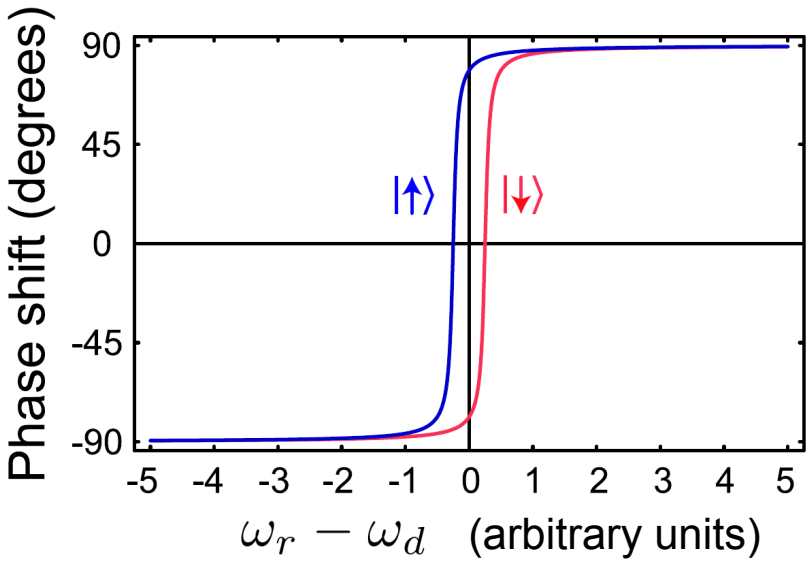

Figure 4.1.: Phase shift of the cavity field as a function of the detuning between the resonance frequency of the cavity ω_r and the drive frequency ω_d for the two possible states of the qubit. We see that in the region around $\Delta_r = \omega_r - \omega_d = 0$, the phase shift depends strongly on the state of the qubit. For large detuning, however, the entanglement is small. (Figure taken from [3], page 10.)

Figure 4.1 shows how the phase shift, which the photons acquire in the cavity, depends on the detuning Δ_r between the cavity and the drive. For $\omega_d \approx \omega_r$ this phase shift depends strongly on the state of the qubit. Thus, the qubit state can be read out by measuring

the phase of the cavity field due to the entanglement described in section 2.2.3.
However, as Blais states in [3], this dependence of the phase shift on the qubit state becomes very small in a regime where the drive frequency is far detuned from ω_r (see figure 4.1), for example for a drive at the qubit frequency $\omega_d = \omega_q \ll \omega_r$. Thus, such a drive can be used to perform gates on the qubit without measuring its state.
This far off-resonant drive does not populate the cavity as a resonant drive would. According to [3], the cavity is only virtually populated with an average photon number of $\bar{n} \approx \xi^2/\Delta^2 \sim 0.1$, where ξ is the amplitude of the drive. This is convenient because this virtual population and depopulation can be realized much faster than the cavity lifetime $1/\kappa$, leading to fast control operations.

4.1.1. Single-qubit gates

As described in [3], a drive on the cavity at frequency ω_d can be modeled by the Hamiltonian

$$H^d(t) = \xi(t)(a^\dagger e^{-i\omega_d t} + a e^{i\omega_d t}), \tag{4.1}$$

where $\xi(t)$ is the pulse envelope. In [10], Bishop presents a method to see how the drive acts on the qubit, using a displacement transformation defined by the Glauber operator

$$D(\alpha) = e^{\alpha(t)a^\dagger - \alpha^*(t)a}.$$

We start with the Jaynes-Cummings Hamiltonian plus the drive as defined in 4.1, but in a rotating frame at frequency ω_d making the drive-term time-independent, that is

$$H = \Delta_r a^\dagger a - \frac{\Delta_q}{2}\sigma^z + g(a^\dagger\sigma^- + a\sigma^+) + \xi(t)(a^\dagger + a), \tag{4.2}$$

where $\Delta_r = \omega_r - \omega_d$ and $\Delta_q = \omega_q - \omega_d$. Using $D^\dagger a^{(\dagger)} D = a^{(\dagger)} + \alpha^{(*)}$ and $D^\dagger a^\dagger a D = a^\dagger a + \alpha a^\dagger + \alpha^* a + |\alpha|^2$ and dropping all non-operator terms yields

$$\begin{aligned}\tilde{H} = D^\dagger H D - iD^\dagger D = \Delta_r a^\dagger a - \frac{\Delta_q}{2}\sigma^z + g\left((a^\dagger + \alpha^*(t))\sigma^- + (a + \alpha(t))\sigma^+\right) \\ + \xi(t)\left(a^\dagger + a\right) + \Delta_r(\alpha(t)a^\dagger + \alpha^*(t)a) - i(\dot{\alpha}(t)a^\dagger - \dot{\alpha}^*(t)a).\end{aligned} \tag{4.3}$$

The second line cancels if we choose $\alpha(t)$ to be the solution of

$$-i\dot{\alpha}(t) + \Delta_r\alpha(t) + \xi(t) = 0.$$

Introducing the Rabi frequency $\Omega(t) = 2g\alpha(t)$, the transformed Hamiltonian is

$$\tilde{H} = \Delta_r a^\dagger a - \frac{\Delta_q}{2}\sigma^z + g(a^\dagger\sigma^- + a\sigma^+) + \underbrace{\frac{1}{2}(\Omega^*(t)\sigma^- + \Omega(t)\sigma^+)}_{=\tilde{H}^d(t)}. \tag{4.4}$$

Comparing the transformed drive term to the original one (equation 4.1), we see that it now acts directly on the qubit. This is the drive term that will be used in the rest of this thesis.
As it is instructive for the further analysis of the system to work with the block diagonal-

ized Hamiltonian derived in section 3.1.2, we will apply the Schrieffer-Wolff transformation to the system including the drive for real $\Omega(t) = \Omega^*(t)$, leading to

$$\tilde{H}_{\text{eff}} = \left(\Delta_r + \frac{g^2}{\Delta}\sigma^z\right) a^\dagger a - \frac{1}{2}\left(\Delta_q - \frac{g^2}{\Delta}\right)\sigma^z + \frac{\Omega(t)}{2}\sigma^x + \frac{g\Omega(t)}{2\Delta}(a^\dagger + a)\sigma^z, \tag{4.5}$$

which is a Hamiltonian that is block-diagonal except for the drive-term that induces transitions between the qubit levels.
In [3], Blais describes a different method to see how the drive affects the qubit. Starting again with the Jaynes-Cummings Hamiltonian plus drive in the rotating frame as in equation 4.2, he directly applies the Schrieffer-Wolff transformation yielding

$$\begin{aligned} H_{\text{eff}} &= H^0 + \frac{1}{2}[H^2, S^{(1)}] + H^d(t) + [H^d(t), S^{(1)}] \\ &= \left(\Delta_r + \frac{g^2}{\Delta}\sigma^z\right) a^\dagger a - \frac{1}{2}\left(\Delta_q - \frac{g^2}{\Delta}\right)\sigma^z + \xi(t)(a^\dagger + a) - \frac{g\xi(t)}{\Delta}\sigma^x. \end{aligned} \tag{4.6}$$

We see that the drive induces a σ^x-rotation on the qubit in the Schrieffer-Wolff frame. A σ^y-rotation is possible with a phase-shifted drive, that is

$$H^d(t) = \xi(t)i(a^\dagger - a),$$

leading to

$$H_{\text{eff}} = \left(\Delta_r + \frac{g^2}{\Delta}\sigma^z\right) a^\dagger a - \frac{1}{2}\left(\Delta_q - \frac{g^2}{\Delta}\right)\sigma^z + \xi(t)i(a^\dagger - a) - \frac{g\xi(t)}{\Delta}\sigma^y.$$

In order to perform an X-gate on the qubit, we have to choose $\omega_d = \omega_q - (2\bar{n} + 1)g^2/\Delta$, where $\bar{n}$ is the mean photon number in the cavity, such that the σ^z-term disappears and we are left with a pure X-rotation. As stated above in section 4.1, the cavity is only virtually populated and $\bar{n} \sim 0.1$.
Similarly, a drive at $\omega_d = \omega_q - (2\bar{n} + 1)g^2/\Delta - 2g\xi(t)/\Delta$ yields

$$H_{\text{eff}} = \Delta_r a^\dagger a + \xi(t)(a^\dagger + a) - \frac{g\xi(t)}{\Delta}(\sigma^x + \sigma^z),$$

which is a Hadamard gate. Thus, arbitrary rotations can be realized by choosing different drive frequencies and phases.
The drive term in equation 4.6 as derived by Blais looks quite different from the one in equation 4.5 as derived by Bishop. In order to connect this, we apply the displacement transformation to 4.6 yielding

$$\begin{aligned} \tilde{H}_{\text{eff}} = \left(\Delta_r + \frac{g^2}{\Delta}\sigma^z\right) a^\dagger a - \frac{1}{2}\left(\Delta_q - \frac{g^2}{\Delta}\right)\sigma^z - \frac{g\xi(t)}{\Delta}\sigma^x + \frac{g^2}{\Delta}(\alpha(t)a^\dagger + \alpha^*(t)a) \\ + \xi(t)\left(a^\dagger + a\right) + \Delta_r(\alpha(t)a^\dagger + \alpha^*(t)a) - i(\dot{\alpha}(t)a^\dagger - \dot{\alpha}^*(t)a). \end{aligned}$$

The second line is the same as in 4.3 and cancels again if we choose $\alpha(t)$ to be the solution of

$$-i\dot{\alpha}(t) + \Delta_r \alpha(t) + \xi(t) = 0.$$

The resulting Hamiltonian is

$$\tilde{H}_{\text{eff}} = \left(\Delta_r + \frac{g^2}{\Delta}\sigma^z\right) a^\dagger a - \frac{1}{2}\left(\Delta_q - \frac{g^2}{\Delta}\right)\sigma^z - \frac{g\xi(t)}{\Delta}\sigma^x + \frac{g^2}{\Delta}(\alpha(t)a^\dagger + \alpha^*(t)a),$$

where the second drive term is obviously equal to the one in equation 4.5 for $\Omega(t) = 2g\alpha(t)$. Comparing the first drive term to the one in equation 4.5 gives an additional condition for $\alpha(t)$

$$-\frac{g\xi(t)}{\Delta} \stackrel{!}{=} \frac{\Omega(t)}{2} = g\alpha(t).$$

Plugging this into the differential equation for $\alpha(t)$ yields

$$-i\dot{\alpha}(t) + \underbrace{(\Delta_r - \Delta)}_{=\Delta_q}\alpha(t) = 0 \Rightarrow \alpha(t) \propto e^{-i\Delta_q t}.$$

Thus, the two methods presented by Bishop and Blais to see how the drive acts on the qubit are consistent.
In the following, we will use the displaced drive term equation 4.4 and apply the Schrieffer-Wolff transformation to the system including the drive, in order to get a Hamiltonian that is block-diagonal except for the drive-term.

4.2. Two-qubit gates

There have been plenty of proposals how to realize entangling gates on superconducting qubits. They can be basically divided into two classes: gates with tunable qubits or gates using fixed-frequency qubits that are driven via microwave radiation. In the introduction of [19] the advantages and disadvantages of both classes are discussed.
The iSWAP gate (see section 4.2.2) belongs to the first class of gates. Two qubits are coupled via a transmission line resonator, the coupling between them can be turned on and off by tuning the qubits in and out of resonance with each other via flux tuning (see section 2.2.2). The biggest advantage of tunable qubits is that they can be operated either in a regime where the interaction is large and two-qubit gates can be performed or in a regime where the qubits are so far detuned that there is almost no interaction between them, such that single-qubit gates can be performed easily. However, these tunable qubits are quite sensitive to flux noise and require additional flux bias lines to tune them.
The second class that includes the Cross-resonance gate (section 4.2.3), the bSWAP or Bell-Rabi gate (section 4.3.1), and the MAP gate (section 4.3.2) are gates using fixed-frequency qubits with fixed always-on interaction, where gates are performed via microwave driving. These qubits have larger coherence times as they can be *parked* at so-called *sweet-spots* of coherence. However, controlling the qubits separately can be more difficult due to the always-on interaction.

4.2.1. Entangling two qubits

Transmission line resonators can be used to couple two qubits together by placing them a bit apart along the resonator as described by Blais in [3]. We assume that there is no direct capacitive coupling between them, but that each qubit is coupled only to the cavity. We can use the Schrieffer-Wolff transformation to derive an effective two-qubit Hamiltonian that shows how the qubits are effectively coupled to each other via the cavity.
We start with a Jaynes-Cummings Hamiltonian for a system of two qubits coupled to the same cavity

$$H = \sum_{i=1}^{2} \omega_r a^\dagger a - \frac{\omega_{q_i}}{2}\sigma_i^z + g_i(a^\dagger \sigma_i^- + a\sigma_i^+),$$

where we assume that the coupling is small and that both qubits are far detuned from the cavity, i.e. $g_i \ll |\omega_r - \omega_{q_i}|$. If we choose the blocks to be $\mathrm{A} \mathrel{\widehat{=}} \{|0,0,n\rangle, |1,1,n\rangle\}$ and $\mathrm{B} \mathrel{\widehat{=}} \{|0,1,n\rangle, |1,0,n\rangle\}$, i.e. even and odd parity states (even/odd photon number blocks would be also possible), the interaction term is block off-diagonal. In analogy to section 3.1.2, we do a Schrieffer-Wolff transformation with

$$S^{(1)} = -\sum\nolimits_i \frac{g_i}{\Delta_i}(a^\dagger \sigma_i^- - a\sigma_i^+),$$

where $\Delta_i = \omega_r - \omega_{q_i}$. The first correction term is

$$\begin{aligned}
\frac{1}{2}[H^2, S^{(1)}] &= \frac{1}{2}\left[\sum\nolimits_i g_i(a^\dagger\sigma_i^- + a\sigma_i^+), -\sum\nolimits_j \frac{g_j}{\Delta_j}(a^\dagger\sigma_j^- - a\sigma_j^+)\right] \\
&= \sum\nolimits_{i=j} g_i^2 \frac{a^\dagger a[\sigma_i^-, \sigma_i^+] - \sigma_i^+\sigma_i^-}{\Delta_i} + \sum\nolimits_{i\neq j} g_i g_j \frac{\Delta_i + \Delta_j}{2\Delta_i\Delta_j}[a^\dagger, a]\sigma_j^+\sigma_i^- \\
&= \sum\nolimits_i \frac{g_i^2}{2\Delta_i}(2a^\dagger a + 1)\sigma_i^z - \sum\nolimits_{i\neq j} g_i g_j \frac{\Delta_i + \Delta_j}{2\Delta_i\Delta_j}\sigma_j^+\sigma_i^-, \quad (4.7)
\end{aligned}$$

where constant terms and two-photon terms were left out. The transformed Hamiltonian to second order in g yields

$$H_{\text{eff}} = \sum_{i=1}^{2}\left(\omega_r + \frac{g_i^2}{\Delta_i}\sigma_i^z\right)a^\dagger a - \frac{1}{2}\left(\omega_{q_i} - \frac{g_i^2}{\Delta_i}\right)\sigma_i^z - \sum\nolimits_{i\neq j} g_i g_j \frac{\Delta_i + \Delta_j}{2\Delta_i\Delta_j}\sigma_j^+\sigma_i^-. \quad (4.8)$$

This is equivalent to the result in section 3.1.2 (equation 3.11), except for the coupling term

$$H_{\text{coupling}} = -\sum\nolimits_{i\neq j} g_i g_j \frac{\Delta_i + \Delta_j}{2\Delta_i\Delta_j}\sigma_j^+\sigma_i^- = J\left(\sigma_1^+\sigma_2^- + \sigma_2^+\sigma_1^-\right), \quad (4.9)$$

where

$$J = -\frac{g_1 g_2(\Delta_1 + \Delta_2)}{2\Delta_1\Delta_2} = \frac{g_1 g_2(\omega_{q_1} + \omega_{q_2} - 2\omega_r)}{2(\omega_r - \omega_{q_1})(\omega_r - \omega_{q_2})} \quad (4.10)$$

is the effective coupling constant. We have thus derived an effective Hamiltonian, where

the qubit-cavity coupling is eliminated and the qubits are directly coupled to each other.

4.2.2. The iSWAP gate

For $g_i \ll \Delta_i$ the two-qubit coupling derived in equation 4.10 is very small compared to the free evolution due to H^0. However, we can move to a rotating frame, where H^0 disappears and the interaction becomes important. For identical resonant qubits with $\omega_{q_1} = \omega_{q_2}$ and $g_1 = g_2$ equation 4.8 yields

$$H_{\text{eff}} = \left(\omega_r + \frac{g^2}{\Delta}\left(\sigma_1^z + \sigma_2^z\right)\right) a^\dagger a - \frac{1}{2}\left(\omega_q - \frac{g^2}{\Delta}\right)\left(\sigma_1^z + \sigma_2^z\right) - \frac{g^2}{\Delta}\left(\sigma_1^+\sigma_2^- + \sigma_2^+\sigma_1^-\right),$$

which is equal to the result in [3] (equation 32) for two Cooper pair box qubits coupled to the same transmission line resonator. In a rotating frame defined by

$$U(t) = e^{iH^0 t} = e^{i\left(\omega_r a^\dagger a - \frac{\omega_q}{2}\left(\sigma_1^z + \sigma_2^z\right)\right)t}$$

H^0 disappears and the Hamiltonian yields

$$H_{\text{eff}} = \frac{g^2}{\Delta}\left(a^\dagger a + \frac{1}{2}\right)\left(\sigma_1^z + \sigma_2^z\right) - \frac{g^2}{\Delta}\left(\sigma_1^+\sigma_2^- + \sigma_2^+\sigma_1^-\right).$$

In this frame, where everything else stands still, the two-qubit interaction becomes important and can be used to entangle the two qubits together and perform gates on them. If the qubits were not resonant, i.e. for $\omega_{q_1} \neq \omega_{q_2}$, the interaction terms like $\sigma_1^+\sigma_2^-$ would acquire a time dependence in the rotating frame. They would rotate at frequency $\omega_{q_1} - \omega_{q_2}$ and average out over time. Therefore, the two-qubit interaction can be turned on and off by tuning the qubits in and out of resonance with each other.
The free evolution generated by this Hamiltonian is

$$U_{\text{eff}}(t) = e^{-i\frac{g^2}{\Delta}\left(a^\dagger a + \frac{1}{2}\right)\left(\sigma_1^z + \sigma_2^z\right)t} \cdot \begin{pmatrix} 1 & & & \\ & \cos\frac{g^2}{\Delta}t & i\sin\frac{g^2}{\Delta}t & \\ & i\sin\frac{g^2}{\Delta}t & \cos\frac{g^2}{\Delta}t & \\ & & & 1 \end{pmatrix}$$

in the $\{|00\rangle, |01\rangle, |10\rangle, |11\rangle\}$-basis. For $t = \pi\Delta/2g^2 \sim 50\,\text{ns}$ the matrix corresponds to the iSWAP gate (see [3]).
While this is a gate that uses tunable qubits, where the interaction can be turned on and off via flux tuning (see section 2.2.2), all the other two-qubit gates presented in this thesis use fixed-frequency qubits with always-on interaction driven via microwave radiation.

4.2.3. The cross-resonance gate

In [20] an all-microwave entangling gate is presented that uses two capacitively-shunted flux qubits (see [4]) coupled via a resonator. In section 4.2, it was demonstrated how a cavity leads to an effective coupling between two qubits. In order to further examine the interaction between them, we consider a two-qubit Hamiltonian as in equation 4.8 without the cavity terms, that is

$$H = -\frac{\omega_1}{2}\sigma_1^z - \frac{\omega_2}{2}\sigma_2^z + J\left(\sigma_1^+\sigma_2^- + \sigma_2^+\sigma_1^-\right),$$

where $\omega_i = \omega_{q_i} - \frac{g_i^2}{\Delta_i}$ and J as defined in equation 4.10. If the qubits are far detuned from the cavity, J is small and we can use another Schrieffer-Wolff with

$$S^{(1)} = -\frac{J}{\Delta_{12}}\left(\sigma_1^+\sigma_2^- - \sigma_2^+\sigma_1^-\right),$$

to diagonalize the Hamiltonian up to second order in J yielding

$$H_{\text{eff}} = -\frac{\tilde{\omega}_1}{2}\sigma_1^z - \frac{\tilde{\omega}_2}{2}\sigma_2^z$$

with shifted frequencies $\tilde{\omega}_1 = \omega_1 + J^2/\Delta_{12}$ and $\tilde{\omega}_2 = \omega_2 - J^2/\Delta_{12}$ and $\Delta_{12} = \omega_1 - \omega_2$ (see [20]). A drive only on qubit one at the shifted frequency of qubit two, $\tilde{\omega}_2$, can be written as

$$H^d(t) = \frac{\Omega(t)}{2}(\sigma_1^+ e^{-i\tilde{\omega}_2 t} + \sigma_1^- e^{i\tilde{\omega}_2 t}),$$

which is the drive-term derived above (equation 4.4). Transferring the drive to the diagonalized frame (Schrieffer-Wolff frame) and to a rotating frame at frequency $\tilde{\omega}_2$ yields

$$H^d_{\text{eff}}(t) = U\left(H^d(t) + [H^d(t), S^{(1)}]\right)U^\dagger = \frac{\Omega(t)}{2}\left(\sigma_1^x - \frac{J}{\Delta_{12}}\sigma_1^z\sigma_2^x\right).$$

Thus, the full effective Hamiltonian yields

$$H_{\text{total}}(t) = -\left(\frac{\tilde{\omega}_1 - \tilde{\omega}_2}{2}\right)\sigma_1^z + \frac{\Omega(t)}{2}\left(\sigma_1^x - \frac{J}{\Delta_{12}}\sigma_1^z\sigma_2^x\right).$$

In this diagonalized and rotating frame, qubit one is rotating at frequency $\tilde{\omega}_1 - \tilde{\omega}_2$ around the Z-axis with a little shift in the X-direction because of the drive term. Qubit two, however, is standing still in this frame except for the drive term, which is an X-gate whose direction depends on the state of qubit one. The fidelity reported in [20] for the cross-resonance gate is $F_{CR} = 81\%$ for a gate time of $t = 220\,\text{ns}$.

4.3. Two-qubit gates using transmons

In the analysis of the iSWAP gate and the cross-resonance gate, we assumed that the qubits were perfect two-level systems. However, as opposed to the Cooper pair box qubit, transmon qubits have much lower anharmonicity and can hardly be approximated as two-level systems. Therefore, the transmon must be considered as a multi-level system, where the higher levels will play a significant role in gate architectures.
In section 4.2, we looked at a Hamiltonian, where two qubits were coupled via a cavity. Using a Schrieffer-Wolff transformation, we derived an effective Hamiltonian, where the qubits are directly coupled to each other (equation 4.8). This is possible for the two-transmon case, too. We consider a Hamiltonian for two transmons coupled to the same cavity, that is

$$H = \omega_r a^\dagger a + \sum_{i=1}^{2}\sum_{j_i}\underbrace{\left(\left(\omega_i - \frac{\delta_i}{2}\right)j_i + \frac{\delta_i}{2}j_i^2\right)}_{\omega_{j_i}}|j_i\rangle\langle j_i| + g_i(a^\dagger c_i + a c_i^\dagger).$$

Just as in section 3.1.4, we make the ansatz

$$S^{(1)} = -\sum_{i=1}^{2} g_i(a^\dagger \tilde{c}_i - a\tilde{c}_i^\dagger),$$

where $\tilde{c} = \sum_j \gamma_{j+1}|j\rangle\langle j+1|$ is the changed annihilation operator from section 3.1.4 with

$$\gamma_{j+1} = \frac{\sqrt{j+1}}{\omega_r - \omega - \delta j}.$$

The first correction term is

$$\begin{aligned}\frac{1}{2}[H^2, S^{(1)}] &= \frac{1}{2}\left[\sum_{i=1}^{2} g_i(a^\dagger c_i + a c_i^\dagger), \sum_{k=1}^{2} g_k(a\tilde{c}_k^\dagger - a^\dagger \tilde{c}_k)\right] \\ &= \sum_{i=k} \frac{g_i^2}{2}\left([a^\dagger c_i, a\tilde{c}_i^\dagger] - [ac_i^\dagger, a^\dagger \tilde{c}_i] - a^{\dagger 2}[c_i, \tilde{c}_i] + a^2[c_i^\dagger, \tilde{c}_i^\dagger]\right) \\ &\qquad + \sum_{i\neq k} \frac{g_i g_k}{2}(c_i\tilde{c}_k^\dagger[a^\dagger, a] - c_i^\dagger \tilde{c}_k[a, a^\dagger]).\end{aligned}$$

Dropping the two-photon terms and defining $\mu_{j_i} = \sqrt{j_i}\gamma_{j_i} = \frac{j_i}{\omega_r - \omega_i - \delta_i(j_i - 1)}$ as in section 3.1.4, this gives

$$\frac{1}{2}[H^2, S^{(1)}] \;=\; \sum_{i=k}\sum_{j_i} g_i^2(a^\dagger a(\mu_{j_i+1} - \mu_{j_i}) - \mu_{j_i})|j_i\rangle\langle j_i| - \sum_{i\neq k}\frac{g_i g_k}{2}(c_i\tilde{c}_k^\dagger + c_i^\dagger \tilde{c}_k).$$

The resulting effective Hamiltonian is

$$H_{\text{eff}} \;=\; \left(\omega_r + \sum_{i=1}^{2}\sum_{j_i}\chi_{j_i}|j_i\rangle\langle j_i|\right)a^\dagger a + \sum_{i=1}^{2}\sum_{j_i}\tilde{\omega}_{j_i}|j_i\rangle\langle j_i| - \sum_{i\neq k}\frac{g_i g_k}{2}(c_i\tilde{c}_k^\dagger + c_i^\dagger\tilde{c}_k), \tag{4.11}$$

with χ_{j_i} and ω_{j_i} as defined in equations 3.16 and 3.17. Apart from the coupling term, this is of course the same result as in section 3.1.4 (equation 3.15). The coupling term can be rewritten as

$$\begin{aligned}H_{\text{coupling}} &= -\sum_{i\neq k}\frac{g_i g_k}{2}(c_i\tilde{c}_k^\dagger + c_i^\dagger\tilde{c}_k) \\ &= \sum_{j_1,j_2}\sqrt{j_1+1}\sqrt{j_2+1}J_{j_1,j_2}\left(|j_1, j_2+1\rangle\langle j_1+1, j_2| + |j_1+1, j_2\rangle\langle j_1, j_2+1|\right)\end{aligned}$$

with

$$J_{j_1,j_2} = \frac{g_1 g_2(\omega_1 + \omega_2 + \delta_1 j_1 + \delta_2 j_2 - 2\omega_r)}{2(\omega_r - \omega_2 - \delta_2 j_2)(\omega_r - \omega_1 - \delta_1 j_1)}$$

which is the same result as Gambetta's in [16] (equation 54). If J_{j_1,j_2} can be approximated by a constant J, that is for low anharmonicity and low transmon level number, we can use the ordinary lowering operators c instead of $\tilde{c}$ and the coupling can be written as

$$H_{\text{coupling}} = J(c_1^\dagger c_2 + c_1 c_2^\dagger),$$

which is the expression used in [14] (equation 1). Just as in the two-qubit case, we now have an effective Hamiltonian where the two transmons are directly coupled to each other.
Making the two-level approximation for H_{coupling} consists in taking only the term for $j_1, j_2 = 0$ into account, that is

$$H_{\text{coupling}} = J_{0,0}\left(|0,1\rangle\langle 1,0| + |1,0\rangle\langle 0,1|\right) = \frac{g_1 g_2(\omega_1 + \omega_2 - 2\omega_r)}{2(\omega_r - \omega_1)(\omega_r - \omega_2)}\left(\sigma_1^+\sigma_2^- + \sigma_1^-\sigma_2^+\right),$$

which is the two-qubit expression derived above (equations 4.9, 4.10).

4.3.1. The bSWAP gate

In [14], Poletto et al. propose a two-transmon entangling gate called bSWAP or Bell-Rabi gate that explicitly uses the existence of higher transmon levels. They exploit particular resonance conditions in order to drive the $|00\rangle \rightarrow |11\rangle$ transition, which is a two-photon transition that is forbidden in harmonic systems. We will derive an effective Hamiltonian for this scheme using *mathematica*, see appendix C for the explicit calculation. These *mathematica* calculations are based on the work of Jay Gambetta.
Consider a Hamiltonian of two coupled transmons modeled as Duffing oscillators without the cavity terms

$$H = \left(\omega_1 - \frac{\delta_1}{2}\right) c_1^\dagger c_1 + \frac{\delta_1}{2}(c_1^\dagger c_1)^2 + \left(\omega_2 - \frac{\delta_2}{2}\right) c_2^\dagger c_2 + \frac{\delta_2}{2}(c_2^\dagger c_2)^2 + J(c_1^\dagger c_2 + c_1 c_2^\dagger),$$

which is a simplified version of the two-transmon Hamiltonian derived in section 4.3 (equation 4.11), where the frequency shift induced by the qubit-cavity coupling is neglected (compare equation 3.17).
Setting up a matrix involving ten two-transmon levels up to three excitations (as for example the levels $|21\rangle$ and $|30\rangle$), we can eliminate the coupling using the full-diagonalizing transformation described in section 3.1.1. In order to reduce the complexity of the calculation, we will only take into account terms up to first order in J here, thus neglecting the frequency shifts induced by the coupling, which are of second order in J. However, when transforming the drive to the diagonalized frame, terms of first order in J will appear.
We move to a rotating frame at the drive frequency, which is near the average value of the two transmon frequencies ω_1 and ω_2, that is

$$\omega_d = (\omega_1 + \omega_2)/2 - \delta,$$

where δ is a small frequency detuning. In this rotating frame, the Hamiltonian is

$$\tilde{H} = \left(\frac{\omega_1 - \omega_2}{2} + \delta - \frac{\delta_1}{2}\right) c_1^\dagger c_1 + \frac{\delta_1}{2}(c_1^\dagger c_1)^2 + \left(\frac{\omega_2 - \omega_1}{2} + \delta - \frac{\delta_2}{2}\right) c_2^\dagger c_2 + \frac{\delta_2}{2}(c_2^\dagger c_2)^2.$$

For $\delta \approx 0$, the levels $|00\rangle$ and $|11\rangle$ have almost energy zero in the rotating frame, see figure 4.2. This low-energy manifold is joined by the level $|20\rangle$ if the anharmonicity of qubit two approaches the detuning between the two qubits $\Delta_{12} = \omega_1 - \omega_2 \to -\delta_1$. The same thing is valid for the level $|02\rangle$, if $\Delta_{12} \to \delta_2$. All the other levels are assumed to be far detuned from this low-energy manifold.

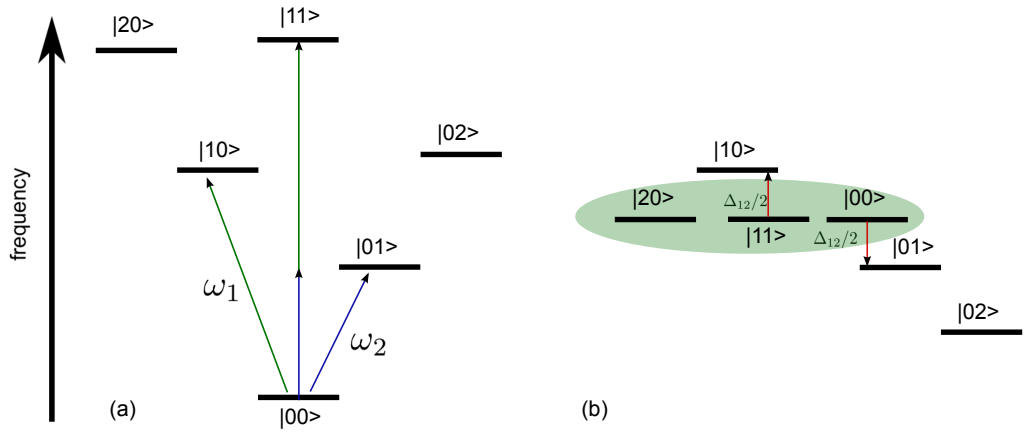

Figure 4.2.: Energy diagram of the system in the laboratory frame (a) and the rotating frame at $\omega_d \approx (\omega_1 + \omega_2)/2$ (b). For $\Delta_{12} = \omega_1 - \omega_2 \to -\delta_1$ the levels $|00\rangle$, $|11\rangle$ and $|20\rangle$ are aligned at energy almost zero in the rotating frame. They make up a low-energy manifold, that is detuned from the other levels by $\Delta_{12}/2$. We assume that the anharmonicities are negative $\delta_1, \delta_2 < 0$ and $\omega_1 > \omega_2$.

The drive on the system can be written as

$$H^d(t) = \frac{\Omega_1}{2}\left(c_1^\dagger e^{-i(\omega_d t+\varphi)} + c_1 e^{i(\omega_d t+\varphi)}\right) + \frac{\Omega_2}{2}\left(c_2^\dagger e^{-i(\omega_d t+\varphi)} + c_2 e^{i(\omega_d t+\varphi)}\right),$$

where Ω_1 and Ω_2 are the driving amplitudes for qubit one and two, respectively. It has to be transferred to the diagonalized frame described above and to the rotating frame at ω_d. We can now use another Schrieffer-Wolff transformation to decouple this low-energy manifold from the other levels. Truncating the system to the two-qubit space, that is $\{|00\rangle, |01\rangle, |10\rangle, |11\rangle\}$, we find

$$H_{\text{eff}} = \begin{pmatrix} \frac{\alpha_{IZ}}{2} + \frac{\alpha_{ZI}}{2} + \frac{\alpha_{ZZ}}{4} & 0 & 0 & \frac{\Omega_B e^{-2i\varphi}}{2} \\ 0 & -\frac{\alpha_{IZ}}{2} + \frac{\alpha_{ZI}}{2} - \frac{\alpha_{ZZ}}{4} & \Omega_S & 0 \\ 0 & \Omega_S & \frac{\alpha_{IZ}}{2} - \frac{\alpha_{ZI}}{2} - \frac{\alpha_{ZZ}}{4} & 0 \\ \frac{\Omega_B e^{2i\varphi}}{2} & 0 & 0 & -\frac{\alpha_{IZ}}{2} - \frac{\alpha_{ZI}}{2} + \frac{\alpha_{ZZ}}{4} \end{pmatrix}. \tag{4.12}$$

By truncating the system like this, we neglect the leakage from the two-qubit space to the non-computational levels, for example between the levels $|11\rangle$ and $|20\rangle$, which is a

possible error source. As shown in appendix C, $\alpha_{IZ} \approx -\alpha_{ZI}$ for small δ, so we can choose δ such that $\alpha_{IZ} + \alpha_{ZI} = 0$. Then we can divide equation 4.12 into three commuting parts

$$\begin{aligned} H_{ZZ} &= \frac{\alpha_{ZZ}}{4} ZZ \\ H_{SZ} &= \frac{\alpha_{IZ}}{2}(IZ - ZI) + \frac{\Omega_S}{2}(XX + YY) \\ H_B &= \frac{\Omega_B}{4}\cos(2\varphi)(XX - YY) + \frac{\Omega_B}{4}\sin(2\varphi)(XY + YX), \end{aligned}$$

where ZZ stands for $\sigma_1^z \sigma_2^z$ etc. The evolution generated by these effective Hamiltonians is

$$U_{\text{eff}}(t) = e^{-iH_{\text{eff}}t} = e^{-iH_{ZZ}t} e^{-iH_{SZ}t} e^{-iH_B t} = U_{ZZ} U_{SZ} U_B,$$

where $U_{ZZ} = \exp(-i\alpha_{ZZ} ZZ t/4)$ leads to phase factors only and

$$U_{SZ}(t) = \begin{pmatrix} 1 & 0 & 0 & 0 \\ 0 & \cos(xt) + i\alpha_{IZ}\frac{\sin(xt)}{x} & -i\Omega_S \frac{\sin(xt)}{x} & 0 \\ 0 & -i\Omega_S \frac{\sin(xt)}{x} & \cos(xt) - i\alpha_{IZ}\frac{\sin(xt)}{x} & 0 \\ 0 & 0 & 0 & 1 \end{pmatrix}$$

with $x = \alpha_{IZ}^2 + \Omega_S^2$ entangles the states $|01\rangle$ and $|10\rangle$, see appendix C for the constants. The last part is the one that generates the bSWAP gate, that is

$$U_B(t) = \begin{pmatrix} \cos(\frac{\Omega_B t}{2}) & 0 & 0 & -ie^{-2i\varphi}\sin(\frac{\Omega_B t}{2}) \\ 0 & 1 & 0 & 0 \\ 0 & 0 & 1 & 0 \\ -ie^{2i\varphi}\sin(\frac{\Omega_B t}{2}) & 0 & 0 & \cos(\frac{\Omega_B t}{2}) \end{pmatrix}$$

with

$$\Omega_B = \frac{-2J\left(-J\Omega_1\Omega_2(\delta_1 + \delta_2) + \Omega_2^2\delta_2(\delta_1 + \Delta_{12}) + \Omega_1^2\delta_1(\delta_2 - \Delta_{12})\right)}{(\delta_2 - \Delta_{12})(\delta_1 + \Delta_{12})(\Delta_{12}^2 - 4\delta^2)}, \tag{4.13}$$

which is equal to the result Gambetta et al. give in the appendix of [14], i.e. equation 2.8 for $U_B(t)$ and equation 2.5 for Ω_B. $U_B(t)$ generates Rabi-like oscillations that entangle the states $|00\rangle$ and $|11\rangle$ as shown in figure 4.3. We can see that Ω_B goes to infinity for the two possible resonance cases $\Delta_{12} \to -\delta_1$ and $\Delta_{12} \to \delta_2$. Thus, by choosing one of these resonance conditions, the $|00\rangle \leftrightarrow |11\rangle$ transition can be made bright.
We might conclude that Ω_B could be tuned to be infinitely large, making the gate infinitely fast. However, the Schrieffer-Wolff transformation is supposed to be a unitary transformation close to a unity matrix. Therefore, all terms in S should be much smaller than one for this to be a reasonable transformation. For the resonance case $\Delta_{12} \to -\delta_1$ though, there are several terms in $S^{(1)}$ that diverge. Setting these terms to one, gives a measure of how close to resonance we can tune our parameters. We find

$$\delta_1 > -\frac{\Delta_{12}(\Delta_{12}^2 - 2\delta\Delta_{12} - 2J\Omega_1)}{\Delta_{12}^2 - 2\delta\Delta_{12} + 2J\Omega_1} \approx -\Delta_{12} + \frac{4J\Omega_1}{\Delta_{12} - 2\delta}. \tag{4.14}$$

This condition puts a limit on how big Ω_B can get, see appendix C.
For a gate time of $t = \pi/\Omega_B \sim 1.6\,\mu\text{s}$, the states swap (bSWAP gate), while the same gate produces the highly entangled Bell state $(|00\rangle + e^{i\varphi}|11\rangle)/\sqrt{2}$ for a gate time of $t = \pi/(2\Omega_B) \sim 800\,\text{ns}$ ($\sqrt{\text{bSWAP}}$ gate). The fidelities reported in [14] for these gates are

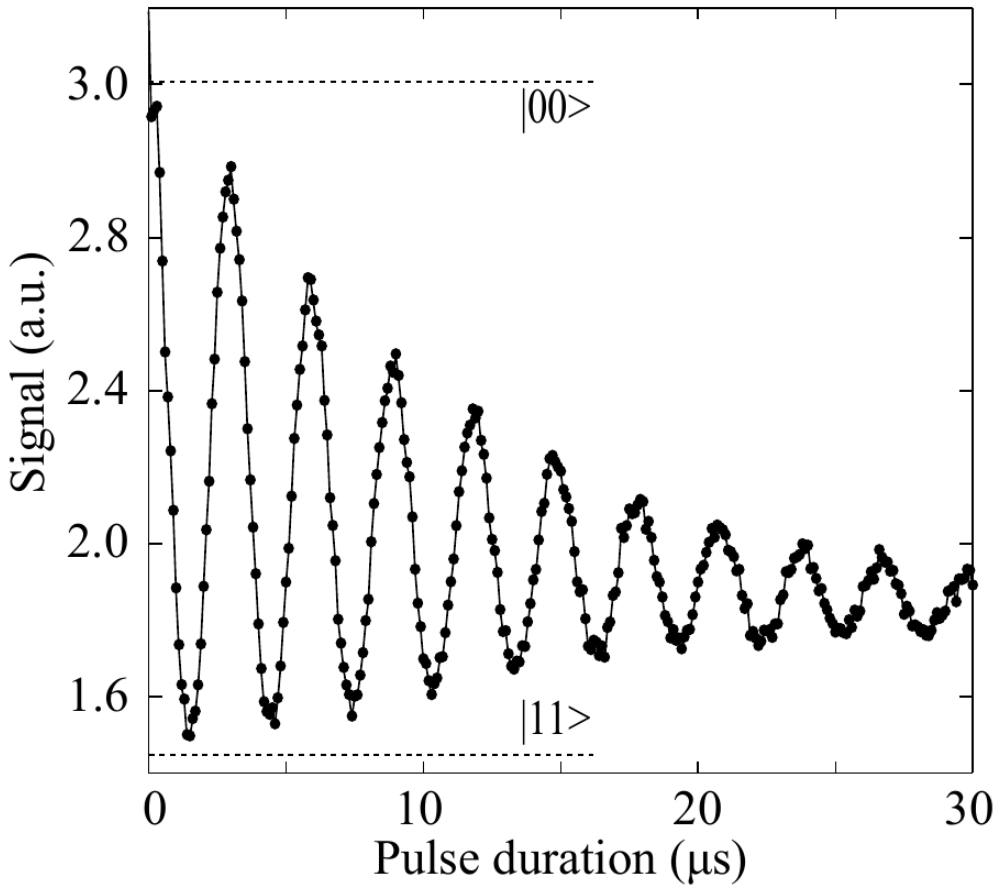

Figure 4.3.: Driving the system at $\omega_d = (\omega_1 + \omega_2)/2 - \delta$ generates a Rabi-like rotation between the states $|00\rangle$ and $|11\rangle$. (Figure taken from [14], page 2.)

$F_{\sqrt{\text{bSWAP}}} = 90\%$ and $F_{\text{bSWAP}} = 87.3\%$.
In principle, we can find the same effect for a pure two-qubit system, too. A strictly analogous procedure with diagonalization, driving and decoupling the low-energy manifold, which is made up by $|00\rangle$ and $|11\rangle$ only in this case, leads to

$$\Omega_B = \frac{-2J(\Omega_1^2 + \Omega_2^2)}{\Delta_{12}^2 - 4\delta^2},$$

which is the limit of 4.13 for $\delta_1, \delta_2 \to \infty$, that is the pure qubit limit. However, this effect remains small, as the qubits can not be tuned to the resonance conditions mentioned above.

4.3.2. The MAP gate

Like the bSWAP gate, the microwave-activated c-Phase (MAP) gate presented in [19] is a two-transmon gate that exploits the existence of higher, non-computational transmon

levels. This calculation will again be executed using *mathematica*, see appendix D.
Two transmon qubits are coupled via a transmission line resonator, as described in section 4.3. The detuning between them is chosen such that the non-computational levels $|12\rangle$ and $|03\rangle$ are aligned, see figure 4.4.

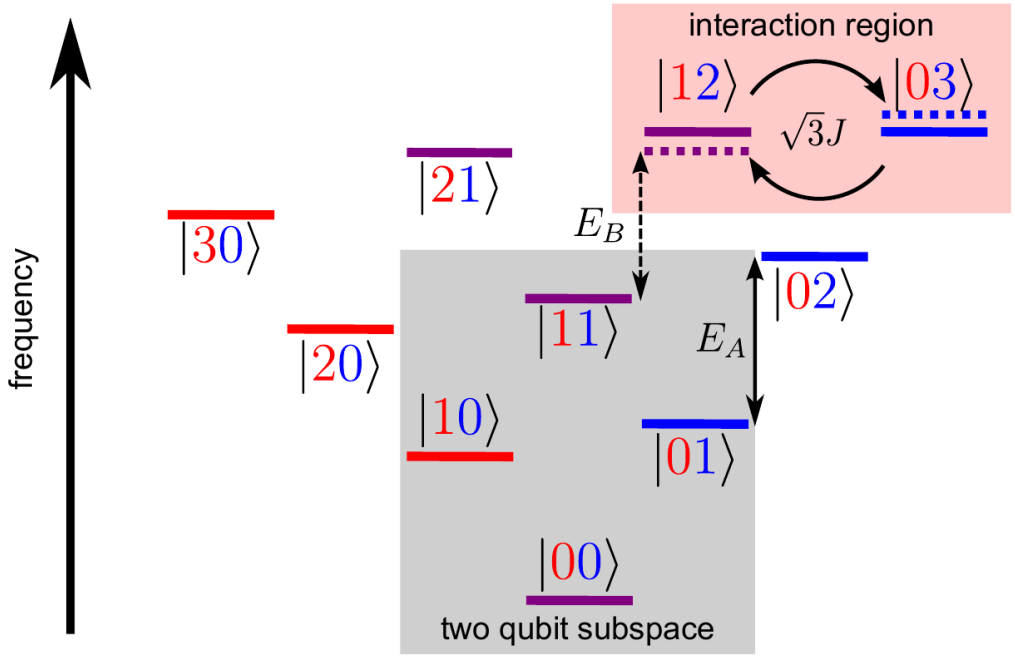

Figure 4.4.: Level diagram of the relevant two-transmon levels. The non-computational levels $|12\rangle$ and $|03\rangle$ are aligned and interact with coupling strength $\sqrt{3}J$. The interaction leads to a dispersive shift ξ, lifting the degeneracy between the $|02\rangle \leftrightarrow |01\rangle$ and the $|12\rangle \leftrightarrow |11\rangle$ transition (E_A and E_B in the diagram). (Figure taken from [19], page 2.)

The corresponding Hamiltonian consists of two coupled Duffing oscillators, just as for the bSWAP gate

$$H = \left(\omega_1 - \frac{\delta_1}{2}\right) c_1^\dagger c_1 + \frac{\delta_1}{2}(c_1^\dagger c_1)^2 + \left(\omega_2 - \frac{\delta_2}{2}\right) c_2^\dagger c_2 + \frac{\delta_2}{2}(c_2^\dagger c_2)^2 + J(c_1^\dagger c_2 + c_1 c_2^\dagger).$$

The resonance condition yields

$$E_{|12\rangle} = \omega_1 + 2\omega_2 + \delta_2 \stackrel{!}{=} 3\omega_2 + 3\delta_2 = E_{|03\rangle} \Leftrightarrow \Delta_{12} = \omega_1 - \omega_2 = 2\delta_2.$$

The Hamiltonian can be diagonalized in the $\{|03\rangle, |12\rangle\}$-space using a simple unitary transformation

$$U = \begin{pmatrix} \cos\theta & \sin\theta \\ -\sin\theta & \cos\theta \end{pmatrix},$$

where θ is chosen such that $\tilde{H} = UHU^\dagger$ is diagonal. It is

$$\tilde{H}_{\{|03\rangle,|12\rangle\}} = \begin{pmatrix} 3\omega_2 + 3\delta_2 + \xi & 0 \\ 0 & \omega_1 + 2\omega_2 + \delta_2 - \xi. \end{pmatrix},$$

We see that both levels are shifted by

$$\xi = \frac{1}{2}\left(\sqrt{12J^2 + (\Delta_{12} - 2\delta_2)^2} + \Delta_{12} - 2\delta_2\right).$$

Inserting the resonance condition yields $\xi = \sqrt{3}J$. Thus, the coupling removes the degeneracy between the two levels and thereby also removes the degeneracy between the $|02\rangle \leftrightarrow |01\rangle$ and the $|12\rangle \leftrightarrow |11\rangle$ transition, see figure 4.4.
It is claimed in [19] that a drive that is almost resonant with the $|n2\rangle \leftrightarrow |n1\rangle$ transition induces a ZZ interaction, that is

$$H^d(t) = \frac{\Omega}{2}\left(c_1^\dagger e^{-i\omega_d t} + c_1 e^{i\omega_d t} + c_2^\dagger e^{-i\omega_d t} + c_2 e^{i\omega_d t}\right),$$

with

$$\omega_d = \omega_2 + \delta_2 - \delta = \frac{\omega_1 + \omega_2}{2} - \delta,$$

where δ is a small frequency detuning. In order to see, where this ZZ interaction comes from, we move to a rotating frame at ω_d and do the full-diagonalizing transformation described in section 3.1.1, where we take the drive and the rest of the coupling as the perturbation. As this transformation only works for non-degenerate energy levels, the degeneracy between the levels $|03\rangle$ and $|12\rangle$ had to be removed before doing the transformation.
We find that the frequency of the $|00\rangle \leftrightarrow |11\rangle$ transition is not equal to the sum of the $|00\rangle \leftrightarrow |01\rangle$ and $|00\rangle \leftrightarrow |10\rangle$ transitions any more, but shifted by

$$\zeta = \omega_{11} - \omega_{01} - \omega_{10} = \zeta_0 + \frac{\Omega^2}{2\delta}\zeta_2, \tag{4.15}$$

where

$$\zeta_0 = \frac{2J^2(\Delta + 2\delta_1)}{\Delta(\Delta + \delta_1)} = J_{11,20}J_{11,02}\left(\frac{1}{\Delta_{11,20}} + \frac{1}{\Delta_{11,02}}\right)$$

is independent of the drive, while

$$\zeta_2 = \frac{3J^2}{3J^2 - \delta^2} = \frac{J_{12,03}^2}{J_{12,03}^2 + \delta(\omega_d - \Delta_{03,11})}$$

is the part of the shift that is induced by the drive. The left-hand-side expressions for ζ_0 and ζ_2 are the results calculated in appendix D. For $J_{11,20} = J_{11,02} = \sqrt{2}J$, $J_{12,03} = \sqrt{3}J$ and $\omega_1 - \omega_2 = 2\delta_2$ they are equal to the right-hand-side expressions, which are the ones given in [19] (equations 2-4).
Thus, the MAP gate induces a phase shift ζ if both qubits are in state 1, which gets large for $\delta \to 0$, see equation 4.15. The effective Hamiltonian in the two-qubit space is

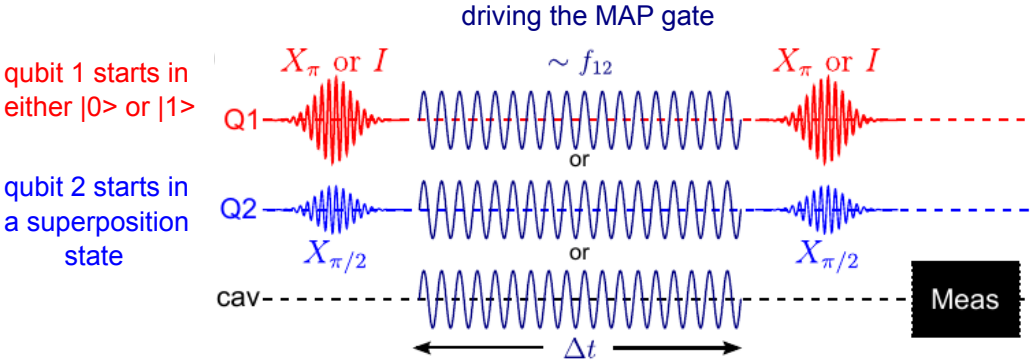

(a) Ramsey-type experiment to show how the MAP gate works. Qubit 1 is either brought to the $|1\rangle$ state by a X_π pulse or left in the $|0\rangle$ state. Qubit 2 is initialized in a superposition state using a $X_{\pi/2}$ pulse. Then the MAP gate is driven for a time Δt.

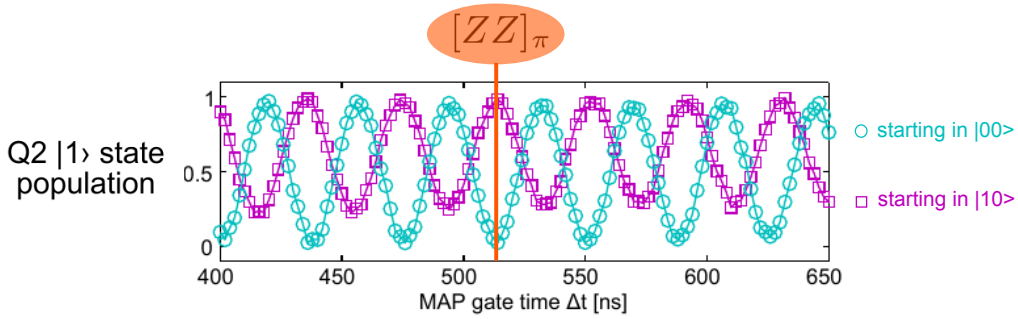

(b) The evolution of the $|1\rangle$ state population of qubit 2 depends on the state of qubit 1 (cyan/purple coloring). After $\Delta t = 514\,\text{ns}$, the two cases have acquired a phase difference of π, realizing a ZZ_π gate.

Figure 4.5.: MAP interaction (figure taken from [19], page 3.)

$$H_{\text{eff}} = \omega_{10}|1,0\rangle\langle 1,0| + \omega_{01}|0,1\rangle\langle 0,1| + (\omega_{10}+\omega_{01}+\zeta)|1,1\rangle\langle 1,1|$$
$$= -\frac{1}{2}\left(\omega_{10}-\frac{\zeta}{2}\right)\sigma_1^z - \frac{1}{2}\left(\omega_{01}-\frac{\zeta}{2}\right)\sigma_2^z + \frac{\zeta}{4}\sigma_1^z\sigma_2^z + const.$$

A c-Phase gate $[ZZ]_\pi = e^{-i\frac{\pi}{4}\sigma_1^z\sigma_2^z}$ is realized with a gate time of $t = 514\,\text{ns}$, which means that the states $|00\rangle$ and $|01\rangle$ have a phase difference of π, see figure 4.5. The gate fidelity is reported to be $F_{\text{MAP}} = 87.6\%$, see [19].

5. Conclusions and outlook

In conclusion, we can say that the transmon qubit presented in chapter 2 is a substantial enhancement of the Cooper pair box qubit, as its insensitivity to charge noise leads to significantly improved coherence times. However, as its anharmonicity is comparatively small, the transmon can not be approximated as a two-level system. Treating it as a multi-level system gives rise to interesting new effects.
Transmon qubits can either be used in fixed-frequency schemes or in tunable schemes, where their transition frequencies are tuned via flux tuning (see section 2.2.2).
Among the perturbative methods for the derivation of effective Hamiltonians presented in chapter 3, the Schrieffer-Wolff transformation (section 3.1) results to be the method of choice. It proves to be extremely useful in the analysis of one- and two-qubit gates, both for two-level and multi-level systems such as transmons. It is easy to implement with computer tools like *mathematica* and adaptable to different requirements on the effective Hamiltonian we want to derive, compare the full diagonalizing transformation presented in section 3.1.1.
The higher levels of the transmons play an important role in two-transmon gate setups, as we saw in chapter 4. By choosing certain resonance conditions between two-transmon states, gates can be driven via microwave radiation. In order to analyze these gates, the Schrieffer-Wolff transformation is again helpful. Treating the coupling between the transmons and the drive terms as a perturbation, we can derive their effect on the two-transmon Hamiltonian. The resonance conditions are used to enhance the desired effects. However, the fidelities of these two-transmon gates are not yet high enough, which is believed to be mostly due to dephasing and leakage to higher levels. This could be improved, to some amount, by pulse shaping techniques to prevent leakage or by optimizing the quantities involved here (driving amplitudes, coupling constants, etc.)
On the other hand, it might be possible to exceed these fidelities with another superconducting qubit. The fluxonium [21], for instance, combines the insensitivity to charge noise of the transmon qubit with the high anharmonicity of the Cooper pair box qubit. With higher anharmonicity, we would not need to worry so much about leakage. Therefore, the fluxonium seems to be a promising candidate for further research.

A. Flux tuning

A tunable transmon as described in [7] consists of two parallel Josephson junctions in a dc-SQUID setup. If these are not identical, the second part of equation 2.10 has to be adjusted to give

$$H_J = -E_{J1}\cos(\hat{\varphi}_1) - E_{J2}\cos(\hat{\varphi}_2),$$

where the phase difference between the two junctions is fixed by the condition that the flux is quantized

$$\varphi_1 - \varphi_2 = 2\pi n + 2\pi\frac{\Phi}{\Phi_0}.$$

Using $\varphi \equiv (\varphi_1 + \varphi_2)/2$, $E_{J\Sigma} \equiv E_{J1} + E_{J2}$ and the junction asymmetry $d = \frac{E_{J2}-E_{J1}}{E_{J1}+E_{J2}}$, the Josephson Hamiltonian yields

$$\begin{aligned}
H_J &= -E_{J\Sigma}\left(\cos(\hat{\varphi})\cos\left(\pi\frac{\Phi}{\Phi_0}\right) + d\sin(\hat{\varphi})\sin\left(\pi\frac{\Phi}{\Phi_0}\right)\right) \\
&= -E_{J\Sigma}\cos\left(\pi\frac{\Phi}{\Phi_0}\right)\left(\cos(\hat{\varphi}) + \sin(\hat{\varphi})\underbrace{d\tan\left(\pi\frac{\Phi}{\Phi_0}\right)}_{\equiv x}\right) \\
&= -E_{J\Sigma}\cos\left(\pi\frac{\Phi}{\Phi_0}\right)\sqrt{1+x^2}\left(\cos(\hat{\varphi})\frac{1}{\sqrt{1+x^2}} + \sin(\hat{\varphi})\frac{x}{\sqrt{1+x^2}}\right) \\
&= -E_{J\Sigma}\cos\left(\pi\frac{\Phi}{\Phi_0}\right)\sqrt{1+x^2}\left(\cos(\hat{\varphi})\cos(\arctan(x)) + \sin(\hat{\varphi})\sin(\arctan(x))\right) \\
&= -E_{J\Sigma}\cos\left(\pi\frac{\Phi}{\Phi_0}\right)\sqrt{1+d^2\tan^2\left(\pi\frac{\Phi}{\Phi_0}\right)}\cos(\hat{\varphi}-\varphi_0)
\end{aligned}$$

with $\tan(\varphi_0) = d\tan(\pi\Phi/\Phi_0)$.

B. Commutators and formulas

The Campbell-Baker-Hausdorff formula is

$$e^X Y e^{-X} = \sum_{m=0}^{\infty} \frac{1}{m!}[X,Y]_m \tag{B.1}$$

with $[X,Y]_m = [X,[X,Y]_{m-1}]$, and $[X,Y]_0 = Y$.

The three Pauli matrices

$$\begin{aligned}
\sigma^x &= |0\rangle\langle 1| + |1\rangle\langle 0| = \sigma^+ + \sigma^- = \left(\begin{smallmatrix} 0 & 1 \\ 1 & 0 \end{smallmatrix}\right) \\
\sigma^y &= i(|1\rangle\langle 0| - |0\rangle\langle 1|) = i(\sigma^+ - \sigma^-) = \left(\begin{smallmatrix} 0 & -i \\ i & 0 \end{smallmatrix}\right) \\
\sigma^z &= |0\rangle\langle 0| - |1\rangle\langle 1| = \left(\begin{smallmatrix} 1 & 0 \\ 0 & -1 \end{smallmatrix}\right)
\end{aligned}$$

obey the following commutation relation

$$[\sigma_i\,,\sigma_j] = \sigma_i\,\sigma_j - \sigma_j\,\sigma_i = 2\,\mathrm{i}\sum_{k=1}^{3}\epsilon_{ijk}\,\sigma_k.$$

Using the Pauli matrices, we can define the operators

$$\sigma^{\pm} = \frac{\sigma^x \mp i\sigma^y}{2}$$

with commutation relations

$$\begin{aligned}
[\sigma^x, \sigma^{\pm}] &= \pm\sigma^z \\
[\sigma^y, \sigma^{\pm}] &= -i\sigma^z \\
[\sigma^z, \sigma^{\pm}] &= \mp 2\sigma^{\pm} \\
[\sigma^-, \sigma^+] &= \sigma^z.
\end{aligned}$$

The photon annihilation operator is defined as

$$a = \sum_n \sqrt{n+1}|n\rangle\langle n+1|$$

with commutation relations

$$
\begin{aligned}
[a, a^\dagger] &= 1 \\
[a^\dagger a, a^\dagger] &= a^\dagger \\
[a^\dagger a, a] &= -a \\
[(a^\dagger a)^2, a^\dagger] &= (2a^\dagger - 1)a^\dagger \\
[(a^\dagger a)^2, a] &= -(2a^\dagger + 1)a.
\end{aligned}
$$

Commutation relations for terms including both qubit and cavity operators:

$$
\begin{aligned}
[a^\dagger \sigma^-, a\sigma^+] &= \left(a^\dagger a + \frac{1}{2}\right)\sigma^z + const. \\
[a^\dagger \sigma^+, a\sigma^-] &= -\left(a^\dagger a + \frac{1}{2}\right)\sigma^z + const.
\end{aligned}
$$

C. bSWAPgate

This calculation was executed using *mathematica* and is based on the work of Jay Gambetta.

Consider two transmons that are coupled via a transmission line resonator. By exploiting certain resonance conditions Rabi oscillations between the states 00 and 11 are induce via an external microwave drive, leading to the highly entangled Bell state $(00 + 11)/\sqrt{2}$.

```
sx = {{0, 1}, {1, 0}};
sy = {{0, -I}, {I, 0}};
sz = {{1, 0}, {0, -1}};
si = {{1, 0}, {0, 1}};
sm = {{0, 1}, {0, 0}};
sp = {{0, 0}, {1, 0}};

ZZ = KroneckerProduct[sz, sz];
II = KroneckerProduct[si, si];
IZ = KroneckerProduct[si, sz];
ZI = KroneckerProduct[sz, si];
XX = KroneckerProduct[sx, sx];
YY = KroneckerProduct[sy, sy];
XY = KroneckerProduct[sx, sy];
YX = KroneckerProduct[sy, sx];

Commutator[A_, B_]:=A.B - B.A;

λ = a;
dim = 10;
```

The eigenvalues of the unperturbed two-transmon Hamiltonian are

```
En[n1_, n2_]:= (ω1 - δ1/2) n1 + δ1/2 n1^2 + (ω2 - δ2/2) n2 + δ2/2 n2^2
```

where $\omega 1$ and $\omega 2$ are the transmon frequencies, $\delta 1$ and $\delta 2$ their anharmonicities and n1 and n2 are the number operators for transmon one and two, respectively.
The corresponding Hamiltonian for the levels 00,01,10,11,02,20,03,12,21,30 is

```
(H0 = Simplify[DiagonalMatrix[{En[0, 0], En[0, 1], En[1, 0], En[1, 1], En[0, 2], En[2, 0], En[0, 3], En[1, 2], En[2, 1], En[3, 0]}]])//MatrixForm
```

$$\begin{pmatrix} 0 & 0 & 0 & 0 & 0 & 0 & 0 & 0 & 0 & 0 \\ 0 & \omega 2 & 0 & 0 & 0 & 0 & 0 & 0 & 0 & 0 \\ 0 & 0 & \omega 1 & 0 & 0 & 0 & 0 & 0 & 0 & 0 \\ 0 & 0 & 0 & \omega 1+\omega 2 & 0 & 0 & 0 & 0 & 0 & 0 \\ 0 & 0 & 0 & 0 & \delta 2+2\omega 2 & 0 & 0 & 0 & 0 & 0 \\ 0 & 0 & 0 & 0 & 0 & \delta 1+2\omega 1 & 0 & 0 & 0 & 0 \\ 0 & 0 & 0 & 0 & 0 & 0 & 3(\delta 2+\omega 2) & 0 & 0 & 0 \\ 0 & 0 & 0 & 0 & 0 & 0 & 0 & \delta 2+\omega 1+2\omega 2 & 0 & 0 \\ 0 & 0 & 0 & 0 & 0 & 0 & 0 & 0 & \delta 1+2\omega 1+\omega 2 & 0 \\ 0 & 0 & 0 & 0 & 0 & 0 & 0 & 0 & 0 & 3(\delta 1+\omega 1) \end{pmatrix}$$

We take the coupling between the states as the perturbation V:

$$V = \begin{pmatrix} 0 & 0 & 0 & 0 & 0 & 0 & 0 & 0 & 0 & 0 \\ 0 & 0 & J & 0 & 0 & 0 & 0 & 0 & 0 & 0 \\ 0 & J & 0 & 0 & 0 & 0 & 0 & 0 & 0 & 0 \\ 0 & 0 & 0 & 0 & \sqrt{2}J & \sqrt{2}J & 0 & 0 & 0 & 0 \\ 0 & 0 & 0 & \sqrt{2}J & 0 & 0 & 0 & 0 & 0 & 0 \\ 0 & 0 & 0 & \sqrt{2}J & 0 & 0 & 0 & 0 & 0 & 0 \\ 0 & 0 & 0 & 0 & 0 & 0 & 0 & \sqrt{3}J & 0 & 0 \\ 0 & 0 & 0 & 0 & 0 & 0 & \sqrt{3}J & 0 & 2J & 0 \\ 0 & 0 & 0 & 0 & 0 & 0 & 0 & 2J & 0 & \sqrt{3}J \\ 0 & 0 & 0 & 0 & 0 & 0 & 0 & 0 & \sqrt{3}J & 0 \end{pmatrix};$$

C.1. Diagonalization

We do a full-diagonalizing transformation as described in section 3.1.1. This perturbative diagonalization is justified, if J<< Δ=ω1-ω2.

```
Hextra1 = V;
S1 = Table[If[n==m, 0, -iHextra1[[n,m]]/(H0[[n]][[n]]-H0[[m]][[m]])], {n, 1, dim}, {m, 1, dim}];
Hextra2 = -Commutator[S1, Commutator[S1, H0]]/2 + iCommutator[S1, V];
S2 = Table[If[n==m, 0, -iHextra2[[n,m]]/(H0[[n]][[n]]-H0[[m]][[m]])], {n, 1, dim}, {m, 1, dim}];
Hextra3 = -Commutator[S1, Commutator[S2, H0]]/2 - Commutator[S2, Commutator[S1, H0]]/2  - iCommutator[S1, Commutator[S1, Commutator[S1, H0]]]/6+
iCommutator[S2, V] -  Commutator[S1, Commutator[S1, V]]/2;
S3 = Table[If[n==m, 0, -iHextra3[[n,m]]/(H0[[n]][[n]]-H0[[m]][[m]])], {n, 1, dim}, {m, 1, dim}];
Hextra4 = -Commutator[S2, Commutator[S2, H0]]/2 - Commutator[S3, Commutator[S1, H0]]/2  - Commutator[S1, Commutator[S3, H0]]/2 -
iCommutator[S1, Commutator[S1, Commutator[S2, H0]]]/6 - iCommutator[S1, Commutator[S2, Commutator[S1, H0]]]/6 - iCommutator[S2, Commutator[S1, Commutator[S1, H0]]]/6 +
Commutator[S1, Commutator[S1, Commutator[S1, Commutator[S1, H0]]]]/24 + iCommutator[S3, V] -  Commutator[S1, Commutator[S2, V]]/2 -  Commutator[S2, Commutator[S1, V]]/2-
iCommutator[S1, Commutator[S1, Commutator[S1, V]]]/6;
S4 = Table[If[n==m, 0, -iHextra4[[n,m]]/(H0[[n]][[n]]-H0[[m]][[m]])], {n, 1, dim}, {m, 1, dim}];

(H1 = Simplify[iCommutator[S1, H0] + Hextra1])//MatrixForm;
```

(H2 = FullSimplify[(*i*Commutator[S2, H0] + Hextra2)/.*ω*1->*ω*2 + Δ/.*ω*2->*ω*1 − Δ])//MatrixForm;

(H3 = Simplify[*i*Commutator[S3, H0] + Hextra3])//MatrixForm;

(H4 = FullSimplify[(*i*Commutator[S4, H0] + Hextra4)/.*ω*1->*ω*2 + Δ/.*ω*2->*ω*1 − Δ])//MatrixForm;

This is the effective Hamiltonian up to second order in J:

(Heff2 = Simplify[H0 + a^2 * H2/.*a* → 1])//MatrixForm;

C.2. Multilevel Schrieffer-Wolff transformation

In the following part, we will just keep terms up to first order in J. This means, that we will work with Heff=H0, as we neglect the dispersive shifts which are of second order in J. We will use the S we just derived in order to transfer the drive Hamiltonian to the diagonalized frame up to first order in J.
First, we go to a rotating frame at frequency ωd, which is close to the average value of ω1 and ω2 with a small detuning δ:

ωd = (*ω*1 + *ω*2)/2 − *δ*;

n1plusn2 corresponds to the sum of the number operators n1+n2 for the levels 00,01,10,11,02,20,03,12,21,30:

n1plusn2 =
$$\begin{pmatrix} 0&0&0&0&0&0&0&0&0&0\\ 0&1&0&0&0&0&0&0&0&0\\ 0&0&1&0&0&0&0&0&0&0\\ 0&0&0&2&0&0&0&0&0&0\\ 0&0&0&0&2&0&0&0&0&0\\ 0&0&0&0&0&2&0&0&0&0\\ 0&0&0&0&0&0&3&0&0&0\\ 0&0&0&0&0&0&0&3&0&0\\ 0&0&0&0&0&0&0&0&3&0\\ 0&0&0&0&0&0&0&0&0&3 \end{pmatrix};$$

(*U* = MatrixExp[*iω**d**t*n1plusn2])//MatrixForm;**

(Udag = MatrixExp[−*iω**d**t*n1plusn2])//MatrixForm;**

(Udot = *D*[*U*, *t*])//MatrixForm;

(H0rot = FullSimplify[(*U*.H0.Udag + *i* * Udot.Udag)])//MatrixForm

$$\begin{pmatrix} 0&0&0&0&0&0&0&0&0&0\\ 0&\frac{1}{2}(2\delta-\omega1+\omega2)&0&0&0&0&0&0&0&0\\ 0&0&\frac{1}{2}(2\delta+\omega1-\omega2)&0&0&0&0&0&0&0\\ 0&0&0&2\delta&0&0&0&0&0&0\\ 0&0&0&0&2\delta+\delta2-\omega1+\omega2&0&0&0&0&0\\ 0&0&0&0&0&2\delta+\delta1+\omega1-\omega2&0&0&0&0\\ 0&0&0&0&0&0&\frac{3}{2}(2\delta+2\delta2-\omega1+\omega2)&0&0&0\\ 0&0&0&0&0&0&0&\frac{1}{2}(6\delta+2\delta2-\omega1+\omega2)&0&0\\ 0&0&0&0&0&0&0&0&\frac{1}{2}(6\delta+2\delta1+\omega1-\omega2)&0\\ 0&0&0&0&0&0&0&0&0&\frac{3}{2}(2\delta+2\delta1+\omega1-\omega2) \end{pmatrix}$$

This is the diagonalized Hamiltonian in the rotating frame. We use the matrix F to swap the levels 01 with 11 and 10 with 20 while the other levels stay where they are, i.e. we now have the

order 00,11,20,01,02,10,03,12,21,30. There are two possible resonance conditions:
for $\Delta \to$-$\delta 1$ the low energy subspace is spanned by the states 00,11 and 20, while for $\Delta \to \delta 2$ the low energy subspace would be 00,11 and 02.

$$\boldsymbol{F} = \begin{pmatrix} 1 & 0 & 0 & 0 & 0 & 0 & 0 & 0 & 0 & 0 \\ 0 & 0 & 0 & 1 & 0 & 0 & 0 & 0 & 0 & 0 \\ 0 & 0 & 0 & 0 & 0 & 1 & 0 & 0 & 0 & 0 \\ 0 & 1 & 0 & 0 & 0 & 0 & 0 & 0 & 0 & 0 \\ 0 & 0 & 0 & 0 & 1 & 0 & 0 & 0 & 0 & 0 \\ 0 & 0 & 1 & 0 & 0 & 0 & 0 & 0 & 0 & 0 \\ 0 & 0 & 0 & 0 & 0 & 0 & 1 & 0 & 0 & 0 \\ 0 & 0 & 0 & 0 & 0 & 0 & 0 & 1 & 0 & 0 \\ 0 & 0 & 0 & 0 & 0 & 0 & 0 & 0 & 1 & 0 \\ 0 & 0 & 0 & 0 & 0 & 0 & 0 & 0 & 0 & 1 \end{pmatrix};$$

(H0 = FullSimplify[(Transpose[$\boldsymbol{F}$].H0rot.$\boldsymbol{F}$)/.ωd->(ω1 + ω2)/2 − δ/.ω1 → Δ + ω2/.ω2 → ω1 − Δ])//MatrixForm

$$\begin{pmatrix} 0 & 0 & 0 & 0 & 0 & 0 & 0 & 0 & 0 & 0 \\ 0 & 2\delta & 0 & 0 & 0 & 0 & 0 & 0 & 0 & 0 \\ 0 & 0 & 2\delta + \Delta + \delta 1 & 0 & 0 & 0 & 0 & 0 & 0 & 0 \\ 0 & 0 & 0 & \delta - \frac{\Delta}{2} & 0 & 0 & 0 & 0 & 0 & 0 \\ 0 & 0 & 0 & 0 & 2\delta - \Delta + \delta 2 & 0 & 0 & 0 & 0 & 0 \\ 0 & 0 & 0 & 0 & 0 & \delta + \frac{\Delta}{2} & 0 & 0 & 0 & 0 \\ 0 & 0 & 0 & 0 & 0 & 0 & 3\delta - \frac{3\Delta}{2} + 3\delta 2 & 0 & 0 & 0 \\ 0 & 0 & 0 & 0 & 0 & 0 & 0 & 3\delta - \frac{\Delta}{2} + \delta 2 & 0 & 0 \\ 0 & 0 & 0 & 0 & 0 & 0 & 0 & 0 & 3\delta + \frac{\Delta}{2} + \delta 1 & 0 \\ 0 & 0 & 0 & 0 & 0 & 0 & 0 & 0 & 0 & \frac{3}{2}(2\delta + \Delta + 2\delta 1) \end{pmatrix}$$

These are again help-matrices corresponding to the transmon lowering operators c1 and c2 for the levels 00,01,10,11,02,20,03,12,21,30, which we need for the drive:

$$\mathbf{c1} = \begin{pmatrix} 0 & 0 & 1 & 0 & 0 & 0 & 0 & 0 & 0 & 0 \\ 0 & 0 & 0 & 1 & 0 & 0 & 0 & 0 & 0 & 0 \\ 0 & 0 & 0 & 0 & 0 & \sqrt{2} & 0 & 0 & 0 & 0 \\ 0 & 0 & 0 & 0 & 0 & 0 & 0 & 0 & \sqrt{2} & 0 \\ 0 & 0 & 0 & 0 & 0 & 0 & 0 & 1 & 0 & 0 \\ 0 & 0 & 0 & 0 & 0 & 0 & 0 & 0 & 0 & \sqrt{3} \\ 0 & 0 & 0 & 0 & 0 & 0 & 0 & 0 & 0 & 0 \\ 0 & 0 & 0 & 0 & 0 & 0 & 0 & 0 & 0 & 0 \\ 0 & 0 & 0 & 0 & 0 & 0 & 0 & 0 & 0 & 0 \\ 0 & 0 & 0 & 0 & 0 & 0 & 0 & 0 & 0 & 0 \end{pmatrix};$$

$$c2 = \begin{pmatrix} 0 & 1 & 0 & 0 & 0 & 0 & 0 & 0 & 0 & 0 \\ 0 & 0 & 0 & 0 & \sqrt{2} & 0 & 0 & 0 & 0 & 0 \\ 0 & 0 & 0 & 1 & 0 & 0 & 0 & 0 & 0 & 0 \\ 0 & 0 & 0 & 0 & 0 & 0 & 0 & \sqrt{2} & 0 & 0 \\ 0 & 0 & 0 & 0 & 0 & 0 & \sqrt{3} & 0 & 0 & 0 \\ 0 & 0 & 0 & 0 & 0 & 0 & 0 & 0 & 1 & 0 \\ 0 & 0 & 0 & 0 & 0 & 0 & 0 & 0 & 0 & 0 \\ 0 & 0 & 0 & 0 & 0 & 0 & 0 & 0 & 0 & 0 \\ 0 & 0 & 0 & 0 & 0 & 0 & 0 & 0 & 0 & 0 \\ 0 & 0 & 0 & 0 & 0 & 0 & 0 & 0 & 0 & 0 \end{pmatrix};$$

We transfer these operators to the diagonalized frame, using the Schrieffer-Wolff transformation defined above.

```
(A = FullSimplify [IdentityMatrix[dim] - iS1λ - iS2λ^2 - S1.S1 λ^2/2/.ω1 → Δ + ω2/.ω2 → ω1 - Δ]) //MatrixForm;

(tc1 = Simplify[Normal[Series[(Transpose[A].c1.A), {a, 0, 1}]]/.a → 1])//MatrixForm;

(tc2 = Simplify[Normal[Series[Transpose[A].c2.A, {a, 0, 1}]]/.a → 1])//MatrixForm;
```

The drive Hamiltonian in the diagonalized frame is:

```
(Hd = Ω1/2 (Transpose[tc1] * Exp[-I(ωd * t + ϕ)] + tc1 * Exp[I(ωd * t + ϕ)]) +  Ω2/2 (Transpose[tc2] * Exp[-I(ωd * t + ϕ)] + tc2 * Exp[I(ωd * t + ϕ)])) //MatrixForm;
```

In the rotating frame, this is not time-dependent anymore:

```
(V = FullSimplify[Transpose[F].(U.Hd.Udag).F])//MatrixForm;
```

Now, we do a Schrieffer-Wolff transformation in order to decouple the low-energy manifold 00,11,20 from the high-energy levels. The drive can be treated as a perturbation, if the its amplitude is much smaller than the detuning, i.e. Ω1,Ω2<< Δ.

```
diml = 3;

Hl0 = Chop[Table[H0[[n, m]], {n, 1, diml}, {m, 1, diml}]];
Hh0 = Chop[Table[H0[[n, m]], {n, diml + 1, dim}, {m, diml + 1, dim}]];
Hextra1 = V;
Hl1 = Chop[Table[Hextra1[[n, m]], {n, 1, diml}, {m, 1, diml}]];
Hh1 = Chop[Table[Hextra1[[n, m]], {n, diml + 1, dim}, {m, diml + 1, dim}]];
S1 = Table [If [(m < diml + 1&&n < diml + 1)||(m > diml&&n > diml), 0, -i Hextra1[[n,m]]/(H0[[n,n]]-H0[[m,m]])] , {n, 1, dim}, {m, 1, dim}] ;
Hextra2 = -Commutator[S1, Commutator[S1, H0]]/2 + iCommutator[S1, V];
(Hl2 = Chop[Table[Hextra2[[n, m]], {n, 1, diml}, {m, 1, diml}]])//MatrixForm;
Hh2 = Chop[Table[Hextra2[[n, m]], {n, diml + 1, dim}, {m, diml + 1, dim}]];
```

The effective Hamiltonian tranformed back to the original order of levels is

```
(Htemp = F.ArrayFlatten[{{Hl0 + aHl1 + a^2Hl2, 0}, {0, Hh0 + aHh1 + a^2Hh2}}].Transpose[F]/.a → 1)//MatrixForm;
```

The effective Hamiltonian to second order in J and Ω1,2 for the computational levels 00,01,10,11 only is

```
(Hqubit = Simplify[Chop[Table[Htemp[[n, m]], {n, 1, 4}, {m, 1, 4}]]/.{a → 1}])//MatrixForm;
```

This Hamiltonian has only terms on the diagonal and the off-diagonal. The terms on the diagonal can be composed of II, IZ, ZI and ZZ-terms:

```
αIIII + αIZ/2IZ + αZI/2ZI + αZZ/4ZZ//MatrixForm
```

$$\begin{pmatrix} \alpha\text{II} + \frac{\alpha\text{IZ}}{2} + \frac{\alpha\text{ZI}}{2} + \frac{\alpha\text{ZZ}}{4} & 0 & 0 & 0 \\ 0 & \alpha\text{II} - \frac{\alpha\text{IZ}}{2} + \frac{\alpha\text{ZI}}{2} - \frac{\alpha\text{ZZ}}{4} & 0 & 0 \\ 0 & 0 & \alpha\text{II} + \frac{\alpha\text{IZ}}{2} - \frac{\alpha\text{ZI}}{2} - \frac{\alpha\text{ZZ}}{4} & 0 \\ 0 & 0 & 0 & \alpha\text{II} - \frac{\alpha\text{IZ}}{2} - \frac{\alpha\text{ZI}}{2} + \frac{\alpha\text{ZZ}}{4} \end{pmatrix}$$

We can find the corresponding constants by solving a system of equations:

```
{αII, αIZ, αZI, αZZ} =
Flatten[{w, x, y, z}/.Solve[{w + x/2 + y/2 + z/4 == Hqubit[[1]][[1]], w - x/2 + y/2 - z/4 == Hqubit[[2]][[2]], w + x/2 - y/2 - z/4 == Hqubit[[3]][[3]], w - x/2 - y/2 + z/4 == Hqubit[[4]][[4]]},
{w, x, y, z}]];
```

To first order in J, this is:

```
FullSimplify[Normal[Series[αZZ, {J, 0, 1}]]]
FullSimplify[Normal[Series[αIZ, {J, 0, 1}]]]
FullSimplify[Normal[Series[αZI, {J, 0, 1}]]]
FullSimplify[Normal[Series[(αIZ + αZI)/2, {J, 0, 1}]]];
FullSimplify[Normal[Series[(αIZ - αZI)/2, {J, 0, 1}]]];
```

$$\frac{\Omega 2\left(2J\left(\left(4\delta^2-\Delta^2\right)(2\delta+\Delta+2\delta 1)+16\Delta\delta 1\delta 2-16\delta 1\delta 2^2\right)\Omega 1-\left(4\delta^2-\Delta^2\right)(2\delta+\Delta+2\delta 1)(\Delta-\delta 2)\Omega 2\right)}{\left(4\delta^2-\Delta^2\right)(2\delta+\Delta+2\delta 1)(\Delta-\delta 2)(2\delta-\Delta+2\delta 2)}$$

$$-(-2\delta+\Delta)^2(2\delta-\Delta+2\delta 2)+\frac{2J\left((2\delta-\Delta)(2\delta+\Delta+2\delta 1)+8\Delta\delta 2-8\delta 2^2\right)\Omega 1\Omega 2}{(2\delta+\Delta+2\delta 1)(\Delta-\delta 2)}+(-2\delta+\Delta-4\delta 2)\Omega 2^2$$
$$2(2\delta-\Delta)(2\delta-\Delta+2\delta 2)$$

$$\frac{(-2\delta+\Delta-2\delta 2)(\Delta-\delta 2)\left((2\delta+\Delta)^2(2\delta+\Delta+2\delta 1)+4\delta 1\Omega 1^2\right)-2J\left(4\delta^2+\Delta^2-6\Delta\delta 1+4\delta(\Delta+\delta 1)+8\delta 1\delta 2\right)\Omega 1\Omega 2+(2\delta+\Delta)(2\delta+\Delta+2\delta 1)(\Delta-\delta 2)\Omega 2^2}{2(2\delta+\Delta)(2\delta+\Delta+2\delta 1)(\Delta-\delta 2)(2\delta-\Delta+2\delta 2)}$$

In the pure qubit limit, where $\delta 1$, $\delta 2 \to$ Infinity, these expressions reduce to the qubit expressions!

```
Limit[Normal[Series[αZZ, {J, 0, 1}]]/.{δ1 → δ2}, δ2 → Infinity]
FullSimplify[Limit[Normal[Series[(αIZ + αZI)/2, {J, 0, 1}]]/.{δ1 → δ2}, δ2 → Infinity]]
FullSimplify[Limit[Normal[Series[(αIZ - αZI)/2, {J, 0, 1}]]/.{δ1 → δ2}, δ2 → Infinity]]
```

$$\frac{8J\Omega 1\Omega 2}{4\delta^2-\Delta^2}$$

$$-\delta-\frac{\Omega 1^2}{2(2\delta+\Delta)}-\frac{\Omega 2^2}{4\delta-2\Delta}$$

$$\frac{1}{2}\left(\Delta+\frac{\Omega 1^2}{2\delta+\Delta}-\frac{\Omega 2^2}{2\delta-\Delta}\right)$$

αIZ and αZI for exemplary values as a function of δ. For δ around zero, αIZ is almost equal to -αZI, so δ can be chosen such that αIZ+αZI=0:

```
αIZ = FullSimplify[αIZ/.{J → 1, δ1 → -10, δ2 → -8, Ω1 → 1, Ω2 → 1, Δ → 12}];
αZI = FullSimplify[αZI/.{J → 1, δ1 → -10, δ2 → -8, Ω1 → 1, Ω2 → 1, Δ → 12}];
Plot[{αIZ, αZI}, {δ, -20, 20}, PlotStyle → {Green, Blue}]
```

The terms on the off-diagonal can be decomposed into XX, XY, YX and YY-terms:

αXXXX + αXYXY + αYXYX + αYYYY//MatrixForm

$$\begin{pmatrix} 0 & 0 & 0 & \alpha\mathrm{XX} - i\alpha\mathrm{XY} - i\alpha\mathrm{YX} - \alpha\mathrm{YY} \\ 0 & 0 & \alpha\mathrm{XX} + i\alpha\mathrm{XY} - i\alpha\mathrm{YX} + \alpha\mathrm{YY} & 0 \\ 0 & \alpha\mathrm{XX} - i\alpha\mathrm{XY} + i\alpha\mathrm{YX} + \alpha\mathrm{YY} & 0 & 0 \\ \alpha\mathrm{XX} + i\alpha\mathrm{XY} + i\alpha\mathrm{YX} - \alpha\mathrm{YY} & 0 & 0 & 0 \end{pmatrix}$$

We want to write them like this:

FullSimplify[ΩBCos[2ϕ]/4(XX − YY) + ΩBSin[2ϕ]/4(XY + YX) + ΩS/2(XX + YY)]//MatrixForm

$$\begin{pmatrix} 0 & 0 & 0 & \frac{1}{2}e^{-2i\phi}\Omega\mathrm{B} \\ 0 & 0 & \Omega\mathrm{S} & 0 \\ 0 & \Omega\mathrm{S} & 0 & 0 \\ \frac{1}{2}e^{2i\phi}\Omega\mathrm{B} & 0 & 0 & 0 \end{pmatrix}$$

We can see that ΩB/2=|Hqubit[[1,4]]|=|Hqubit[[4,1]]| and ΩS=Htemp[[2,3]]=Htemp[[3,2]]:

ΩB = 2FullSimplify[Htemp[[1, 4]]/Exp[2Iϕ]]

ΩS = FullSimplify[Htemp[[2, 3]]]

$$\frac{2J\left(\delta1(\Delta-\delta2)\Omega1^2+J(\delta1+\delta2)\Omega1\Omega2-(\Delta+\delta1)\delta2\Omega2^2\right)}{\left(4\delta^2-\Delta^2\right)(\Delta+\delta1)(\Delta-\delta2)}$$

$$\Big(2J\left(-\Delta^2\delta1(\Delta+\delta1)(\Delta-\delta2)\Omega1((\Delta+\delta1)\Omega1+J\Omega2)+4\delta^3\Omega2\left(J\left(-\delta1^2+\Delta\delta2\right)\Omega1-(\Delta+\delta1)^2\delta2\Omega2\right)+4\delta^2(\Delta+\delta1)\left(-\delta1(\Delta+\delta1)(\Delta-\delta2)\Omega1^2+J(-\delta1(\Delta+2\delta1)+(2\Delta+\delta1)\delta2)\Omega1\Omega2-2(\Delta+\delta1)^2\delta2\Omega2^2\right)\right)$$
$$+\delta\left(-4\delta1(\Delta+\delta1)^3(\Delta-\delta2)\Omega1^2+J\left(12\Delta\delta1^2(-\delta1+\delta2)+4\delta1^3(-\delta1+\delta2)+\Delta^3(-4\delta1+3\delta2)+\Delta^2\delta1(-11\delta1+12\delta2)\right)\Omega1\Omega2-(\Delta+\delta1)^2(\Delta+2\delta1)(3\Delta+2\delta1)\delta2\Omega2^2\right)\Big)$$
$$/\left((2\delta-\Delta)\Delta(2\delta+\Delta)(\Delta+\delta1)^2(2\delta+\Delta+2\delta1)(2\delta+3\Delta+2\delta1)(\Delta-\delta2)\right)$$

ΩB is only slightly bigger than ΩS for δ around zero and exemplary values of the other quantities:

```
ΩB = 2FullSimplify[Htemp[[1, 4]]/Exp[2Iϕ]/.{J → 1, δ1 → −10, δ2 → −8, Ω1 → 1, Ω2 → 1, Δ → 12}];
ΩS = FullSimplify[Htemp[[2, 3]]/.{J → 1, δ1 → −10, δ2 → −8, Ω1 → 1, Ω2 → 1, Δ → 12}];
Plot[{Abs[ΩB], Abs[ΩS]}, {δ, −1, 1}, PlotStyle → {Green, Blue}]
```

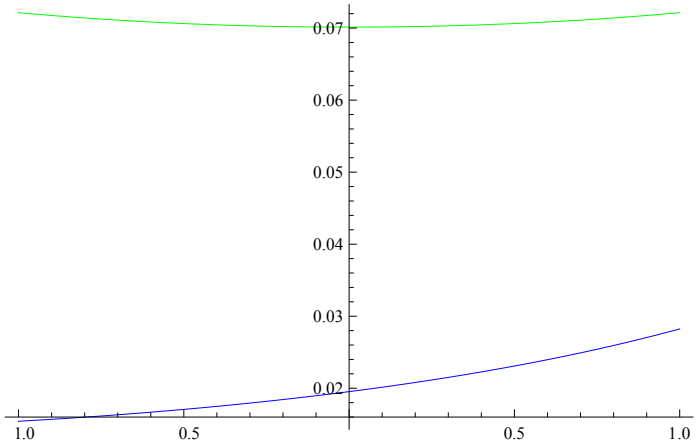

ΩB and ΩS both go to infinity for the resonance cases Δ=-δ1 and Δ=δ2:

```
ΩB = 2FullSimplify[Htemp[[1, 4]]/Exp[2Iϕ]/.{J → 1, δ1 → −10, δ2 → −8, Ω1 → 1, Ω2 → 1, δ → 0.01}];
ΩS = FullSimplify[Htemp[[2, 3]]/.{J → 1, δ1 → −10, δ2 → −8, Ω1 → 1, Ω2 → 1, δ → 0.01}];
Plot[{Abs[ΩB], Abs[ΩS]}, {Δ, 5, 15}, PlotStyle → {Green, Blue}]
Plot[{Abs[ΩB], Abs[ΩS]}, {Δ, −13, −3}, PlotStyle → {Green, Blue}]
```

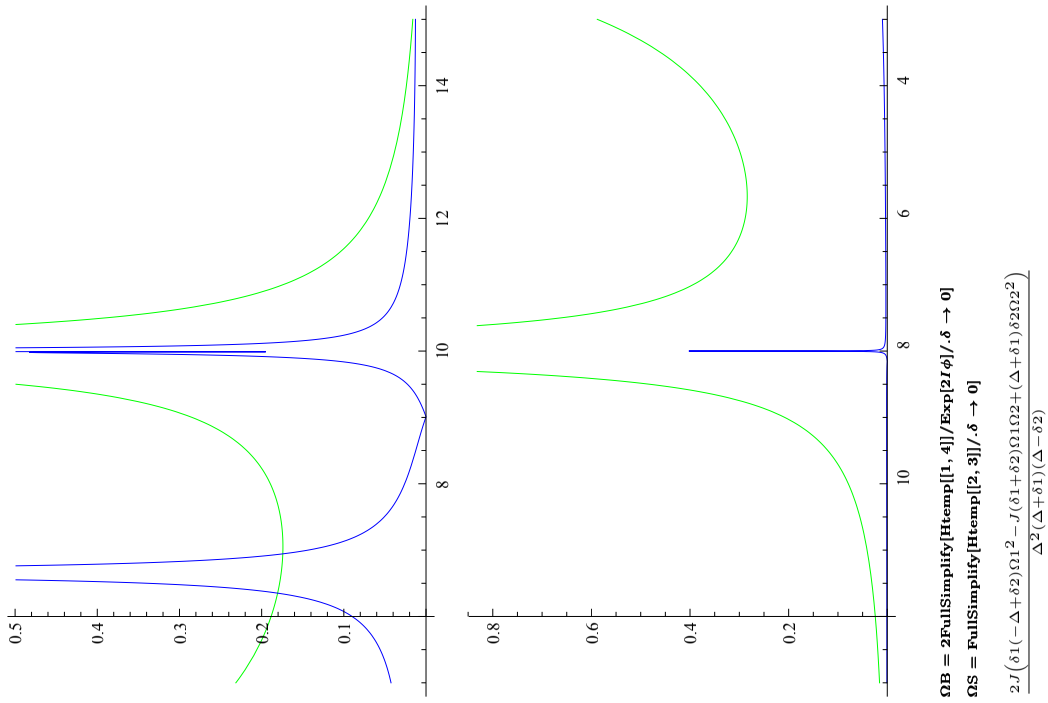

ΩB = 2FullSimplify[Htemp[[1, 4]]/Exp[2 I ϕ]/.δ → 0]

ΩS = FullSimplify[Htemp[[2, 3]]/.δ → 0]

$$\frac{2J\left(\delta 1(-\Delta+\delta 2)\Omega 1^2-J(\delta 1+\delta 2)\Omega 1\Omega 2+(\Delta+\delta 1)\delta 2\Omega 2^2\right)}{\Delta^2(\Delta+\delta 1)(\Delta-\delta 2)}$$

$\frac{2J\delta1\Omega1((\Delta+\delta1)\Omega1+J\Omega2)}{\Delta(\Delta+\delta1)(\Delta+2\delta1)(3\Delta+2\delta1)}$

In the pure qubit limit, where $\delta1$, $\delta2\to$Infinity, these expressions reduce to the qubit expressions!

```
ΩB = Limit[2FullSimplify[Htemp[[1, 4]]/Exp[2Iϕ]]/.{δ1 → δ2}, δ2 → Infinity]
ΩS = Limit[FullSimplify[Htemp[[2, 3]]]/.{δ1 → δ2}, δ2 → Infinity]
```

$$\frac{2J\left(\Omega1^2+\Omega2^2\right)}{4\delta^2-\Delta^2}$$

$$\frac{2J\delta\left(-\Omega1^2+\Omega2^2\right)}{4\delta^2\Delta-\Delta^3}$$

In the case where $\delta1\to0$ and $\delta2\to0$, i.e. when the transmon becomes a harmonic oscillator, Bell Rabi does not work:

```
ΩB = 2FullSimplify[Htemp[[1, 4]]/Exp[2Iϕ]/.{δ1 → 0, δ2 → 0}]
ΩS = FullSimplify[Htemp[[2, 3]]/.{δ1 → 0, δ2 → 0}]
```

0

0

In order for the last Schrieffer-Wolff to be a reasonable transformation,all terms in S should be much smaller than zero.This defines,how close we can get to the resonance condition $\Delta\to$-$\delta1$.

```
FullSimplify[S1/.δ1 → -Δ];
```

There are seven terms in S1 that diverge for $\delta1\to$-Δ:

```
FullSimplify[S1[[2]][[6]]]
```

$$-\frac{ie^{-i\phi}(J(-\Delta+\delta1)\Omega1+\Delta(\Delta+\delta1)\Omega2)}{(2\delta-\Delta)\Delta(\Delta+\delta1)}$$

In order to see,how close we can get to $\delta1\to$-Δ without any big terms in S1,we set the term in S1[[2]][[6]] that diverges for $\delta1\to$-Δ equal to 1:

```
δcrit = Flatten[δ1/.Simplify[Solve[J(-Δ+δ1)Ω1/((δ-Δ/2)Δ(Δ+δ1)) == 1, δ1]]]
```

$$\left\{-\frac{\Delta\left(-2\delta\Delta+\Delta^2-2J\Omega1\right)}{-2\delta\Delta+\Delta^2+2J\Omega1}\right\}$$

This is an estimation for how close $\delta1$ can get to-Δ,to first order in J:

```
Normal[Series[δcrit, {J, 0, 1}]]
```

$$\left\{-\Delta+\frac{4J\Omega1}{-2\delta+\Delta}\right\}$$

```
ΩB = 2FullSimplify[Htemp[[1, 4]]/Exp[2Iϕ]/.δ1 → δcrit]
```

$$\left\{-\frac{\Delta(\Delta-\delta2)\Omega1\left(2\delta\Delta-\Delta^2+2J\Omega1\right)+J((2\delta-\Delta)\Delta(\Delta-\delta2)+2J(\Delta+\delta2)\Omega1)\Omega2-4J\Delta\delta2\Omega2^2}{2\Delta\left(-4\delta^2+\Delta^2\right)(\Delta-\delta2)}\right\}$$

C.3. Interpretation

The Hamiltonian has only terms on the diagonal and the off diagonal. We saw above that we can write it like this:

```
Clear[αIZ, αZI, αZZ, ΩS, ΩBR, ΩBI, ΩB];
(H = FullSimplify[αIZ/2IZ + αZI/2ZI + αZZ/4ZZ + ΩBCos[2ϕ]/4(XX − YY) + ΩBSin[2ϕ]/4(XY + YX) + ΩS/2(XX + YY)])//MatrixForm
```

$$\begin{pmatrix} \frac{1}{4}(2(\alpha\mathrm{IZ}+\alpha\mathrm{ZI})+\alpha\mathrm{ZZ}) & 0 & 0 & \frac{1}{2}e^{-2i\phi}\Omega\mathrm{B} \\ 0 & \frac{1}{4}(-2\alpha\mathrm{IZ}+2\alpha\mathrm{ZI}-\alpha\mathrm{ZZ}) & \Omega\mathrm{S} & 0 \\ 0 & \Omega\mathrm{S} & \frac{1}{4}(2\alpha\mathrm{IZ}-2\alpha\mathrm{ZI}-\alpha\mathrm{ZZ}) & 0 \\ \frac{1}{2}e^{2i\phi}\Omega\mathrm{B} & 0 & 0 & \frac{1}{4}(-2(\alpha\mathrm{IZ}+\alpha\mathrm{ZI})+\alpha\mathrm{ZZ}) \end{pmatrix}$$

We can choose δ such that αIZ+αZI=0:

αZI = $-\alpha$IZ;

We divide H into three commuting parts:

HZZ = $\begin{pmatrix} \frac{\alpha ZZ}{4} & 0 & 0 & 0 \\ 0 & -\frac{\alpha ZZ}{4} & 0 & 0 \\ 0 & 0 & -\frac{\alpha ZZ}{4} & 0 \\ 0 & 0 & 0 & \frac{\alpha ZZ}{4} \end{pmatrix}$;

HSZ = $\begin{pmatrix} \frac{(\alpha IZ+\alpha ZI)}{2} & 0 & 0 & 0 \\ 0 & \frac{(-\alpha IZ+\alpha ZI)}{2} & \Omega S & 0 \\ 0 & \Omega S & \frac{(\alpha IZ-\alpha ZI)}{2} & 0 \\ 0 & 0 & 0 & -\frac{(\alpha IZ+\alpha ZI)}{2} \end{pmatrix}$;

HB = $\begin{pmatrix} 0 & 0 & 0 & \frac{1}{2}e^{-2i\phi}\Omega B \\ 0 & 0 & 0 & 0 \\ 0 & 0 & 0 & 0 \\ \frac{1}{2}e^{2i\phi}\Omega B & 0 & 0 & 0 \end{pmatrix}$;

Commutator[HZZ, HSZ]

Commutator[HZZ, HB]

Commutator[HB, HSZ]

Simplify[H − HZZ − HSZ − HB]

{{0, 0, 0, 0}, {0, 0, 0, 0}, {0, 0, 0, 0}, {0, 0, 0, 0}}

{{0, 0, 0, 0}, {0, 0, 0, 0}, {0, 0, 0, 0}, {0, 0, 0, 0}}

{{0, 0, 0, 0}, {0, 0, 0, 0}, {0, 0, 0, 0}, {0, 0, 0, 0}}

{{0, 0, 0, 0}, {0, 0, 0, 0}, {0, 0, 0, 0}, {0, 0, 0, 0}}

The evolution generated by these Hamiltonians is:

(UZZ = MatrixExp[$-It$HZZ])//MatrixForm

(USZ = FullSimplify[MatrixExp[$-It$HSZ], {αIZ > 0, ΩS > 0}])//MatrixForm

(UB = MatrixExp[$-It$HB])//MatrixForm

$$\begin{pmatrix} e^{-\frac{1}{4}it\alpha ZZ} & 0 & 0 & 0 \\ 0 & e^{\frac{it\alpha ZZ}{4}} & 0 & 0 \\ 0 & 0 & e^{\frac{it\alpha ZZ}{4}} & 0 \\ 0 & 0 & 0 & e^{-\frac{1}{4}it\alpha ZZ} \end{pmatrix}$$

$$\begin{pmatrix} 1 & 0 & 0 & 0 \\ 0 & \mathrm{Cos}\left[t\sqrt{\alpha \mathrm{IZ}^2+\Omega \mathrm{S}^2}\right]+\frac{i\alpha \mathrm{IZSin}\left[t\sqrt{\alpha \mathrm{IZ}^2+\Omega \mathrm{S}^2}\right]}{\sqrt{\alpha \mathrm{IZ}^2+\Omega \mathrm{S}^2}} & -\frac{i\Omega \mathrm{SSin}\left[t\sqrt{\alpha \mathrm{IZ}^2+\Omega \mathrm{S}^2}\right]}{\sqrt{\alpha \mathrm{IZ}^2+\Omega \mathrm{S}^2}} & 0 \\ 0 & -\frac{i\Omega \mathrm{SSin}\left[t\sqrt{\alpha \mathrm{IZ}^2+\Omega \mathrm{S}^2}\right]}{\sqrt{\alpha \mathrm{IZ}^2+\Omega \mathrm{S}^2}} & \mathrm{Cos}\left[t\sqrt{\alpha \mathrm{IZ}^2+\Omega \mathrm{S}^2}\right]-\frac{i\alpha \mathrm{IZSin}\left[t\sqrt{\alpha \mathrm{IZ}^2+\Omega \mathrm{S}^2}\right]}{\sqrt{\alpha \mathrm{IZ}^2+\Omega \mathrm{S}^2}} & 0 \\ 0 & 0 & 0 & 1 \end{pmatrix}$$

$$\begin{pmatrix} \mathrm{Cos}\left[\frac{t\Omega \mathrm{B}}{2}\right] & 0 & 0 & -ie^{-2i\phi}\mathrm{Sin}\left[\frac{t\Omega \mathrm{B}}{2}\right] \\ 0 & 1 & 0 & 0 \\ 0 & 0 & 1 & 0 \\ -ie^{2i\phi}\mathrm{Sin}\left[\frac{t\Omega \mathrm{B}}{2}\right] & 0 & 0 & \mathrm{Cos}\left[\frac{t\Omega \mathrm{B}}{2}\right] \end{pmatrix}$$

U = MatrixExp[$-ItH$];

FullSimplify[U − UZZ.USZ.UB, {αIZ > 0, ΩS > 0}]

{{0, 0, 0, 0}, {0, 0, 0, 0}, {0, 0, 0, 0}, {0, 0, 0, 0}}

UZZ creates phase factors only, but USZ entangles the states 01 and 10, while UB is the Bell-Rabi part that entangles the states 00 and 11.

D. Map gate

This calculation was executed using *mathematica* and is based on the work of Jay Gambetta.

Consider two transmons that are coupled via a transmission line resonator. By exploiting certain resonance conditions of the higher transmon levels, a ZZ interaction is induced via an external microwave drive.

```
sx = {{0, 1}, {1, 0}};
sy = {{0, -I}, {I, 0}};
sz = {{1, 0}, {0, -1}};
si = {{1, 0}, {0, 1}};
sm = {{0, 1}, {0, 0}};
sp = {{0, 0}, {1, 0}};

ZZ = KroneckerProduct[sz, sz];
II = KroneckerProduct[si, si];
IZ = KroneckerProduct[si, sz];
ZI = KroneckerProduct[sz, si];

λ = a;
dim = 10;

Commutator[A_, B_]:=A.B - B.A;
dagger[a_]:=Transpose[Conjugate[a]];
```

The eigenvalues of the unperturbed two-transmon Hamiltonian are

```
En[n1_, n2_]:= (ω1 - δ1/2) n1 + δ1/2 n1^2 + (ω2 - δ2/2) n2 + δ2/2 n2^2
```

where $\omega 1$ and $\omega 2$ are the transmon frequencies, $\delta 1$ and $\delta 2$ their anharmonicities and n1 and n2 are the number operators for transmon one and two, respectively.
The corresponding Hamiltonian for the levels 00,01,10,11,02,20,03,12,21,30 is

```
(H0 = DiagonalMatrix[{En[0, 0], En[0, 1], En[1, 0], En[1, 1], En[0, 2], En[2, 0], En[0, 3], En[1, 2], En[2, 1], En[3, 0]}])//MatrixForm
```

$$\begin{pmatrix}
0 & 0 & 0 & 0 & 0 & 0 & 0 & 0 & 0 & 0 \\
0 & \omega 2 & 0 & 0 & 0 & 0 & 0 & 0 & 0 & 0 \\
0 & 0 & \omega 1 & 0 & 0 & 0 & 0 & 0 & 0 & 0 \\
0 & 0 & 0 & \omega 1+\omega 2 & 0 & 0 & 0 & 0 & 0 & 0 \\
0 & 0 & 0 & 0 & 2\delta 2+2\left(-\frac{\delta 2}{2}+\omega 2\right) & 0 & 0 & 0 & 0 & 0 \\
0 & 0 & 0 & 0 & 0 & 2\delta 1+2\left(-\frac{\delta 1}{2}+\omega 1\right) & 0 & 0 & 0 & 0 \\
0 & 0 & 0 & 0 & 0 & 0 & \frac{9\delta 2}{2}+3\left(-\frac{\delta 2}{2}+\omega 2\right) & 0 & 0 & 0 \\
0 & 0 & 0 & 0 & 0 & 0 & 0 & 2\delta 2+\omega 1+2\left(-\frac{\delta 2}{2}+\omega 2\right) & 0 & 0 \\
0 & 0 & 0 & 0 & 0 & 0 & 0 & 0 & 2\delta 1+2\left(-\frac{\delta 1}{2}+\omega 1\right)+\omega 2 & 0 \\
0 & 0 & 0 & 0 & 0 & 0 & 0 & 0 & 0 & \frac{9\delta 1}{2}+3\left(-\frac{\delta 1}{2}+\omega 1\right)
\end{pmatrix}$$

We will choose the resonance condition Δ=ω1-ω2=2δ2, such that the levels 03 and 12 are aligned. The coupling between these two states yields

$$\mathbf{Hint} = \begin{pmatrix}
0 & 0 & 0 & 0 & 0 & 0 & 0 & 0 & 0 & 0 \\
0 & 0 & 0 & 0 & 0 & 0 & 0 & 0 & 0 & 0 \\
0 & 0 & 0 & 0 & 0 & 0 & 0 & 0 & 0 & 0 \\
0 & 0 & 0 & 0 & 0 & 0 & 0 & 0 & 0 & 0 \\
0 & 0 & 0 & 0 & 0 & 0 & 0 & 0 & 0 & 0 \\
0 & 0 & 0 & 0 & 0 & 0 & 0 & 0 & 0 & 0 \\
0 & 0 & 0 & 0 & 0 & 0 & 0 & \sqrt{3}J & 0 & 0 \\
0 & 0 & 0 & 0 & 0 & 0 & \sqrt{3}J & 0 & 0 & 0 \\
0 & 0 & 0 & 0 & 0 & 0 & 0 & 0 & 0 & 0 \\
0 & 0 & 0 & 0 & 0 & 0 & 0 & 0 & 0 & 0
\end{pmatrix};$$

We want to diagonalize the Hamiltonian in the {03,12}-space only, using the unitary transformation Ud:

```
Ud = IdentityMatrix[10];
Ud[[8, 8]] = Cos[θ];
Ud[[7, 7]] = Cos[θ];
Ud[[7, 8]] = Sin[θ];
Ud[[8, 7]] = −Sin[θ];
Ud//MatrixForm
```

$$\begin{pmatrix}
1 & 0 & 0 & 0 & 0 & 0 & 0 & 0 & 0 & 0 \\
0 & 1 & 0 & 0 & 0 & 0 & 0 & 0 & 0 & 0 \\
0 & 0 & 1 & 0 & 0 & 0 & 0 & 0 & 0 & 0 \\
0 & 0 & 0 & 1 & 0 & 0 & 0 & 0 & 0 & 0 \\
0 & 0 & 0 & 0 & 1 & 0 & 0 & 0 & 0 & 0 \\
0 & 0 & 0 & 0 & 0 & 1 & 0 & 0 & 0 & 0 \\
0 & 0 & 0 & 0 & 0 & 0 & \mathrm{Cos}[\theta] & \mathrm{Sin}[\theta] & 0 & 0 \\
0 & 0 & 0 & 0 & 0 & 0 & -\mathrm{Sin}[\theta] & \mathrm{Cos}[\theta] & 0 & 0 \\
0 & 0 & 0 & 0 & 0 & 0 & 0 & 0 & 1 & 0 \\
0 & 0 & 0 & 0 & 0 & 0 & 0 & 0 & 0 & 1
\end{pmatrix}$$

```
(H0d = FullSimplify[Ud.(H0 + Hint).Transpose[Ud]])//MatrixForm;
```

We choose θ such that the non-diagonal terms disappear.

```
(*√3JCos[2θ] + (-2δ2 + ω1 - ω2)Cos[θ]Sin[θ] == 0*)

(*√3JCos[2θ] + (-2δ2+ω1-ω2)/2 Sin[2θ] == 0*)

(*Tan[2θ] = -2√3J/(-2δ2+ω1-ω2)

Cos[2θ] = (-Δ+2δ2)/√((2√3J)^2+(-2δ2+ω1-ω2)^2)
Sin[2θ] = 2√3J/√((2√3J)^2+(-2δ2+ω1-ω2)^2)
*)
```

The diagonalization leads to a shift $+\xi$ on the level 03 and -ξ on the level 12. The shift yields

```
FullSimplify[Solve[H0[[7]][[7]] + ξ==H0d[[7]][[7]], ξ]/.Sin[2θ] → 2√3J/√((2√3J)^2+(-Δ+2δ2)^2) /. Cos[2θ] → (-Δ+2δ2)/√((2√3J)^2+(-Δ+2δ2)^2) /.ω1 → Δ + ω2]
```

$$\left\{\left\{\xi \to \frac{1}{2}\left(\Delta + \sqrt{12J^2 + (\Delta - 2\delta 2)^2} - 2\delta 2\right)\right\}\right\}$$

```
FullSimplify[Solve[H0[[8]][[8]] - ξ==H0d[[8]][[8]], ξ]/.Sin[2θ] → 2√3J/√((2√3J)^2+(-Δ+2δ2)^2) /. Cos[2θ] → (-Δ+2δ2)/√((2√3J)^2+(-Δ+2δ2)^2) /.ω1 → Δ + ω2]
```

$$\left\{\left\{\xi \to \frac{1}{2}\left(\Delta + \sqrt{12J^2 + (\Delta - 2\delta 2)^2} - 2\delta 2\right)\right\}\right\}$$

We define the transmon lowering operators c1 and c2. Hintd includes what is left of the coupling between the transmons (without the coupling between 03 and 12). H0d is the unperturbed Hamiltonian plus the shifts +-ξ. Htot is Hintd plus a drive at frequency ωd.

```
c1 = {{0,0,1,0,0,0,0,0,0,0},{0,0,0,1,0,0,0,0,0,0},{0,0,0,0,0,√2,0,0,0,0},{0,0,0,0,0,0,0,0,√2,0},{0,0,0,0,0,0,0,1,0,0},{0,0,0,0,0,0,0,0,0,√3},{0,0,0,0,0,0,0,0,0,0},{0,0,0,0,0,0,0,0,0,0},{0,0,0,0,0,0,0,0,0,0},{0,0,0,0,0,0,0,0,0,0}};
```

$$c1 = \begin{pmatrix} 0 & 0 & 1 & 0 & 0 & 0 & 0 & 0 & 0 & 0 \\ 0 & 0 & 0 & 1 & 0 & 0 & 0 & 0 & 0 & 0 \\ 0 & 0 & 0 & 0 & 0 & \sqrt{2} & 0 & 0 & 0 & 0 \\ 0 & 0 & 0 & 0 & 0 & 0 & 0 & 0 & \sqrt{2} & 0 \\ 0 & 0 & 0 & 0 & 0 & 0 & 0 & 1 & 0 & 0 \\ 0 & 0 & 0 & 0 & 0 & 0 & 0 & 0 & 0 & \sqrt{3} \\ 0 & 0 & 0 & 0 & 0 & 0 & 0 & 0 & 0 & 0 \\ 0 & 0 & 0 & 0 & 0 & 0 & 0 & 0 & 0 & 0 \\ 0 & 0 & 0 & 0 & 0 & 0 & 0 & 0 & 0 & 0 \\ 0 & 0 & 0 & 0 & 0 & 0 & 0 & 0 & 0 & 0 \end{pmatrix};$$

$$\mathbf{c2} = \begin{pmatrix} 0 & 1 & 0 & 0 & 0 & 0 & 0 & 0 & 0 & 0 \\ 0 & 0 & 0 & 0 & \sqrt{2} & 0 & 0 & 0 & 0 & 0 \\ 0 & 0 & 0 & 1 & 0 & 0 & 0 & 0 & 0 & 0 \\ 0 & 0 & 0 & 0 & 0 & 0 & 0 & \sqrt{2} & 0 & 0 \\ 0 & 0 & 0 & 0 & 0 & 0 & \sqrt{3} & 0 & 0 & 0 \\ 0 & 0 & 0 & 0 & 0 & 0 & 0 & 0 & 1 & 0 \\ 0 & 0 & 0 & 0 & 0 & 0 & 0 & 0 & 0 & 0 \\ 0 & 0 & 0 & 0 & 0 & 0 & 0 & 0 & 0 & 0 \\ 0 & 0 & 0 & 0 & 0 & 0 & 0 & 0 & 0 & 0 \\ 0 & 0 & 0 & 0 & 0 & 0 & 0 & 0 & 0 & 0 \end{pmatrix};$$

$$(\mathbf{Hintd} = J(\mathbf{dagger[c1].c2} + \mathbf{dagger[c2].c1}) - \mathbf{Hint})\mathbf{//MatrixForm};$$

$$\left(\mathbf{H0d} = \mathbf{H0} + \begin{pmatrix} 0 & 0 & 0 & 0 & 0 & 0 & 0 & 0 & 0 & 0 \\ 0 & 0 & 0 & 0 & 0 & 0 & 0 & 0 & 0 & 0 \\ 0 & 0 & 0 & 0 & 0 & 0 & 0 & 0 & 0 & 0 \\ 0 & 0 & 0 & 0 & 0 & 0 & 0 & 0 & 0 & 0 \\ 0 & 0 & 0 & 0 & 0 & 0 & 0 & 0 & 0 & 0 \\ 0 & 0 & 0 & 0 & 0 & 0 & 0 & 0 & 0 & 0 \\ 0 & 0 & 0 & 0 & 0 & 0 & \xi & 0 & 0 & 0 \\ 0 & 0 & 0 & 0 & 0 & 0 & 0 & -\xi & 0 & 0 \\ 0 & 0 & 0 & 0 & 0 & 0 & 0 & 0 & 0 & 0 \\ 0 & 0 & 0 & 0 & 0 & 0 & 0 & 0 & 0 & 0 \end{pmatrix}\right)\mathbf{//MatrixForm};$$

$$\left(\mathbf{Htot} = \mathbf{Ud.Hintd.Transpose[Ud]} + \mathbf{Ud.}\left(\frac{\Omega}{2}(\mathbf{c1Exp}[I\omega dt] + \mathbf{dagger[c1]Exp}[-I\omega dt] + \mathbf{c2Exp}[I\omega dt] + \mathbf{dagger[c2]Exp}[-I\omega dt])\right)\mathbf{.Transpose[Ud]}\right)\mathbf{//MatrixForm};$$

We go to a rotating frame at frequency ωd via the unity transformation U. n1plusn2 corresponds to the sum of the number operators n1+n2 for the levels 00,01,10,11,02,20,03,12,21,30.

$$\mathbf{n1plusn2} = \begin{pmatrix} 0 & 0 & 0 & 0 & 0 & 0 & 0 & 0 & 0 & 0 \\ 0 & 1 & 0 & 0 & 0 & 0 & 0 & 0 & 0 & 0 \\ 0 & 0 & 1 & 0 & 0 & 0 & 0 & 0 & 0 & 0 \\ 0 & 0 & 0 & 2 & 0 & 0 & 0 & 0 & 0 & 0 \\ 0 & 0 & 0 & 0 & 2 & 0 & 0 & 0 & 0 & 0 \\ 0 & 0 & 0 & 0 & 0 & 2 & 0 & 0 & 0 & 0 \\ 0 & 0 & 0 & 0 & 0 & 0 & 3 & 0 & 0 & 0 \\ 0 & 0 & 0 & 0 & 0 & 0 & 0 & 3 & 0 & 0 \\ 0 & 0 & 0 & 0 & 0 & 0 & 0 & 0 & 3 & 0 \\ 0 & 0 & 0 & 0 & 0 & 0 & 0 & 0 & 0 & 3 \end{pmatrix};$$

$$(U = \mathbf{MatrixExp}[i\omega dt\,\mathbf{n1plusn2}])\mathbf{//MatrixForm};$$

$$(\mathbf{Udag} = \mathbf{MatrixExp}[-i\omega dt\,\mathbf{n1plusn2}])\mathbf{//MatrixForm};$$

$$(\mathbf{Udot} = D[U, t])\mathbf{//MatrixForm};$$

$$(\mathbf{H0rot} = \mathbf{FullSimplify}[(U.\mathbf{H0d.Udag} + i * \mathbf{Udot.Udag})])\mathbf{//MatrixForm}$$

$$\begin{pmatrix} 0 & 0 & 0 & 0 & 0 & 0 & 0 & 0 & 0 & 0 \\ 0 & \omega 2-\omega \mathrm{d} & 0 & 0 & 0 & 0 & 0 & 0 & 0 & 0 \\ 0 & 0 & \omega 1-\omega \mathrm{d} & 0 & 0 & 0 & 0 & 0 & 0 & 0 \\ 0 & 0 & 0 & \omega 1+\omega 2-2\omega \mathrm{d} & 0 & 0 & 0 & 0 & 0 & 0 \\ 0 & 0 & 0 & 0 & \delta 2+2\omega 2-2\omega \mathrm{d} & 0 & 0 & 0 & 0 & 0 \\ 0 & 0 & 0 & 0 & 0 & \delta 1+2\omega 1-2\omega \mathrm{d} & 0 & 0 & 0 & 0 \\ 0 & 0 & 0 & 0 & 0 & 0 & 3\delta 2+\xi+3\omega 2-3\omega \mathrm{d} & 0 & 0 & 0 \\ 0 & 0 & 0 & 0 & 0 & 0 & 0 & \delta 2-\xi+\omega 1+2\omega 2-3\omega \mathrm{d} & 0 & 0 \\ 0 & 0 & 0 & 0 & 0 & 0 & 0 & 0 & \delta 1+2\omega 1+\omega 2-3\omega \mathrm{d} & 0 \\ 0 & 0 & 0 & 0 & 0 & 0 & 0 & 0 & 0 & 3(\delta 1+\omega 1-\omega \mathrm{d}) \end{pmatrix}$$

(V = FullSimplify[U.Htot.Udag])//MatrixForm

$$\begin{pmatrix} 0 & \frac{\Omega}{2} & \frac{\Omega}{2} & 0 & 0 & 0 & 0 & 0 & 0 & 0 \\ \frac{\Omega}{2} & 0 & J & \frac{\Omega}{2} & \frac{\Omega}{\sqrt{2}} & 0 & 0 & 0 & 0 & 0 \\ \frac{\Omega}{2} & J & 0 & \frac{\Omega}{2} & 0 & \frac{\Omega}{\sqrt{2}} & 0 & 0 & 0 & 0 \\ 0 & \frac{\Omega}{2} & \frac{\Omega}{2} & 0 & \sqrt{2}J & \sqrt{2}J & \frac{\Omega \mathrm{Sin}[\theta]}{\sqrt{2}} & \frac{\Omega \mathrm{Cos}[\theta]}{\sqrt{2}} & \frac{\Omega}{\sqrt{2}} & 0 \\ 0 & \frac{\Omega}{\sqrt{2}} & 0 & \sqrt{2}J & 0 & 0 & \frac{1}{2}\Omega\left(\sqrt{3}\mathrm{Cos}[\theta]+\mathrm{Sin}[\theta]\right) & \frac{1}{2}\Omega\left(\mathrm{Cos}[\theta]-\sqrt{3}\mathrm{Sin}[\theta]\right) & 0 & 0 \\ 0 & 0 & \frac{\Omega}{\sqrt{2}} & \sqrt{2}J & 0 & 0 & 0 & 0 & \frac{\Omega}{2} & \frac{\sqrt{3}\Omega}{2} \\ 0 & 0 & 0 & \frac{\Omega \mathrm{Sin}[\theta]}{\sqrt{2}} & \frac{1}{2}\Omega\left(\sqrt{3}\mathrm{Cos}[\theta]+\mathrm{Sin}[\theta]\right) & 0 & 0 & 0 & 2J\mathrm{Sin}[\theta] & 0 \\ 0 & 0 & 0 & \frac{\Omega \mathrm{Cos}[\theta]}{\sqrt{2}} & \frac{1}{2}\Omega\left(\mathrm{Cos}[\theta]-\sqrt{3}\mathrm{Sin}[\theta]\right) & 0 & 0 & 0 & 2J\mathrm{Cos}[\theta] & 0 \\ 0 & 0 & 0 & \frac{\Omega}{\sqrt{2}} & 0 & \frac{\Omega}{2} & 2J\mathrm{Sin}[\theta] & 2J\mathrm{Cos}[\theta] & 0 & \sqrt{3}J \\ 0 & 0 & 0 & 0 & 0 & \frac{\sqrt{3}\Omega}{2} & 0 & 0 & \sqrt{3}J & 0 \end{pmatrix}$$

H0 = H0rot;

We do a Schrieffer-Wolff transformation that diagonalizes the Hamiltonian. To second order in J and Ω the effective Hamiltonian is

Hextra1 = V;
S1 = Table $\left[\text{If}\left[n==m, 0, -\frac{i\text{Hextra1}[[n,m]]}{\text{H0}[[n]][[n]]-\text{H0}[[m]][[m]]}\right], \{n, 1, \text{dim}\}, \{m, 1, \text{dim}\}\right]$;
Hextra2 = −Commutator[S1, Commutator[S1, H0]]/2 + iCommutator[S1, V];
S2 = Table $\left[\text{If}\left[n==m, 0, \frac{-i\text{Hextra2}[[n,m]]}{\text{H0}[[n]][[n]]-\text{H0}[[m]][[m]]}\right], \{n, 1, \text{dim}\}, \{m, 1, \text{dim}\}\right]$;
H1 = Simplify[iCommutator[S1, H0] + Hextra1];
H2 = FullSimplify[(iCommutator[S2, H0] + Hextra2)];
(Heff2 = Simplify[H0 + a^2 * H2/.a → 1])//MatrixForm;

We calculate the transitions frequencies ωij between the level ij and 00. We see that ω11 is not just the sum of ω10 and ω01, but shifted by ζ.

ω0 = Heff2[[1]][[1]];
ω11 = FullSimplify[Heff2[[4]][[4]] − ω0];
ω10 = FullSimplify[Heff2[[3]][[3]] − ω0];
ω01 = FullSimplify[Heff2[[2]][[2]] − ω0];
ζ = FullSimplify[ω11 − (ω10 + ω01)]

$$\frac{1}{4}\left(-\frac{8J^2(\delta1+\delta2)}{(\delta1+\omega1-\omega2)(\delta2-\omega1+\omega2)}+\frac{2\Omega^2}{\delta2+\omega2-\omega d}-\frac{2\Omega^2\mathrm{Cos}[\theta]^2}{\delta2-\xi+\omega2-\omega d}-\frac{2\Omega^2\mathrm{Sin}[\theta]^2}{3\delta2+\xi-\omega1+2\omega2-\omega d}\right)$$

We evaluate ζ for the resonance condition $\delta2=(\omega1\text{-}\omega2)/2=\Delta/2$ and a drive close to the n2->n1 transition $\omega d=(\omega1+\omega2)/2\text{-}\delta$, where δ is a small frequency detuning. Choosing $\theta=\pi/4$ corresponds to the diagonalization condition from above.
The shift consists of a term $\zeta0$ that is independent of the drive and a term $\zeta2$ that is induced by the drive.

ζ = FullSimplify[$\omega11-(\omega10+\omega01)/.\delta2\to(\omega1-\omega2)/2/.\omega d\text{->}(\omega1+\omega2)/2-\delta/.\omega1\to\Delta+\omega2/.\theta\to\pi/4$]

$$\frac{2J^2(\Delta+2\delta1)}{\Delta(\Delta+\delta1)}-\frac{\xi^2\Omega^2}{2\delta^3-2\delta\xi^2}$$

Taking a look at the computational levels only, i.e. the levels 00,01,10,11, we find

(Hqubit = FullSimplify[Chop[Table[Heff2[[n, m]], {n, 1, 4}, {m, 1, 4}]]/.$\delta2\to(\omega1-\omega2)/2/.\omega d\text{->}(\omega1+\omega2)/2-\delta/.\omega1\to\Delta+\omega2/.\theta\to\pi/4$])//MatrixForm;

This Hamiltonian consists of IZ and ZI terms plus a ZZ interaction and some constants

(Hcheck = FullSimplify[$-\frac{1}{2}\left(\omega01+\frac{\zeta}{2}\right)IZ-\frac{1}{2}\left(\omega10+\frac{\zeta}{2}\right)ZI+\frac{\zeta}{4}ZZ+\left(\frac{\omega01}{2}+\frac{\omega10}{2}+\frac{\zeta}{4}+\omega0\right)II/.\delta2\to(\omega1-\omega2)/2/.\omega d\text{->}(\omega1+\omega2)/2-\delta/.\omega1\to\Delta+\omega2/.\theta\to\pi/4$]) //MatrixForm

$$\begin{pmatrix} -\frac{2\delta\Omega^2}{4\delta^2-\Delta^2} & 0 & 0 & 0 \\ 0 & \frac{-\delta\left(4\delta^2-\Delta^2\right)\left(2J^2+\Delta(-2\delta+\Delta)\right)+\Delta\left(-4\delta^2+2\delta\Delta+\Delta^2\right)\Omega^2}{8\delta^3\Delta-2\delta\Delta^3} & 0 & 0 \\ 0 & 0 & \delta+\frac{J^2}{\Delta}+\frac{\Delta}{2}+\frac{2(\delta(2\delta+\Delta)+\Delta\delta1)\Omega^2}{\left(-4\delta^2+\Delta^2\right)(2\delta+\Delta+2\delta1)} & 0 \\ 0 & 0 & 0 & 2\delta+\frac{2J^2(\Delta+2\delta1)}{\Delta(\Delta+\delta1)}+\frac{\left(-8\delta^4+4\delta^2\Delta^2-2\Delta^2\xi^2+\delta(\Delta+2\delta1)\left(\Delta^2-4\xi^2\right)\right)\Omega^2}{2\left(4\delta^2-\Delta^2\right)(2\delta+\Delta+2\delta1)(\delta-\xi)(\delta+\xi)} \end{pmatrix}$$

Check that this is the same:

FullSimplify[Hqubit − Hcheck]

{{0, 0, 0, 0}, {0, 0, 0, 0}, {0, 0, 0, 0}, {0, 0, 0, 0}}

Bibliography

[1] Richard P. Feynman. "Simulating physics with computers". In: *International Journal of Theoretical Physics 21* (1982).

[2] Peter Shor. "Algorithms for quantum computation: discrete logarithms and factoring ". In: *35th Annual Symposium on Foundations of Computer Science* (1994).

[3] A. Blais et al. "Cavity quantum electrodynamics for superconducting electrical circuits: An architecture for quantum computation". In: *Physical Review A* 69.6, 062320 (June 2004), p. 062320. DOI: 10.1103/PhysRevA.69.062320. eprint: arXiv:cond-mat/0402216.

[4] M. Steffen et al. "High-Coherence Hybrid Superconducting Qubit". In: *Physical Review Letters* 105.10, 100502 (Sept. 2010), p. 100502. DOI: 10.1103/PhysRevLett.105.100502. arXiv:1003.3054 [cond-mat.supr-con].

[5] John M. Martinis et al. "Rabi Oscillations in a Large Josephson-Junction Qubit". In: *Phys. Rev. Lett.* 89 (11 2002), p. 117901. DOI: 10.1103/PhysRevLett.89.117901. URL: http://link.aps.org/doi/10.1103/PhysRevLett.89.117901.

[6] B. M. Terhal. "Quantum Error Correction for Quantum Memories". In: *ArXiv e-prints* (Feb. 2013). arXiv:1302.3428 [quant-ph].

[7] J. Koch et al. "Introducing the Transmon: a new superconducting qubit from optimizing the Cooper Pair Box". In: *eprint arXiv:cond-mat/0703002* (Feb. 2007). eprint: arXiv:cond-mat/0703002.

[8] Roland Winkler. *Spin-Orbit Coupling Effects in Two-Dimensional Electron and Hole System*. Springer, 2003.

[9] S. Bravyi, D. P. Divincenzo, and D. Loss. "Schrieffer-Wolff transformation for quantum many-body systems". In: *Annals of Physics* 326 (Oct. 2011), pp. 2793–2826. DOI: 10.1016/j.aop.2011.06.004. arXiv:1105.0675 [quant-ph].

[10] Lev Bishop. "Circuit Quantum Electrodynamics". PhD thesis. Yale University, 2010.

[11] Audrey Cottet. "Implementation of a quantum bit in a superconducting circuit". PhD thesis. Université Paris VI, 2002.

[12] Matthew David Reed. "Entanglement and Quantum Error Correction with Superconducting Qubits". PhD thesis. Yale University, 2013.

[13] Steven M. Girvin. "Superconducting Qubits and Circuits: Artificial Atoms Coupled to Microwave Photons". In: *Lecture Notes delivered at Les Houches Summer School, July 2011*. to be published by Oxford University Press.

[14] S. Poletto et al. "Entanglement of Two Superconducting Qubits in a Waveguide Cavity via Monochromatic Two-Photon Excitation". In: *Physical Review Letters* 109.24, 240505 (Dec. 2012), p. 240505. DOI: 10.1103/PhysRevLett.109.240505. arXiv:1208.1287 [quant-ph].

[15] J. B. Chang et al. "Improved superconducting qubit coherence using titanium nitride". In: *Applied Physics Letters* 103.1, 012602 (July 2013), p. 012602. DOI: 10.1063/1.4813269. arXiv:1303.4071 [quant-ph].

[16] Jay M. Gambetta. "Control of Superconducting Qubits". In: *Lecture Notes of the 44th IFF Spring School*. Ed. by David DiVincenzo. Schriften des Forschungszentrums Jülich. 2013.

[17] V. Paulisch et al. "Beyond adiabatic elimination: A hierarchy of approximations for multi-photon processes". In: *ArXiv e-prints* (Sept. 2012). arXiv:1209.6568 [quant-ph].

[18] Daniel F. V. James and Jonathan Jerke. "Effective Hamiltonian Theory and Its Applications in Quantum Information". In: *Canadian Journal of Physics* (2007).

[19] J. M. Chow et al. "Microwave-activated conditional-phase gate for superconducting qubits". In: *ArXiv e-prints* (July 2013). arXiv:1307.2594 [quant-ph].

[20] J. M. Chow et al. "Simple All-Microwave Entangling Gate for Fixed-Frequency Superconducting Qubits". In: *Physical Review Letters* 107.8, 080502 (Aug. 2011), p. 080502. DOI: 10.1103/PhysRevLett.107.080502. arXiv:1106.0553 [quant-ph].

[21] V. E. Manucharyan et al. "Fluxonium: Single Cooper-Pair Circuit Free of Charge Offsets". In: *Science* 326 (Oct. 2009), pp. 113–. DOI: 10.1126/science.1175552. arXiv:0906.0831 [cond-mat.mes-hall].